FREEZE-THAW DURABILITY OF HIGH STRENGTH SILICA FUME CONCRETE

by

MOHSEN GHOLAM-REZA KASHI

DISSERTATION submitted to the Faculty of the
Virginia Polytechnic Institute and State University
in partial fulfillment of the requirements for the degree of
DOCTOR OF PHILOSOPHY
in
CIVIL ENGINEERING

APPROVED:

RICHARD E. WEYERS, (CHAIRMAN)

RICHARD D. WALKER

RICHARD M. BARKER

THANGAVELU KUPPUSAMY

GEORGE W. SWIFT

December, 1988

Blacksburg, Virginia

FREEZE-THAW DURABILITY OF HIGH STRENGTH SILICA FUME CONCRETE

by

MOHSEN GHOLAM-REZA KASHI

CIVIL ENGINEERING

(ABSTRACT)

Specimens from 27 batches of concrete with water to cementitious (cement plus silica fume) ratio of 0.25 to 0.32, with and without entrained air, were tested for freeze-thaw durability in accordance with ASTM C666, procedure A (freezing and thawing in water). In addition, another set of similar specimens were moist cured for 28 days instead of 14 days and tested in accordance with ASTM C666 , Procedure A to determine the effect of curing time on the freeze- thaw durability of high strength concrete. Results show that non air- entrained high strength concrete with water-cementitious ratio of less than 0.30, regardless of the length of curing time, is frost resistant. Non-air-entrained concrete with water-cement ratio of 0.32 is also durable if silica fume is not used.

Acknowledgements

The author would like to express his appreciation to the chairman of graduate committee Dr. R.E. Weyers. The author is deeply indebted to him for his advice, guidance and sincere concern during my studies and dissertation.

Thanks are also extended to the members of the committee, Dr. R.D. Walker Dr. R.M. Barker, Dr. T. Kuppusamy, and Dr. G.W. Swift for their fruitful suggestions. Appreciation is gratefully expressed to Dr. R.D. Walker for his sound advice.

The author express his deepest appreciation to his wife for her continuous help, encouragements, and patience which without, this work was not possible. This work is dedicated to the memory of the author's father .

Table of Contents

List of Illustrations

List of Tables

Chapter I

BACKGROUND

1.1 INTRODUCTION

Concrete is the single most used material in the construction industry throughout the world. This is mainly attributed to its abundance and flexibility to be cast in different geometrical shapes. Although the modulus of elasticity of concrete is low as compared to steel (about 10%), its cost per psi and other factors such as relatively good resistance to harsh environments and low maintenance requirements, have made it so popular that today most of the major structures such as dams, bridges, underground sewage system, and a large percentage of pavements are made of concrete. According to statistical abstracts of the United States, the current value of concrete-based structures on U.S. territory alone is about 6 trillion dollars (1) .

A concrete structure, although adequately designed to withstand the imposed loads, can and often will fail if its ability to perform in the expected environmental exposure is overlooked. Durability in concrete refers to its capability to withstand the environmental conditions anticipated during its intended service life without any significant damage. The potentially destructive forces

that might influence the durability of concrete are numerous and include: wetting and drying, freezing and thawing, and attack by acid, chloride, and sulfate.

1.2 FREEZING AND THAWING OF CONCRETE

Damage to the concrete structures (such as pavements and bridges) as the result of freezing and thawing is very serious and costly in the northern hemisphere. Concrete is a porous material and its vulnerability to alternate freezing and thawing is a function of its pore structure (2). The pores and bleeding channels in hardened concrete provide passage for the water. The water bearing spaces in the concrete cover a wide range of sizes. It varies from 15 to 40 Å for the spaces within the hydrated cement particles (gel pores) in their densest possible form (3), to 5,000 Å for the channels created by unused portion of mixing water from hydration process (capillary pores) (4). Much larger ones are created by entrapped pockets of air. By decreasing temperatures, in a partially saturated concrete, there is a progressive freezing process starting from the water in the largest cavities to the smaller ones. In an ordinary freezing environment a great portion of the water present in the smaller cavities, and in particular the water in the gel pores, does not freeze. This is because of a strong force acting between water molecules and the walls of the cavity in smaller pores. Alternate freezing and thawing of the stored water inside the intermediate size pores, called capillaries, is responsible for the destruction of concrete.

In ordinary concrete with water to cement ratio of greater than about 0.38, the presence of residual water from the hydration process creates the capillary channels. To protect such a concrete from frost damage, deliberate entrainment of a system of microscopic air bubbles has been the only practical counter measure. Air bubbles are created using air entraining chemical admixtures at the initial mixing stage. They are in the size range of 1 to 1,000 μm and they act as reservoirs for the water expelled during the freezing process and prevent the build up of destructive pressure. For the

air-bubbles to function properly, they have to be distributed uniformly throughout the hardened cement paste.

In an environment where concrete (for one inch top size aggregate) is exposed to severe freezing and thawing, the American Concrete Institute (ACI)(5) recommends an average air content of 6 percent or higher (by volume), as measured by the pressure meter (ASTM C 231). The spacing factor as a representation of the spaces between the air bubbles and specific surface which is the ratio of air bubble's peripherial surface area, to its volume, are the other two important freezing and thawing parameters. According to ACI recommendation, for a concrete to be frost resistant, its spacing factor, as measured in a hardened state has to be less than 0.008 inches and the specific surface should be greater than 600 $\frac{in^2}{in^3}$ (6).

Porosity and permeability in concrete have a direct relationship to its water to cement ratio. By decreasing this ratio, the number and the size of interconnecting channels within the hardened paste decreases. Powers (3) suggested that theoretically it is possible to have concrete with no capillary channels, provided that such a concrete is sufficiently low in water-cement ratio and the curing period is prolonged until all the water present in the system is depleted through hydration and internal self desiccation. Such a concrete would naturally survive freezing and thawing since it does not contain any freezable water. Unless the water-cement ratio is extremely low, the lack of uniformity in the distribution of water throughout the mass of fresh concrete makes the existence of some pockets with a higher water-cement ratio inevitable. For the water to diffuse to the other regions of concrete and enter the process of hydration, years of curing are needed. Freezing of freezable water in the concrete can exert a force in excess of 30,000 psi (4). This is beyond the tensile strength of any normal portland cement concrete currently produced, and regardless of strength, there is a need for air-entrainment.

The inherent problem with very low water cement ratio concrete is the lack of workability which has been the major stumbling block in the practicality of such concrete.

1.3 NEW DEVELOPMENTS

In the last two decades, the development of a large variety of materials such as water reducers and mineral admixtures has given a new direction to the concrete industry. In the past few years, a new generation of concrete with very high compressive strength has emerged and has been used in some major projects in the United States (7). This is usually accomplished by employing a high range water reducer (HRWR) and a very low water-cement ratio concrete in conjunction with pozzolans such as fly ash or silica fume. Due to the adverse effect of air entrainment on the compressive strength , there has been a general reluctance in the industry to use this material in an exposed environment, hampering its great potential. The following are several hypotheses regarding freeze-thaw durability of high strength silica fume concrete (4).

1. Silica fume, due to its fineness, can reduce the size of capillary pores to a degree that water cannot freeze under normal environmental temperature in its pore system.

2. Reliable durability results can be obtained in the laboratory using ASTM C666, procedure A, provided the concrete is cured for more than 14 days in order for the hydration of silica fume to fully develop.

3. Even if air entraining is needed for high strength concrete, the current recommendations (spacing factor of less than 0.008 inches and air content of 6%) are too conservative to be used for high strength concrete.

1.4 EXPERIMENTAL METHODS

Resistance of concrete to repeated cycles of freezing and thawing can be measured in the laboratory in accordance to standardized testing methods ASTM C666 procedures A and B, or ASTM C671 (8).

According to ASTM C666 (Resistance of Concrete to Rapid Freezing and Thawing), concrete specimens after 14 days of moist curing are usually exposed to 300 cycles of freezing and thawing. The freeze-thaw cycles for both procedures (A & B) consist of alternately lowering the temperature of the specimens from 40 to 0 °F and raising it back to 40 °F in not less than 2 nor more than 5 hours. In procedure A concrete specimens are frozen and thawed in water, while according to procedure B the specimens are frozen in the air and thawed in the water.

Deleterious effects of freezing and thawing on the concrete specimens are detected nondestructively by measuring its dynamic modulus of elasticity (ASTM C215). The decrease in dynamic modulus of elasticity as the result of exposure to freezing and thawing is the measure of frost susceptibility of concrete.

The other standard test method for evaluation of concrete resistance to freezing and thawing is ASTM C671 (Critical Dilation of Concrete Specimens Subjected to Freezing). In this method the specimen, after being cured in an environment similar to the field condition, is cooled in a water saturated kerosene bath from 35 to 15 °F at the rate of $5° \pm 1°F$. Then specimen is immediately transferred to a water bath with a temperature of 35 °F until the next test cycle, which is carried out every two weeks. In this method the residual dilation after a designated number of freezing cycles is the measure of frost resistance in the concrete.

1.5 OBJECTIVES

The objectives of this study are:

1. To test the performance of high strength silica fume concrete according to a " standard test method for resistance of concrete to rapid freezing and thawing " (ASTM C666, procedure A).

2. To test the effect of curing time on freeze-thaw durability for high strength silica fume concrete.

3. To ascertain any possible correlation between air void parameters and freeze-thaw durability performance.

Chapter II

HIGH STRENGTH CONCRETE

2.1 INTRODUCTION

In civil engineering as in other fields of technology engineers are faced with increasing demands for efficiency. This has been the bases for a general improvement in concrete's properties and particularly its compressive strength. In the 1950s, concrete with a compressive strength of 5,000 psi was considered as high strength. In the 1960s, concrete with 6,000 to 7,500 psi, and in early 1970s concrete with compressive strength of 9,000 psi was being produced commercially but in limited quantity. More recently concrete with compressive strengths over 16,000 psi has been used in cast-in-place and prestressed structural members.

In general, high strength concrete refers to concrete which has a uniaxial compressive strength greater than that which is ordinarily obtained in a region. This definition has been generally accepted and used by ACI Committee 363(committee on high strength concrete) (9), because maximum strength of concrete currently being produced varies considerably from region to region throughout the world. In a country where concrete with a compressive strength of 8,000 psi is already being produced commercially, high strength concrete might be in the range of 10,000 to

14,000 psi. However, in a country where the upper limit on commercially available material is currently 5,000 psi, 8,000 psi concrete is considered high strength. Currently 5,000 to 10,000 psi concrete can be produced nearly anywhere in the U.S. by using conventional production techniques (10).

2.2 USE OF HIGH STRENGTH CONCRETE

There are many possible structural applications where concrete with high compressive strength can be employed to an advantage. In bridge construction, the paradox of dead structural weight and span length can be solved by using smaller but equally strong sections. In rehabilitation of old bridges for accommodation of new and higher traffic load, super-structure weight can be reduced through the use of smaller and lighter girders, beams, and deck.

In highrise structures, column and beam dimensions can be reduced resulting in substantial increase in expensive office space. In one case it is reported (11) that in a 50 story structure using 8,000 psi concrete instead of 4,000 psi resulted in a reduction of 33 percent in column diameters. At this juncture, it is appropriate to consider the saving in costs of scaffolding and form works, by the reduction of dead load and cross sectional area. Equivalently substantial benefits can be named for other structures such as pavements, foundations, and underground structures. Despite all these advantages, the concrete industry has been very slow in adoption and utilization of high strength concrete's potentials. This reluctance is basically due to the lack of adequate information on the behavior of high strength concrete under actual field conditions.

2.3 PRODUCTION METHODS

A variety of methods are used in production of concrete with high compressive strength but most are produced through exotic procedures and materials either in the laboratory or for special application. The following is a list of several methods used for production of high strength concrete.

1. Alteration in conventional mix proportioning through the use of lower water to cement ratio and chemical and/or mineral admixtures.

2. Fiber reinforcement.

3. High speed slurry mixing.

4. Compaction by pressure.

5. Modification with polymers.

6. Autoclave curing.

Performance of high strength concrete which is produced through the reduction of water to cement ratio (first category) is the concern of this research. The inherent problem with lowering water to cement ratio without help of chemical admixtures, is the loss of workability. Concrete made with a W/C ratio less than 0.40 by weight is generally not practical for field use. The introduction of chemical admixtures such as water-reducing agents and more recently high-range-water-reducing agents (super plasticizers) provide the opportunity of producing concrete with a W/C ratio as low as 0.20 with a considerable increase in compressive strength.

Factors that would permit the production of high strength concrete is not a drastic change in material properties or in production technique. The proper material selection, concrete mix proportioning, batching, mixing, transporting, placing, and finally the control procedures are responsible for the attainment of higher strength concrete.

2.3.1 Cement

Variations in the chemical composition and physical properties of the cement affect the concrete compressive strength. According to ACI committee 363 (9), if the tricalcium silicate content in the cement varies by more than 0.5 percent, or the fineness by more than 375 cm^2/g (Blaine), then problem in maintaining a uniform high compressive strength may result. Other than the above requirement, the use of an optimum amount of good quality type I cement is sufficient to produce high strength concrete. "Optimum amount" refers to an amount beyond which no additional strength can be achieved.

2.3.2 Fine Aggregate.

Generally, rounded aggregate particles help workability or in other words requires less water to maintain the same workability as when angular aggregate is used. Consequently in the production of high strength concrete, sands with rounded particles are recommended. In addition, since high strength concrete typically contains a large amount of fine cementitious materials, use of relatively coarse sand with a fineness modulus in the range between 2.7 and 3.2 has been recommended (10).

2.3.3 Coarse Aggregate.

For concrete with less than 5,000 psi compressive strength, aggregate is normally stronger than the cement paste matrix. In high strength concrete this is not necessarily true. In the production of high strength concrete, the use of strong aggregate is recommended. Gradation of coarse aggregate is of prime importance, since the probability of flaws and micro fractures in the transition zone (between the aggregate particles and cement paste) as well as within the aggregate structure itself is higher for the larger aggregate particles. The maximum size aggregate recommended by ACI Committee 363 is 1 inch. The second factor to be considered is that in low water to cement ratio concrete, hydration causes desiccation, and, if water is not available to the unhydrated cement particles, the cement matrix cannot develop its full compressive strength capability. Desiccation during hydration process produces some vacuum which, if available to the paste, can draw water from the surroundings. Using coarse aggregate with moderate absorption can be the source for such curing water.

Other than the gradations, both fine and coarse aggregate should meet the requirements of ASTM C 33 (8).

2.3.4 Water

Mixing water for high strength concrete, like ordinary concrete, should be potable.

2.3.5 Chemical Admixtures

2.3.5.1 High Range Water Reducers (Super Plasticizers)

In normal cement pastes where particles come into close contact with each other there is a tendency for cement particles to form large conglomerations. This is due to the Van der Waals forces attracting particles together. The addition of a water-reducing admixture to a cement suspension neutralizes the force field and reduces the interparticle friction in the system so that the energy required to induce flow into the system is reduced (12). A normal water reducer is capable of reducing water requirements by about 10 to 15 percent. Further reduction can be obtained with a higher dosage, but this may result in undesirable effects on other properties of concrete such as time of setting, air content, and potential for segregation. High range water reducers (super plasticizers) are chemically different from the normal water reducers and they are capable of reducing water content by about 30 percent. This class of chemical is capable of producing a better than normal workability in concrete with a lower than normal amount of water. Introduction of super plasticizers has been the major breakthrough in the production of high strength concrete.

2.3.5.2 Retarders

Dispersion of cement in a superplasticized concrete causes the individual cement particles to have more exposure to water. This will foster a higher rate of hydration which in turn causes a fast reduction in workability (slump loss). In high strength concrete, because of the large quantity of cement, this is even more significant. In such a situation a repeated dosage of superplasticizers or another but similar class of chemical admixtures called retarders is recommended. These chemicals are able to lengthen the time available for transport, handling and placing of the concrete.

2.3.5.3 Air Entraining Agents

Air Entraining agents belong to a class of chemicals called surfactants. A surfactant, which is short for surface active substance, is a material whose molecules are absorbed strongly at air-water or solid-water interfaces. On addition to cement paste and agitation, the solution of air entraining agent produces air bubbles which are stabilized later as microscopic spheres (13). For concrete to resist the destructive effect of freezing and thawing, the air entrainment is vital and it is the only remedy known today. The reduction in compressive strength of concrete is the only drawback associated with the use of air entraining agents. It should be noted that for most normal strength concrete, air-entrainment has little or no effect on strength because of reduction of W/C ratio.

2.3.6 Mineral Admixtures

Mineral admixtures are fine granulated materials that are normally added to portland cement concrete in large quantities as a percentage of cement weight. Many industrial by-products such as fly ash, rice husks ash, and silica fume are rapidly becoming the primary source of mineral admixtures. The mineral admixtures are primarily used for their pozzolanic or both pozzolanic and cementitious properties.

According to ASTM C618 (8), a pozzolan is defined as "siliceous or siliceous and aluminous materials which in themselves possess little or no cementitious value but will, in finely divided form and in the presence of moisture, chemically react with calcium hydroxide at ordinary temperature to form compounds possessing cmentitious properties ".

However, many industrial by products such as fly ash and slag contain 10 to 40 percent CaO. If a part or all of this calcium becomes available for the pozzolanic reaction, the material becomes self-cementing. Such materials are considered as cementitious and pozzolanic (13). Since silica

fume was the only mineral admixture used for this study, its properties and effects on concrete as well as its production methods are presented in this section.

In ordinary concrete the water-cement ratio as defined by the ASTM C125 (8), is referred to as the amount of water, exclusive only of that absorbed by the aggregates, to the amount of cement in concrete. But when a pozzolan is present, normally the water-cementitious ratio or W/(C+P) instead of water-cement ratio (W/C) is used. Where (C+P) is the amount of cement plus the amount of pozzolan in the concrete.

2.4 SILICA FUME

Silica fume is a material made of finely graded spherical particles which is a by-product from the reduction of high-purity quartz with coal in electric arc furnaces during the production of silicon and ferrosilicon alloys (14). It is known by such terms as microsilica, silica powder, and condensed silica fume. Silica fume has a high content of amorphous silicon dioxide (SiO_2). Table 2.1 shows the chemical composition of a typical silica fume sample (15).

2.4.1 Physical Properties

- Specific Gravity - The specific gravity of silica fume is approximately 2.2 as compared to 3.15 for normal type 1 portland cement (16).

- Fineness - The particle-size distribution of a typical silica fume shows that most of the particles are smaller than one micrometer (1 μm) with an average diameter of about 0.1 μm. This is approximately two orders of magnitude smaller than the average cement particle. Using

Table 2.1. Silica Fume Chemical Composition Ref. (15)

CHEMICAL COMPOSITION	%
SiO_2	87.20
Al_2O_3	0.26
Fe_2O_3	2.26
CaO	1.24
MgO	0.79
SO_3	0.26
Loss on Ignition	3.80
Total Alkalies	0.56

surface area as another index for the particle size, the following table illustrates the extreme fineness of silica fume (16).

	m^2/kg	Measuring Method
Silica Fume	20,000	Nitrogen adsorption
Fly Ash	400 to 700	Blaine
Ground Granulated Blast-Furnace slag	350 to 600	Blaine
Normal Portland cement	300 to 400	Blaine

- Unit Weight - The bulk unit weight of silica fume in powder form is about 39 lb/ft^3(16).

2.4.2 Mechanism of Reaction

The process of the pozzolanic reaction of silica fume was studied by Grutzeck et al (17). Adding silica fume to a solution of calcium hydroxide, his observations pertaining to its reaction in portland cement concrete are:

1. In solution form, a silica gel forms during the first minutes of mixing. The large amount of water absorbed by silica gels at this stage explains the loss of workability in fresh concrete when silica fume is added.

2. The silica gels would soon react with $Ca(OH)_2$ liberated from the cement minerals and form calcium silicate hydrate (C-S-H).

3. C-S-H growing outward from the hydrating cement particles produces a rigidly cemented C-S-H network.

In another study (18), the amount of $Ca(OH)_2$ in specimens of portland cement mortar with 0 to 30 percent silica fume was measured. All the available $Ca(OH)_2$ in the mortar containing 30 percent silica fume and with a water to cementitious ratio of 0.45 after 3 days of curing and mortar with water to cementitues ratio of 0.60 after 14 days of curing were consumed by silica fume's pozzolanic reaction. But Sarker et al (19) investigating the pozzolanic reaction of silica fume on very low water to cementitues ratio (0.24) concluded that, the low water content in such a concrete effectively delays the dissolution of silica fume particles. In such a concrete, the effective dissolution process continues (with a diminishing rate) even up to 90 days.

2.5 EFFECT OF SILICA FUME ON COMPRESSIVE STRENGTH OF CONCRETE

Silica fume has been used in concrete along two different paths:

1. Silica fume as a partial replacement for cement, mainly to enhance the concrete's properties and cost saving. According to Sellevold (20,21) the efficiency of silica fume in terms of producing compressive strength is about 2 to 4 times greater than cement. In other words, 1 lb. of silica fume can replace 2 to 4 lbs. of cement.

2. Use of silica fume to produce concrete with superior compressive strength. In a literature survey by Jahren (22), more than 70 percent of the literature internationally available on silica fume concrete suggests that the admixture significantly increases the compressive strength of concrete. Garette (23) in an experimental investigation using silica fume and fly ash in concrete, concluded that regardless of water to cement ratio, the compressive strength of concrete using silica fume was significantly higher than the controls from age 7 to 91 days. Several other literatures reviewed by the author regarding this subject acknowledge the increase in compressive strength of concrete due to addition of silica fume (24-34).

The optimum amount of silica fume, beyond which no increase in compressive strength is achieved, was determined to be about 15 percent by the weight of cement (35).

Another advantage precipitated to the use of silica fume in concrete is the improvement in the bond between cement paste and aggregate. Cement paste in the periphery zones of aggregates is called transition zone and has different characteristics than the bulk of cement paste matrix. This zone which in ordinary portland cement concrete is about 50 μm thick, is more porous and structurally weaker than both aggregate and paste. Using x-ray diffraction, Carles-Gibergues (36) observed that the crystals of hydrated cement in the transition zone grow with a preferential orientation on the surface of aggregate. This in turn makes the transition zone more susceptible to crack propagation.

There are indications that addition of silica fume to concrete has a definite effect on transition zone. Some investigators partially attribute the higher strength in silica fume concrete to the superior bond between aggregate and the paste (18,37,38).

2.6 EFFECT OF SILICA FUME ON PERMEABILITY OF HARDENED CONCRETE

When silica fume is mixed with portland cement and hydrated, it produces a pore structure fundamentally different from ordinary hardened cement paste. The addition of silica fume substantially reduces the permeability of concrete (14,15,27,32,37,39). Using hydraulic conductivity as a measure of permeability Gjory (40) observed that permeability reduced from about $1.6x10^{-7}$m/sec for plain mix to about$4.0x10^{-10}$ m/sec for the mix with 10 percent silica fume. Nagataki et al (41) studied the effect of silica fume on air permeability of concrete. He reported that when silica fume is added to concrete its coefficient of air permeability decreases regardless of curing period. A comprehensive study about the effect of silica fume on the pore structure of concrete

was carried out by Sellevold et al (21). They prepared several mixes with a constant W/C ratios and various dosages of silica fume. Using mercury porsimitery, they reported that although the permeability decreases by increasing the dosage of silica fume, the total porosity remains unchanged. The results indicate that the addition of silica fume actually causes refinement in the pore structure of concrete.

The studies regarding the effect of silica fume on pore size distribution of concrete indicates that, while the amount of capillary pores substantially decreases, the number of smaller voids, particularly those below 400Å, are increased (30,40,42).

2.7 FREEZE-THAW DURABILITY OF SILICA FUME CONCRETE

A survey of the available literature concerning the effect of silica fume on the freeze-thaw durability of concrete indicates a general variation and sometimes contradicting results. This can be attributed to variations inherent in the laboratory procedures, materials, and equipment used.

Some investigators imply that addition of silica fume improves the freeze-thaw resistance of concrete (27,43,44). Cjorv (40) reported that the addition of 10 percent silica fume to a mix with 250 Kg/m^3 cement, gives the same resistance to freezing and thawing (using ASTM C666) as a mix with 400 Kg/m^3 of cement.

The overwhelming bulk of data indicates that the addition of silica fume in high dosage (above 15%) is harmful to the freeze-thaw durability of concrete. The densification of the internal pore system and refinement of the migratory path for the moving water as the result of freezing is generally blamed for the adversity (12,21,29,30,45).

Sorensen (46) tested concrete with a W/(C+SF) ratio ranging from 0.37 to 0.67 with various silica fume contents. The samples of concrete with and without entrained air, were tested according

to ASTM C671. Non-air-entrained samples with W/(C+SF) of 0.37 and 10 percent silica fume demonstrated an outstanding frost resistance as compared to control concrete. Sellevold et al (21) suggest that at very low water to cement ratios, perhaps less than 0.3, with silica fume dosage of around 10 percent air entrainement might not be necessary. Yamato et. al. (30) conducted research on the freeze-thaw durability of concrete according to ASTM C666 procedure A, with W/(C+SF) ranging from 0.25 to 0.55, incorporating 0 to 30 percent silica fume. The results indicate that regardless of the amount of silica fume, the concrete with W/(C+SF) of 0.25 (without air entrainment) is immune to frost damage. But for concrete with W/(C+SF) of higher than 0.25 air entrainment is mandatory.

In another study (35), concrete with W/(C+SF) of 0.34, and containing 0 to 30 percent silica fume, was tested for freeze-thaw durability according to ASTM C666. The results indicate that regardless of strength level and silica fume content, air entrainment is necessary to insure an adequate freeze-thaw durability. A comprehensive research study was carried out by Malhotra (47) on the durability of high strength silica fume concrete. W/(C+SF) for the mixes ranged from 0.25 to 0.35 and the silica fume content was 0 to 20 percent by the weight of cement. All the non air-entrained samples that were subjected to freezing and thawing according to ASTM C666 procedure A failed in less than 50 cycles of exposure. Samples with 10 and 20 percent silica fume, although they were air-entrained (from 3.7 to 5.4%), showed very poor resistance to freezing and thawing as compared to the controls.

The densification in the paste structure caused by silica fume have shown to be detrimental to the air void parameters and in particular to the concept of critical spacing factor. In a study concerning the effect of silica fume on freeze-thaw durability (48), concrete with a water-cement ratio of 0.50 incorporating 10 percent silica fume were submitted to freeze-thaw cycles in accordance with ASTM C666 procedure A. Analyzing the air void parameters according to ASTM C457, the value of the critical spacing factor was found to be smaller for silica fume concrete as compared to the concrete without silica fume. In another study by the same authors (49), although the water to cementitous ratio was 0.30, the same conclusion was drawn. The critical spacing factor were 300

μm for silica fume concrete and 400 μm for the control. The critical spacing factor specified by ACI for ordinary portland cement concrete is 200 μm.

2.8 FREEZE-THAW DURABILITY OF HIGH STRENGTH CONCRETE (NO SF)

As in the case of concrete with silica fume, the literature available on the durability of high strength concrete showed conflicting results.

High strength concrete samples with a nominal 28 days compressive strength of 6,000 to 10,000 psi (water to cementitious ratio ranging from 0.52 to 0.26), incorporating class C fly ash with the cement content of 600 to 960 lb/yd^3 were subjected to 300 cycles of freezing and thawing under water. Testing was conducted at two cycles per day. Some samples were kept under water for 28 days prior to testing while the others were air dried for 21 days after 7 days of moist curing. All non air-entrained samples performed poorly irrespective of strength level. The period of air drying did not have any significant effect on the durability of the concrete. Entrainment of 3 to 4 percent air (top aggregate size of 0.5 in.) was found to be necessary in order to insure its durability (50).

Foy et. al. (51), in a study on the durability of high strength concrete exposed some samples of air-entrained and non air-entrained concrete specimens with water cement ratio of 0.20 to freezing and thawing in accordance with ASTM C666 procedure A. All the specimens performed excellently after 300 cycles. Air void parameters calculated, using the result of microscopical analysis (ASTM C457), revealed a critical spacing factor of about 750 μm. In another study concrete with a water- cement ratio as low as 0.32 and a compressive strength as high as 8,000 psi was tested according to ASTM C666 procedure A and ASTM C671 (52). All the samples with a water-cement ratio of less than 0.40, and especially the ones with water-cement ratio of 0.32 (without air entrainment), exhibited good resistance when they were tested according to ASTM C671, while

they all failed according to ASTM C666 procedure A. This raises a question on the validity of the results obtained from ASTM C666 procedure A for the field use.

Chapter III

FROST MECHANISM

3.1 INTRODUCTION

The vulnerability of concrete to alternate freezing and thawing is an attribute of the pore structure of cement paste and aggregate. In this chapter a brief explanation of the kinds of damages, as well as the role of the aggregate and paste, are presented.

The deterioration of concrete caused by freezing and thawing is usually manifested in cracking, scaling, and spalling which produces uneven and unsightly surfaces. Several distinguished modes of deteriorations have been identified.

3.1.1 D-Cracking

One of the common signs of freezing and thawing deterioration is the appearance of cracks that run approximately parallel to joints or edges of concrete section. These cracks initiate near the

joint and propagate further away as deterioration progresses. The most logical explanation for the occurrence of D-cracking in concrete is that debris and moisture normally accumulates within the joints. Saturated concrete sections in these regions fall victim to the destructive effect of freezing and thawing (53).

3.1.2 Map Cracking

Map cracking is a kind of deterioration whereby random cracks develop over the concrete's surface. It is caused mainly by the expansive properties of unsound aggregate aggravated by alkaline-silica reactions, freezing and thawing, or excessive heat (54).

3.1.3 Pop-Outs

Large and saturated pieces of porous aggregate near the surface of concrete are removed from the concrete by an exertion of bond braking force to the surrounding paste induced by expanding frozen water inside the aggregate. Cherts are the most frequent cause of pop-outs. If a large quantity of this aggregate is present in the concrete, appearance or even the integrity of the structure may be damaged.

3.1.4 Scaling

Progressive crumbling of mortars from the exposed surface of poor quality concrete is called scaling. This can be caused by the exertion of pressure developed in the underlying unsound aggregate, lack of entrained air, or weak (high W/C) concrete at the surface resulting from overfinishing the surface.

3.2 AGGREGATE

Although it is beyond the scope of this study to explain durability as related to aggregate, it is necessary to explain briefly the mechanism of frost action in the aggregate for the sake of completeness and to show the similarities as well as the differences in the freezing mechanisms that exist between these two prime components of concrete.

There are two ways in which the aggregate in concrete may be deleterious. The first is when a porous aggregate has low permeability. In this case the aggregate has a very large capacity for storing water, but, if it is exposed to freezing, the small size of the pores will offer a high resistance to the migrating water that is pushed by the expanding ice. Depending on the size of aggregate particles and the length of migratory path, the pressure can reach a magnitude large enough to crack the aggregate or at least abnormally expand it. To minimize the deleterious effect of this kind of aggregate, the smallest possible top size should be used. The second kind of frost-susceptible aggregates are those with both high porosity and permeability. Although in this case the aggregate itself is immune to frost action, the high volume of water that is expelled during freezing will damage the surrounding bonded paste. The use of this kind of aggregate in a concrete exposed to freezing environment should be avoided (55).

3.3 CEMENT PASTE

For a better understanding of frost action in cement paste matrix, it is necessary to define the internal microstructure of the cement paste.

During the hydration process cement particles are replaced by granular substances called cement gel. Such particles are of colloidal nature and have a characteristic porosity of approximately 25 to 30 percent (56,57). This can be compared to typical rock which has approximately a 1 percent

capacity (by volume) for storing water. The space occupied by hydrated cement gel is more than twice that of the cement consumed in producing it. Portland cement concrete does not have a net expansion in volume after hardening. Consequently, the gel particles not only replace the original cement but also fill some of the original water-filled space. The degree to which the originally water-filled space becomes filled with gel products depends on two factors. First is the amount of cement that becomes hydrated, and the second is the volume of water-filled spaces originally present in the paste matrix. In other words, the water-cement ratio of the concrete is the single major factor in the paste's physical characteristics.

For all the cement (Type I) in a mass of concrete to become hydrated, a water-cement ratio of 1.2 by volume (0.38 by weight) is required. In a concrete with a water-cement ratio less than 0.38 some of the cement particles remain unhydrated and the water-cement ratio more than the above value causes some excess water to remain in the paste structure. This residual water forms an interconnected network of channels throughout the gel called capillary pores. Gel pores are the smallest space in the structure and range in size between 15 to 40 Å as compared to the gel particles, which if expressed as a sphere, have a diameter of about 140Å(3). Capillary cavities are estimated to average approximately 5000Å in diameter (53). In the process of saturation, the smaller pores in the paste fill with water before larger cavities. Water is held in the cement paste matrix by three distinct mechanisms. In the first mechanism, water is chemically bonded to the hydrated products. In the second, water is held by the gel's surface traction, and in the third, water is held in bulk under capillary action in the pores. The water held by chemical bond has been classified as non-evaporable, compared to the rest which is evaporable. The total amount of evaporable and non- evaporable water in a concrete specimen depends on both age and curing condition. As the length of curing period increases, the amount of hydrated product increases with a corresponding decrease in space causes a decrease in evaporable water (3).

The freezing mechanism in the cement paste has been the subject of numerous research for several decades. Over the years several different hypotheses have emerged. The reason for this lies in the complexity of hardened cement's internal structure. Regardless of all the different theories,

there are two facts that are generally accepted. First, when damage occurs, whether due to excess stress in the paste or the aggregate, it causes dilation of the component directly affected by freezing. Second, a system of uniformly scattered air bubbles throughout the cement matrix is the best remedy known to make the mortar phase of the concrete resistant to frost damage.

The oldest hypothesis is the hydraulic pressure theory developed by Powers during the middle 1940s. Although several other researchers and, in one case, Powers himself (58), dismissed this theory for the mortar phase, most of the literature and texts today refer to this theory more than the others. In the following section, the hydraulic pressure theory and other theoretical hypotheses are presented.

3.3.1 Hydraulic Pressure Theory (59)

In a saturated paste, the capillary pores and the gel pores are filled with water. As a result of decreasing the temperature below the freezing point of water, ice crystals appear first in the largest cavities. When the water changes to ice, its volume increases by 9 percent, exceeding the capacity of the cavity. During this time, the cavity must dilate to accommodate the increase in the volume or the excess water must be expelled from it. Movement of this expelled water in the paste toward the escape boundary causes pressure which is proportional to the following factors:

1. The coefficient of permeability of the materials through which the water is forced.

2. The distance from the escape boundary.

3. The rate of freezing which determines the speed of the water movement.

If a point in the paste is sufficiently remote from an escape boundary, the pressure may be high enough to stress the surrounding gel beyond its elastic limit or strength and produce permanent damage. Air-bubbles produced by an air entraining agent in the cement paste matrix serve as the escape boundary for the gels. An abundance of such bubbles shortens the distance for the moving water. The mathematical explanation is as follows (60):

If it is assumed that the air bubbles are dispersed in a unit volume of the paste at equal distance from each other, each bubble is actually responsible to collect water from a sphere around it. This sphere is called the sphere of influence and it is bound by the mid-point between two adjacent air bubbles (Figure 3.1). If each bubble is located at the center of a spherical element where r' is the radius and $\Delta r'$ the thickness, the volume of the gel within this spherical element is:

$$V = 4\pi(r')^2\Delta r' \tag{1}$$

$$\Delta V = (1.09 - \frac{1}{S})\Delta W_f A\pi r'^2\Delta r' \tag{2}$$

where

$\Delta V =$ Amount of water expelled from the gel by freezing

$\Delta W_f =$ Amount of water frozen gr/c^3 of paste

$S =$ Coefficient of saturation

The coefficient of saturation is the ratio of the capillary water present to the capillary porosity. The Amount of water frozen in the capillary is a function of temperature:

$$\frac{dV}{d\theta} = (1.09 - \frac{1}{S})\frac{dW_f}{d\theta} 4\pi(r')^2\Delta r' \tag{3}$$

where

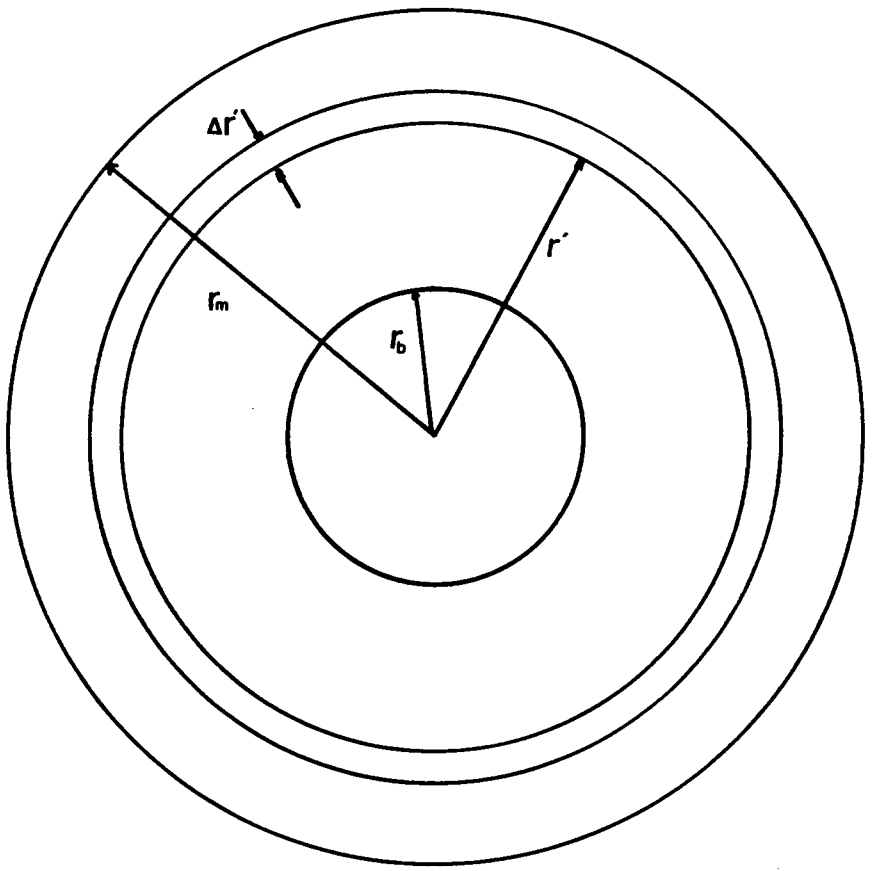

Figure 3.1. Cross Section of an Air Bubble

θ = Temperature $x-1$ °C

The rate of the water expelled from the element will be:

$$\frac{dV}{dt} = (1.09 - \frac{1}{S}) \frac{d\theta}{dt} \frac{dW_f}{d\theta} 4\pi(r')^2 dr' \tag{4}$$

where

$\frac{d\theta}{dt}$ = Rate of cooling

The total volume of water expelled is:

$$\frac{dV}{dt} = (1.09 - \frac{1}{S}) \frac{d\theta}{dt} \frac{dW_f}{d\theta} 4\pi \int_r^{r_m} (r')^2 dr' \qquad r_b \le r \le r_m \tag{5}$$

The area through which the flow takes place is:

$$a = 4\pi r^2 \tag{6}$$

Integrating equation 5 and dividing it by the area we get:

$$\frac{dV}{dt} \frac{1}{a} = C(\frac{r_m^3}{r^2} - r) \tag{7}$$

where C is defined as:

$$C = \frac{1}{3} (1.09 - \frac{1}{S}) \frac{d\theta}{dt} \frac{dW_f}{d\theta} \tag{8}$$

According to Darcy's Law

$$\frac{dP}{dr} = \frac{\eta}{K}\frac{dV}{dt}\frac{1}{a} \tag{9}$$

where

P = Hydraulic pressure dyne/sq cm

K = Coefficient of permeability

η = Coefficient of viscosity of the water

Combining 9 and 5

$$\frac{dP}{dr} = \frac{\eta}{K} C \left[\frac{r_m^3}{r^2} - r\right] \tag{10}$$

Integrating this over the paste thickness from r_b to r we obtain:

$$P = \frac{\eta}{K} C \int_{r_b}^{r} \left[\frac{r_m^3}{r^2} - r\right] dr = \frac{\eta}{K} C \left[\frac{r_m^3}{r_b} + \frac{r_b^2}{2} - \frac{r_m^3}{r} - \frac{r^2}{2}\right] \tag{11}$$

The maximum pressure will be at the outer boundary of the sphere of influence, or at $r = r_m$ Then:

$$P_{\max} = \frac{\eta}{K} C \left[\frac{r_m^3}{r_b} + \frac{r_b^2}{2} - r_m^2 - \frac{r_m^2}{2}\right] \tag{12}$$

If L is the thickness of the paste within the sphere of influence or $L = r_m - r_b$

$$P_{\max} = \frac{\eta}{K} C\phi(L) \tag{13}$$

where

$$\phi(L) = \frac{L^3}{r_b} + \frac{3L^2}{2} \tag{14}$$

In the case of saturated paste:

$S = 1$

Then

$$C = 0.03 \frac{d\theta}{dt} \frac{dW_f}{d\theta}$$

and

$$P_{max} = \frac{0.03\eta}{K} \frac{d\theta}{dt} \frac{dW_f}{d\theta} \phi(L)$$

If

$R = \frac{d\theta}{dt}$ (freezing rate)

$u = \frac{dW_f}{d\theta}$ (Water expelled per degree decrease temperature)

Then:

$$P_{max} = \frac{\eta}{3}(1.09 - \frac{1}{S}) \frac{uR}{K} \phi(L)$$

and for saturated paste:

$$P_{max} = 0.03\eta \frac{UR}{K} \phi(L) \qquad (15)$$

Where U = the value of u when the paste is saturated, i.e., when S = 1.0

If the maximum pressure is divided by tensile strength of the paste:

$$\frac{P_{max}}{T} = 0.03\eta \frac{R}{Z} \phi(L) \tag{16}$$

where

$$Z = \frac{KT}{U}$$

Then $\phi(L)_{max}$ as an expression for maximum bubble spacing is:

$$\phi(L)_{max} = \frac{1}{0.03\eta} \frac{Z}{R} \tag{17}$$

Substituting

$\eta = 0.019$ Poise for water at $-2°C$ (Coefficient of viscosity)

then:

$$\phi(L)_{max} = 1775 \frac{Z}{R} \tag{18}$$

R is the cooling rate and Z has to be determined experimentally for each specimen. The derivation is valid for the bubble system in which each bubble is equal in size and dispersed uniformly in the matrix. These two assumptions are far from reality.

3.3.2 Arguments For Theories Alternate to Hydraulic Pressure

According to Helmuth (61), the expansion-producing mechanism in a moist-cured hardened paste, regardless of being air-entrained or not, is not due to the development of pressure by the 9

percent expansion of freezing water. His arguments against the hydraulic pressure theory are as follows:

1. The continuous process of hydration in the concrete is at the expense of water in the capillaries. This would cause self desiccation or lack of saturation in the paste.

2. The capillary water of saturated paste flows into the gel pores when the temperature falls from $25°C$ to about $4°C$. This is due to higher free energy of capillary water as compared to gel water. During this process the gel pores become super-saturated but capillary spaces become partly empty. By further cooling to below $0°C$, the freezing water should have enough space to expand without inducing any internal pressure.

Helmuth explains that the expansion mechanism is a result of the growth of ice dendrites in the capillaries (62). He believes that the freezing of water in the cement paste can only be initiated through an external seeding. After the seeding, the ice front will propagate as a continuous phase through the interconnected pores of the paste. The different sizes and the texture of the capillary channels offer restriction to the propagation process unless the temperatures get cold enough for the ice dendrites to penetrate the openings (63). Helmuth experimentally showed that the large expansion began when it was cold enough for ice crystals to penetrate into water-filled capillaries, rather than by filling up partly empty capillary space.

Litvan (64) measured the amount of water that was expelled during the cooling of two thinly sliced cement paste samples. The total water expelled was greater than 3 to 4 times the specific volume increase of freezing water. Another researcher (65) actually dried a sample of cement paste and resaturated it with benzene. Specific volumes of benzene, unlike the water, decrease on freezing. When this specimen was exposed to freezing, expansion rather than contraction was observed at the freezing point of the absorbed liquid.

3.3.3 Diffusion Theory

In a saturated paste the water in the gel and capillaries is in a state of thermodynamic equilibrium. Reducing the temperature from 25°*C* to about 4°*C* causes the water in the capillary to diffuse toward the gel (66). A further decrease in temperature causes the water in larger capillaries to freeze. Bulk water in the gel and ice in the capillaries can be in thermodynamic equilibrium only if either the gel water is under pressure or the ice is under tension. Without such pressure, the gel water has a free energy much higher than that of the ice in the capillary. As a consequence, the gel water acquires an energy potential enabling it to move into the cavity and cause the ice crystal to grow and enlarge the cavity.

In a sufficiently air-entrained concrete, volume of the air bubbles are much more than the capillaries and it is practically impossible for the water to fill these voids. When exposed to freezing, the ice in the air bubbles cannot fill the space and no pressure will be created. The ice in the air bubbles is in the state of least energy (Gibbs free energy), compared to super cooled water in the gels and capillaries which are under pressure. Consequently, excess water in the capillaries and the gels flow into the bubbles relieving the destructive hydraulic pressure. This process actually takes place in the following manner: At the beginning of the freezing period, the free energy of gel water is much higher than the two bodies of ice in the capillary and the air bubbles. The gel water diffuses toward both the air bubble and the capillaries. Capillaries having a smaller volume than air bubbles fill first, and the excessive water causes the ice in the capillary to pressurize causing its free energy to increase. From this point on the water from both capillaries and gels diffuses toward the air bubbles (59).

3.3.4 Osmotic Pressure Theory

When solutions containing different concentrations of soluble materials are separated by a semi-permeable membrane, the differential head created at two sides of the barrier causes the solvent particles to move through the membrane toward the solution of greater concentration. The water present in the capillaries and the gels of cement paste normally contain a concentration of salts and alkalis. As water freezes in the large capillaries, the ions of these solutes move in front of the freezing water, increasing the concentration of the unfrozen pocket of water in the capillaries. The high concentration gradient between the solution in capillary and the surrounding gels causes a diffusion of the gel water toward the freezing site, causing excess ice and subsequent pressure and dilation (53,59).

3.3.5 Litvan's Hypothesis

Water absorbed in the pores of cement paste does not freeze since it is under surface traction forces. For ice crystals to form, the water molecules should be mobile enough to arrange themselves in the proper order required for ice crystal lattices (67). The surface forces imposed on water molecules restrict them from such mobility. When a saturated sample of hardened cement paste is cooled, for example from 0 to $-2°C$, supercooled water in the gels and ice in the large capillaries will be present simultaneously. Higher vapor pressure in the surrounding gels causes some of the water to flow into the capillary and subsequently freeze. If the temperature is kept constant at $-2°C$, the remaining liquid water in the gel and the ice in the capillary equilibrize themselves through the decrease in the radius of meniscus curvature of the gel water (68). Since the difference in the vapor pressure of ice and supercooled water increases with decreasing temperature, any further cooling will upset the equilibrium and cause further desorption of the gel pores toward the freezing sites.

This mechanism can damage the concrete in several ways. If the cooling rate is high in a sample with a very low permeability and porosity, the rate of water expulsion is much higher than an orderly migration and causes a rapid expansion (69). Freezing normally initiates in the largest pores; if there is a flaw in the paste matrix, it acts as a freezing site and attracts all the water from surrounding paste. Growth of this ice would propagate the flaw. During water expulsion, if the passage ways are blocked by ice crystals, the internal pressure can cause fracture and subsequent destruction of the cement paste matrix.

Theoretically damage can be avoided (67) if:

1. The amount of water that has to be expelled is small. That is, the porosity or degree of saturation or both are low.

2. The freezing rate is so low that expelled water can move with minimum resistance from the channel's boundary.

3. The permeability is high enough to facilitate a smooth and orderly migration.

4. The migratory path to the escape boundary is short. This can be achieved with low spacing factor.

Chapter IV

LINEAR TRAVERSE (ROSIWAL) METHOD

4.1 INTRODUCTION

The systematic study of the relationship between resistance of concrete to freezing and thawing and characteristics of the internal void system such as void size, concentration, and uniformity is only feasible by investigation of concrete in hardened state.

4.2 THEORETICAL DEVELOPMENT

Late in the nineteenth century Rosiwal (70) showed that the volume of a constituent in a solid as the percentage of the overall volume of the solid can be obtained as follows:

First, a random plane should be cut through the solid, and the surface should be thoroughly polished. Second the surface is microscopically traversed along straight and preferably parallel lines uniformly placed throughout the plane. Lengths of segments or chords intercepted are summed

separately for each constituent. The proportion for any constituent is simply calculated by dividing the cumulative summation for that constituent by the summation of all constituents. For example if a solid consists of A,B,C,....etc. A as a percentage of total solid i.e:

$$\%A = \frac{(Ax100)}{(A+B+C+...)}$$

The initial purpose of the method was to determine the mineral composition of natural rock, but later was introduced by Brown and Pierson (70) for measurement of air content in hardened concrete. In the process of traversing the surface, the bubble sections intersected by the traverse line are counted and the individual length of chords intersected are measured and recorded. As per to-day, the parameters recommended by ASTM C457 (8) as index for evaluation of air void characteristics in hardened concrete are:

1. Air Content (A) - A percent ratio of total volume of air to the volume of concrete

2. Specific Surface (α) - The ratio of total surface area to the total volume of air bubbles in hardened concrete, expressed as square inch per cubic inch.

3. Average chord intercept (l) - The arithmetic mean of the intercepted chords expressed in inch.

4. Spacing factor (L) - An index related to maximum distance of any point in the hardened cement paste to the nearest periphery of an air bubble expressed in inch.

All the above quantities are function of the true diameters of air bubbles. However the measured chords in linear traverse procedure are not the same as true bubble diameter and the bubbles in hardened concrete cover a wide range of size and geometric shapes. The above parameters were originally calculated by Powers (60) but later were modified by Willies (60) who con-

sidered some statistical variation . Since the above parameters are widely used today, their theoretical derivations as were done by Powers and Willies are given as follows:

All the air voids are assumed to have spherical shape and dispersed randomly throughout a unit volume of concrete . If in a unit volume of concrete, M is the total number of bubbles and F(u)du a function representing quantity-proportion of different sizes, having diameters in the range of u to u + du, then: MF(u)du = Actual number of bubbles within the size range of u and u + du.

and

$$\int_0^u F(u)du = 1 \qquad u < r < u + du \tag{1}$$

If a unit cube with a single air bubble ($d = u_1$) is penetrated by an arbitrary line, the probability of intersecting the bubble is equal to the ratio of maximum air bubble cross section area to the face area of the cube, or

$$\frac{(\frac{\pi u_1^2}{4})}{1}$$

If there are n_1 bubbles of diameter u_1, the above probability is:

$$\frac{n_1(\pi u_1^{\,2})}{4} \tag{2}$$

If u_1 is within the domain of function F(u)du, then:

$$n_1 = MF(u)du$$

Substituting this into equation (2) we get the number of bubbles within the boundary domain of the function which have been intersected by the line:

$$\frac{\pi}{4} u^2 MF(u)du \tag{3}$$

Extending the above reasoning for all the bubbles of different size such as u_1, u_2, u_3, ... etc:

Probability of intersection by an arbitrary line is:

$$\frac{\pi}{4}(n_1u_1^2 + n_2u_2^2 + \cdots + n_uu_u^2) = \frac{\pi}{4} M[u]_2$$

where

$$[u]_2 = \frac{n_1u_1^2 + n_2u_2^2 + \cdots + n_uu_u^2}{M}$$

and $[u]_2$ is the second moment of u.

From all the bubbles penetrated by a line, let f(u)du be the proportion which have diameters of u to u + du. Then the actual number of this size penetrated by the line is:

$$\frac{\pi}{4} M\ [u]_2\ f(u)du$$

This is in effect equivalent to equation (3):

$$\frac{\pi}{4}\ M[u]_2\ f(u)du$$

$$f(u)du = \frac{u^2}{[u]_2} F(u)du \tag{4}$$

The above equation shows the relationship between the bubbles in the concrete and those penetrated by a line.

Figure 4.1 shows a hypothetical air bubble that has been penetrated by an arbitrary traverse line. If the line passes a distance y from the center of the bubble, the probability that a sphere of diameter u to u + du has its center at a distance y to y + dy from a randomly penetrated line is:

$$\frac{dA}{A} \quad \text{and} \quad dA = 2\pi y dy, \quad A = \frac{\pi u^2}{4}$$

$$\frac{dA}{A} = \frac{(8\pi y dy)}{u^2} = \frac{(8y dy)}{u^2}$$

Intercepted chord length at a distance y to y + dy from the bubble will have a length of l + dl:

$$y = \frac{\sqrt{u^2 - l^2}}{2}$$

and

$$dy = \frac{l dl}{2\sqrt{u^2 - l^2}}$$

$$\frac{dA}{A} = \frac{2l dl}{u^2}$$

f(u)du = Proportion of all the bubbles with diameter u < d < u + du penetrated by the line.

$(\frac{2l}{u^2})dl =$ Probability proportion of intercepted chords being l to $l + dl$ long.

Then the proportion of chords with length l to $l + dl$ resulting from intersection with bubbles having diameters u to u + du is:

$$(\frac{2l dl}{u^2}) f(u) du$$

From equation (4):

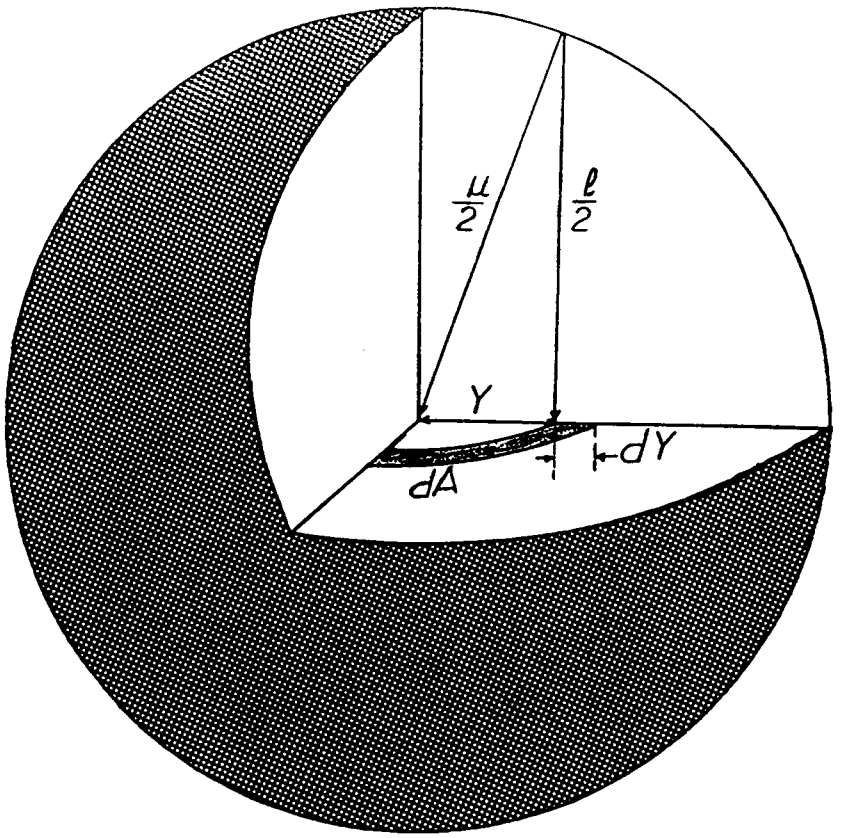

Figure 4.1. An Air Bubble Penetrated By a Traverse Line

$$\left(\frac{2ldl}{u^2}\right)\left(\frac{u^2}{[u]_2}\right) f(u)du = \left(\frac{2ldl}{[u]_2}\right) F(u)du \quad l < u$$

Since there are a distribution of bubble sizes, l may have value up to U, the diameter of largest bubble in the system. The proportion or probability of a chord with the length of l to $l + dl$ penetrating all bubble size is $\phi(l)dl$ where:

$$\phi(l)dl = \left(\frac{2ldl}{[u]_2}\right) \int_l^U F(u)du$$

and

$$\phi(l) = \left(\frac{2l}{[u]_2}\right) \int_l^U F(u)du \tag{5}$$

The above equation is the relative frequency function of the distribution of measured chord intercepts.

$[l]_i = i^{th}$ moment of chord intercepts

$$[l]_i = \frac{n_1 l_1^i}{M} + \frac{n_2 l_2^i}{M} + \cdots + \frac{n_j l_j^i}{M}$$

$\frac{n_j}{M}$ = Proportional number of one size to the total number andin the case ofl_i:

$$\frac{n_j}{M} = \phi(l_j)dl$$

Therefore

$$[I]_i = \phi(l_1)\, l_1^i dl + \phi(l_2)\, l_2^i dl + \cdots + \phi(l_j)\, l_j^i dl = \int_0^U l^i\, \phi(l) dl$$

From equation (5)

$$[I]_i = \frac{2}{[u]_2} \int_0^U l^i\, ldl \int_l^U F(u) du = \frac{2}{[u]_2} \int_0^U l^{(i+1)}\, dl \int_l^U F(u) du$$

Changing the order of integration:

$$[I]_i = \frac{2}{[u]_2} \int_0^U F(u) du \int_0^U l^{i+1} dl$$

Integration of the second part yields

$$[I]_i = \frac{2}{(i+2)[u]_2} \int_0^U u^{(i+2)}\, F(u) du \qquad (6)$$

Using similar approach

$$[u]_i = \int_0^U u^i F(u) du$$

and

$$[u]_{i+2} = \int_0^U u^{(i+2)}\, F(u) du$$

Substituting in equation (6)

$$[l]_i = \frac{2[u]_{(i+2)}}{(i+2)[u]_2} \tag{7}$$

If r = radius of bubble

$[u]_1 = 2[r]_1$

$[u]_2 = 4[r]_2$

$[u]_3 = 8[r]_3$

$$[l]_1 = \frac{2[u]_3}{3[u]_2} = \frac{16[r]_3}{12[r]_2} = \frac{4[r]_3}{3[r]_2} \tag{8}$$

In a system of air bubbles with radius of $r_1, r_2, r_3, \ldots$ etc., the second moment $[r]_2$ is multiplied by 4π and the total number of bubbles M gives the total surface area of all the bubbles, i.e:

$S_T = 4\pi M[r]_2$

and the third moment $[r]_3$ multiplied by $\frac{4\pi}{3}$ and total number of bubbles in the system M gives the total volume of all the bubbles (Air content A) in a unit volume of concrete.

$A = V_T = \frac{4\pi}{3} M[r]_3$

from equation (3):

$n = \frac{\pi M[u]_2}{4} = \pi M[r]_2$

where n is the total number of bubbles intersected by traversing line.

$$\frac{A}{n} = \frac{4[r]_3}{3[r]_2} \tag{9}$$

This is equivalent to equation (8) or arithmetic mean of intercepted chords:

$$\bar{l} = \frac{A}{n} \quad \text{and} \quad A = n\bar{l} \tag{10}$$

Specific surface or total surface area per unit volume of air voids in hardened concrete is calculated from:

$$\alpha = \frac{S_T}{V_T} = \frac{3[r]_2}{[r]_3}$$

and considering equations (8) & (9) we get:

$$\alpha = \frac{4}{\bar{l}} \tag{11}$$

In a hypothetical system where all of the air bubbles have equal size and they are uniformly dispersed throughout the hardened paste and, further, if it is assumed that all the bubbles have a specific surface as calculated in equation. In this system the radius of the hypothetical air bubbles $r_h$are:

$$r_h = \frac{3}{\alpha} = \frac{3l}{4}$$

Each bubble can be assumed to be located at the center of a cube and sum of all the volumes of these small cubes is equal to the total volume of the paste an the air voids. Volume of one cube is:

$$V = \frac{P + A}{N}$$

where :

P = The paste content in percent (by volume).

A = The air content in percent (by volume).

N = The number of voids of radius r_h equivalent to the actual air content (A) in the concrete. N is not the actual number of bubbles.

The edge of each small cube enclosing an air bubble is:

$$(\frac{P + A}{N})^{\frac{1}{3}}$$

The spheres circumscribing each cube are called the spheres of influence. Radius of each sphere is denoted by r_m and it is equal to:

$$r_m = \frac{\sqrt{3}}{2}(\frac{P + A}{N})^{\frac{1}{3}}$$

The thickness of paste between each air bubble and the periphery of each sphere or the length of migratory path for the water to the nearest air bubble is called spacing factor and it is :

$$\bar{L} = r_m - r_h$$

Therefore

$$\bar{L} = \frac{\sqrt{3}}{2}(\frac{P + A}{N})^{\frac{1}{3}} - r_h$$

and

$$N = \frac{\alpha^3 A}{36\pi}$$

then

$$\bar{L} = \frac{3}{\alpha}[1.4(\frac{P}{A}+1)^{\frac{1}{3}} - 1] \qquad (12)$$

When P/A is equal to 4.33 the computed spacing factor from both $\frac{P}{4n}$ and the above equation is the same. But when P/A > 4.33, the equation results in a smaller spacing factor and vice versa. According to Powers (60) the spacing factor obtained from either equation exceeds the actual spacing factor.

4.3 PHILLEO'S FACTOR.

Philleo (71) suggests that the spacing factor as calculated by equation 12 is derived from the total air content and it is only applicable to the concrete with similar distribution in air void size. He introduced another parameter believed to be more realistic called Philleo's factor. Philleo's factor has been defined in the American Concrete Institute, Cement and Concrete Terminology (72) as " a distance used as an index of the extent to which hardened cement paste is protected from the effect of freezing, so selected that only a small portion of the cement paste (usually 10%) lies farther than that distance from the perimeter of the nearest air void ". The factor is calculated based on the number of bubbles per unit volume of paste.

$$S = \frac{0.62}{N^{\frac{1}{3}}}[(\ln\frac{1}{1-A} + 2.303)^{\frac{1}{3}} - (\ln\frac{1}{1-A})^{\frac{1}{3}}] \qquad (13)$$

where

S = Philleo's factor

A = Air content of the paste

N = The number of air bubbles in a unit volume of the paste

Air content of the paste (A), and the number of the voids in a unit volume of the paste (N) can be calculated from the material's mixture proportion data and the linear traverse measurements.

$$A = \frac{AIRCONTENT}{PASTECONTENT \times (1 - AIRCONTENT) + (AIRCONTENT)}$$

and

$$N = \frac{\text{The number of voids per unit volume of concrete}(N')}{PASTECONTENT(1 - AIRCONTENT) + (AIRCONTENT)}$$

Willis (73) has shown that if the length of chords measured in a linear traverse is classified and discretesized into size group, the chord lengths included in the smallest group is sufficient to determine the number of voids per unit volume of concrete. The relation is as follows:

$$N' = \frac{2N_c}{\pi i \Delta l}$$

where

N' = The number of air voids per unit volume of concrete

N_c = The number of voids in the smallest size group per total traverse length

l = The width of size group

Δl = The median of smallest size group

In an experimental study Larson et al (74) compared the correlation between concrete's actual performance in freeze-thaw environment to the several different parameters calculated based on linear traverse measurements. They reported that Philleo's factor is superior to the other parameters in predicting the frost resistance of concrete.

Chapter V

EXPERIMENTAL DESIGN

5.1 SCOPE

A total of 54 specimens 3x4x16 in. from 27 batches of high strength silica fume concrete, with various levels of water-cementitious ratio and different amounts of air content, were tested for evaluation of their freeze-thaw durability. All the specimens were placed, after curing, in stainless steel containers in the freeze-thaw machine. The freeze-thaw apparatus was manufactured by Logan, in Utah, and functionally conforms to specification designated by ASTM C 666-84, procedure A " standard test method for resistance of concrete to rapid freezing and thawing " (8). A complete cycle in this machine should consist of cooling from 40 to 0°*F* and warming back to 40°*F* in approximately 4 hours and 45 minutes. Freezing proceeds from bottom of the sample toward the top and temperature decreases at the rate of 11°*F* per hour. A schematic of the apparatus is shown in the Figure 5.1 (75). The actual performance of the freeze-thaw apparatus was monitored in the laboratory and its detailed description is given in Appendix B. The specimens were measured for weight and dynamic modulus before beginning the test, and every 20 to 30 cycles thereafter. A brief description of the dynamic modulus and the apparatus for its measurement is

presented in Appendix C. Out of 27 batches, specimens from 19 were cured for 28 days and the samples from the remaining eight batches were cured for just 14 days prior to freeze-thaw testing. This was done in order to determine the effect of concrete's maturity on its freeze-thaw durability.

From each batch of concrete, three beams (3x4x16 in.), and eight cylinders (3x6 in.) were made. Two beams from each batch were used for freeze-thaw testing and the third one was used for air void measurement. Two slabs from each beam, one 4x6x1 in., and the other 3x4x1 in., were cut. One of the slabs (4x6x1 in.) was polished and the air-void parameters were measured microscopically in accordance with the ASTM C457-82, Rosiwal linear traverse (8). The second cut sections (3x4x1 in.) from each beam were placed in an oven operating at 240 °F after weighing in a surface dry condition. The specimens were dried for 24 days during which the specimens were taken out of the oven and weighed, after they were cooled down to room temperature in a desiccator. Accuracy of the scale was within $\pm$ 0.1 grams. This was done in order to find any possible correlation between the amount of water loss and other parameters of concrete such as water-cement ratio or air content.

5.2 MATERIALS

5.2.1 Coarse Aggregate

The coarse aggregate used was crushed limestone from Ridgen Valley quarry in Blacksburg, Virginia. This material has been used as the stock aggregate in the Virginia Tech laboratory for the past 28 years. Throughout these years the characteristics including its freeze-thaw durability, which is 100%, remained unchanged (76). The gradation of the material conforms to no. 57 as designated by ASTM C33-86 (8). The results of the sieve analysis are presented in Appendix A, Table A-1. The other parameters of the coarse aggregate are also presented in Appendix A, Table A-2.

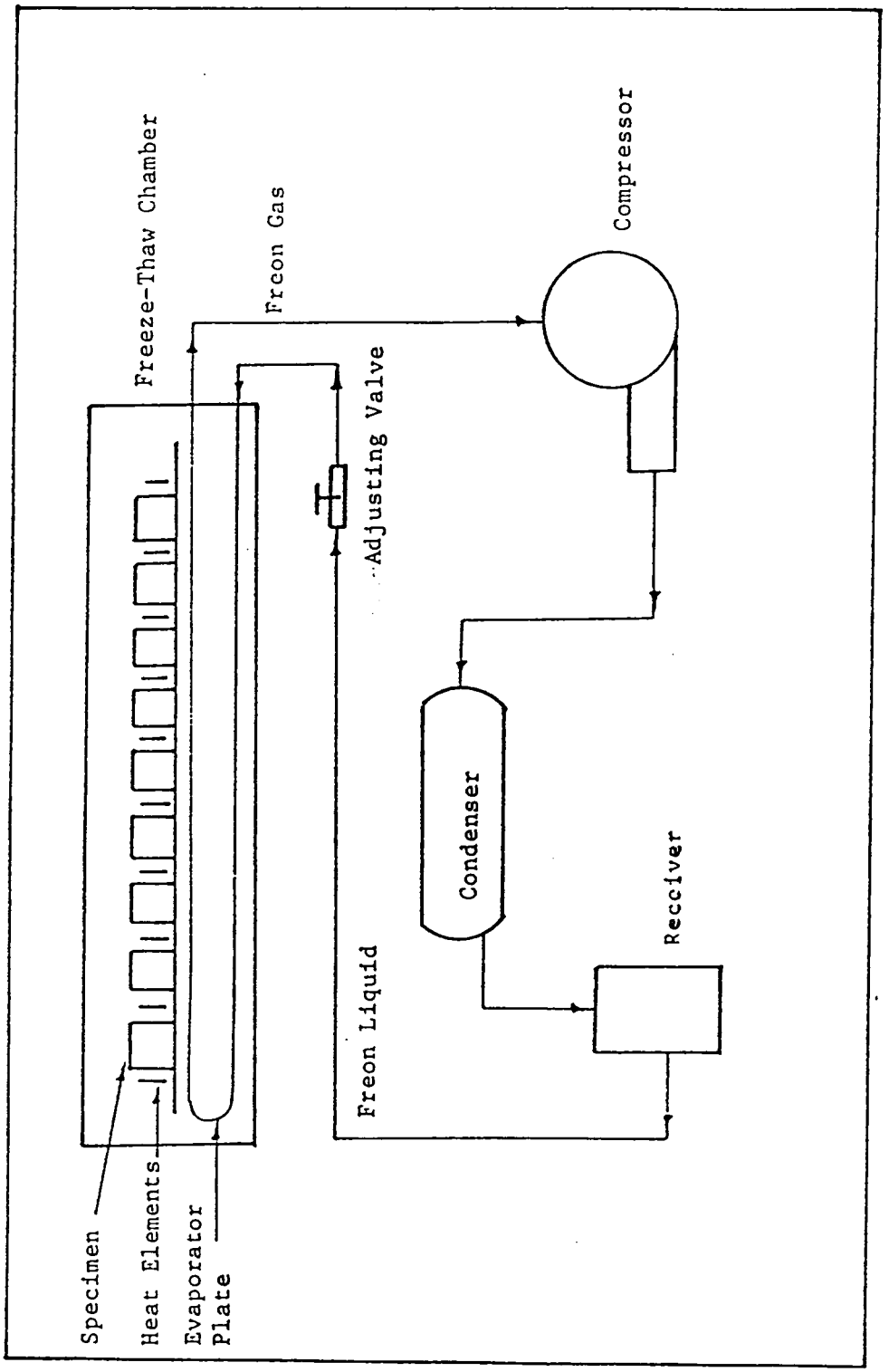

Figure 5.1. A Schematic of Logan Freeze-Thaw Apparatus

5.2.2 Fine Aggregate

Fine aggregate used throughout this investigation was natural brown sand. It primarily contained mica, quartz, and sandstone. Its gradation and other physical characteristics are given in Appendix A., Tables A-1 and A-2.

5.2.3 Cement

Type one Portland cement manufactured by LONESTAR was used throughout the study. Its specific gravity was assumed to be 3.15.

5.2.4 Silica Fume

Silica fume was supplied by Elkem Chemical, Pittsburgh, Pennsylvania. It was in powder form marketed under brand name FT 100 and according to manufacturer it contains 93% silica dioxide and 7% an unknown plasticizer. The physical parameters are given in Appendix A, Table A-2.

5.2.5 Chemical Admixtures

Air-Entraining admixture and high range water reducer were supplied by Master Builder. They are marketed under brand names, MICRO AIR, and REHOBUILD.

5.3 Mixing Procedure

Mixture design quantities are given in Appendix A, Table A-3. The procedure for mixing and making specimens was in accordance with the specifications given by ASTM C192-81 (8). A counter flow pan mixer with a capacity of 2 ft^3 was used for mixing the concrete. Prior to the mixing of each batch, a small quantity (0.005 yd^3) of concrete with a components ratio similar to the actual batch was mixed in the pan and it was subsequently discharged. The mortar adhering to the mixer pan and blades after discharge of this concrete prevents the loss of mortar from the actual batch. This process according to ASTM C 192-81 (8), is called buttering. The actual volume of each testing batch was 0.04 yd^3. The mixing procedure was as follows.

Coarse and fine aggregates were placed in the pan along with one-third of the mixing water. The mixer was allowed to rotate for approximately one minute. Cement and silica fume were added and, whenever applicable, the chemical admixtures were mixed with the remaining water and it was added to the mixture in the pan. The machine was operated for three minutes, followed by three minutes of rest and two additional minutes of mixing. Prior to making the specimens, the temperature, slump, unit weight and air-content were measured. Table A-4 in Appendix A present the data pertaining to plastic characteristics of the concretes. In a few cases where the slump was not satisfactory, some additional superplasticizers were added, and the concrete was allowed to mix an additional two minutes. In general, the target slump was 3 ± 1 in.

In the process of mixing the concrete, it proved to be impossible to get 6% air content. Using many trial batches, the amount of air entraining agent was increased several times. But due to the lack of workability, air content as measured by pressure meter, did not increase to more than 4 percent (Figure 5.2). This is consistent with the results Whiting (77) obtained from air entraining a low slump dense concrete. He reported that air content in low slump dense concrete is not sensitive to change in air entraining agent dosage, but it is very sensitive to the changes in workability. To obtain 6% air in the concrete mixtures, high range water reducers had to be used.

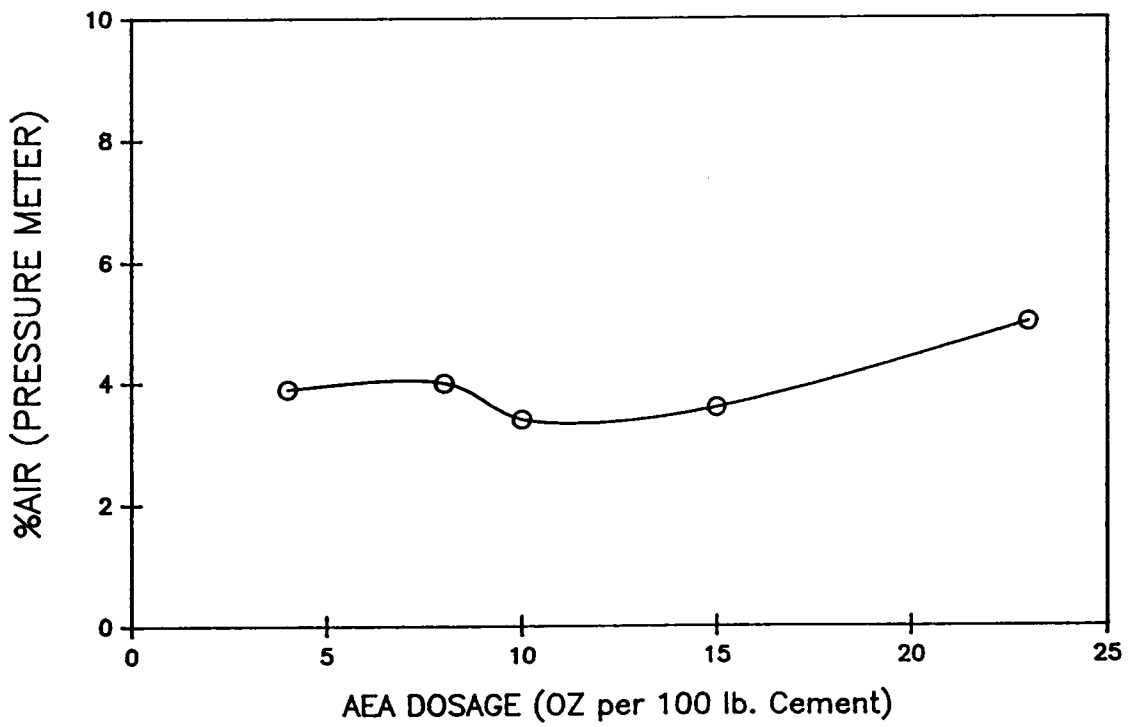

Figure 5.2. Effectiveness of Air Entraining Agent

Plastic molds were used for the cylinders and steel forms were used to make the beams. The concrete in the cylinders was placed in three layers and each layer was rodded 25 times, and the concrete in the beams was placed in two layers and each layer was rodded 48 times. The steel forms for the beams were tapped with rubber mallet in order to minimize entrapped air voids and honey combs. All the specimens were taken out of the molds after 24 hours and after marking, they were transferred to a moist room. The beams were placed in a bath of saturated lime water for the entire curing period.

5.4 Testing Procedure

Experimental testing was done in three phases. In the first phase, twenty-two specimens from eleven batches of concrete, with a W/(C+SF) ratio of 0.32, were cured for 28 days and subsequently tested for freeze-thaw durability. The prime objective of this phase was to assess the consistency in strength and freeze-thaw durability among similar mixes. In the second and the third phase of the experiment, specimens from batches with W/(C+SF) of 0.32, 0.30, 0.28, and 0.25 were subjected to freezing and thawing. In all three phases of the study, the concrete specimens were exposed to 300 cycles of freezing and thawing, except for the ones that failed and had to be removed earlier. The only difference between phase two and three was that the specimens tested in phase two were cured for 28 days while the ones tested in the third phase were cured just for 14 days.

In addition to the above, one beam from each batch was cut with a masonry saw after approximately one month of moist curing. A slab 4x6 in. from each beam was polished using a vibrating lapping machine. The portion used for microscopic examination is shown in Figure 5.3. Each specimen was traversed for 95 inches using a computer controlled Linear Traverse apparatus.

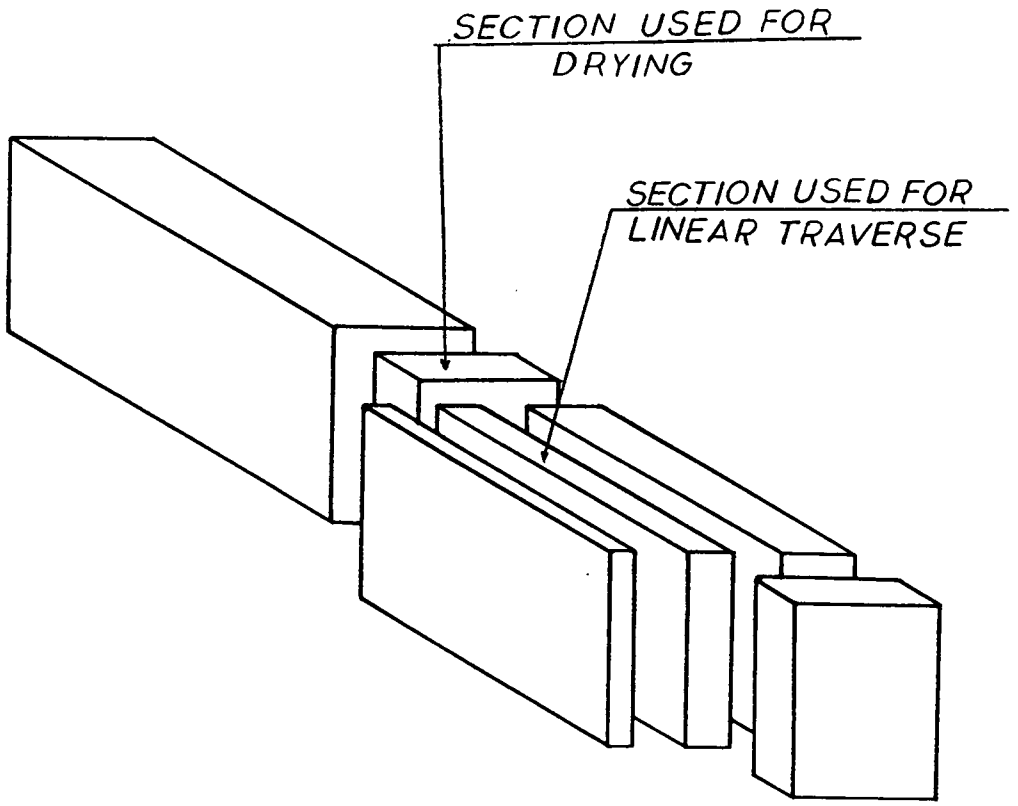

Figure 5.3. Concrete Section Used for Air Void Analysis and Drying

All the individual chords intercepted by the microscope were measured digitally and stored by the computer. Air void parameters were subsequently calculated using a spread sheet on a personal computer. Picture of Linear Traverse apparatus is presented in Appendix D, Figure D-1.

Chapter VI

RESULTS AND DISCUSSION

Throughout the course of this study, the following topics were subjects of the investigation:

1. Freeze-thaw durability of air-entrained and non air entrained high strength concrete.

2. The effect of curing duration on the performance of air-entrained and non air-entrained high strength concrete exposed to freeze-thaw environments.

3. Air void parameters and their relation to the freeze-thaw durability of high strength, silica fume concrete.

In addition to the above, concrete cylinders (3x6 in.) were tested for compressive strength at different ages. The results from the compression tests as well as the impact of entraining air on the compressive strength of concrete are also discussed here.

6.1 COMPRESSIVE STRENGTH

A total of eight cylinders (3x6 in.) from each mix were tested for compressive strength. Two cylinders were capped and tested at the ages of 7, 14, 28, and 56 days. Figure 6.1 shows compressive strength versus age for the concrete with W/(C+SF) ratio ranging from 0.25 to 0.32 without air entrainment. Figure 6.2 shows the strength for similar concrete but with an average air content of 4 percent. Each data point on the plots in Figure 6.1 and 6.2 represents an average of four cylinders tested for compressive strength. As shown in Figure 6.3, the reduction of water to cementitious ratio from 0.32 to 0.25 caused a 37 percent increase in compressive strength as tested after 56 days of curing.

Regardless of water to cementitious ratio the rate of increase in compressive strength was similar among all of the mixes. But there was a 30 to 35 percent increase in compressive strength between the ages of 7 to 28 days, while between the ages of 28 to 56 days the samples gained only 2 to 10 percent additional strength.

Figure 6.4, shows compressive strength of mixes all with water to cementitious ratio of 0.32 but with different levels of silica fume content (0%, 10%, 15%). The plots shown for the 0% and 10% silica fume concrete belongs to the mixtures without air-entrainment, while the plot for the mixtures with 15% silica fume contained an average of 6% air. All the mixes had same strength at 7 days of age, but beyond the 7 days the concrete with higher amount of silica fume had higher strength. Figure 6.5 shows the increase in compressive strength for three levels of silica fume content as a percentage of 7 days strength. It also shows that the concrete with higher amount of silica fume had a higher rate of increase in compressive strength. For example the mix with no silica fume at 56 days of age showed an increase of 26 percent as compared to 7 days strength, while the mix with 10 percent silica fume had and increase of 35 percent and the mix with 15 percent silica fume increased 40 percent as compared to its 7 days compressive strength.

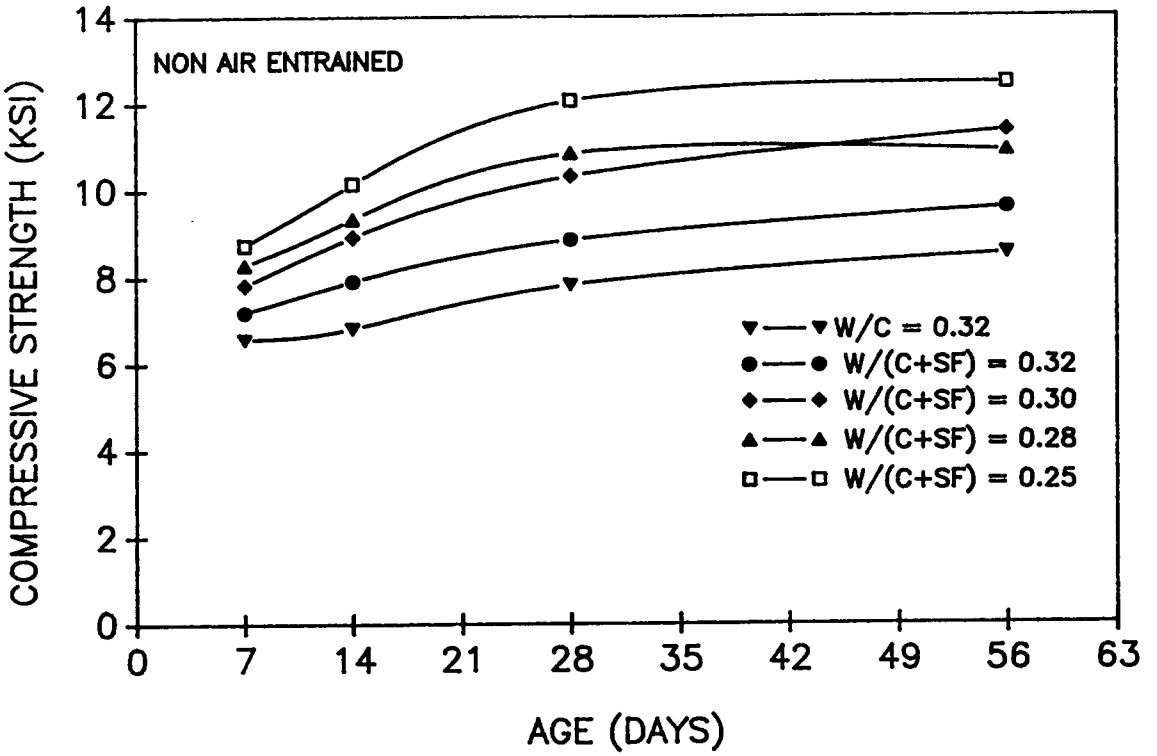

Figure 6.1. Compressive Strength Versus Age

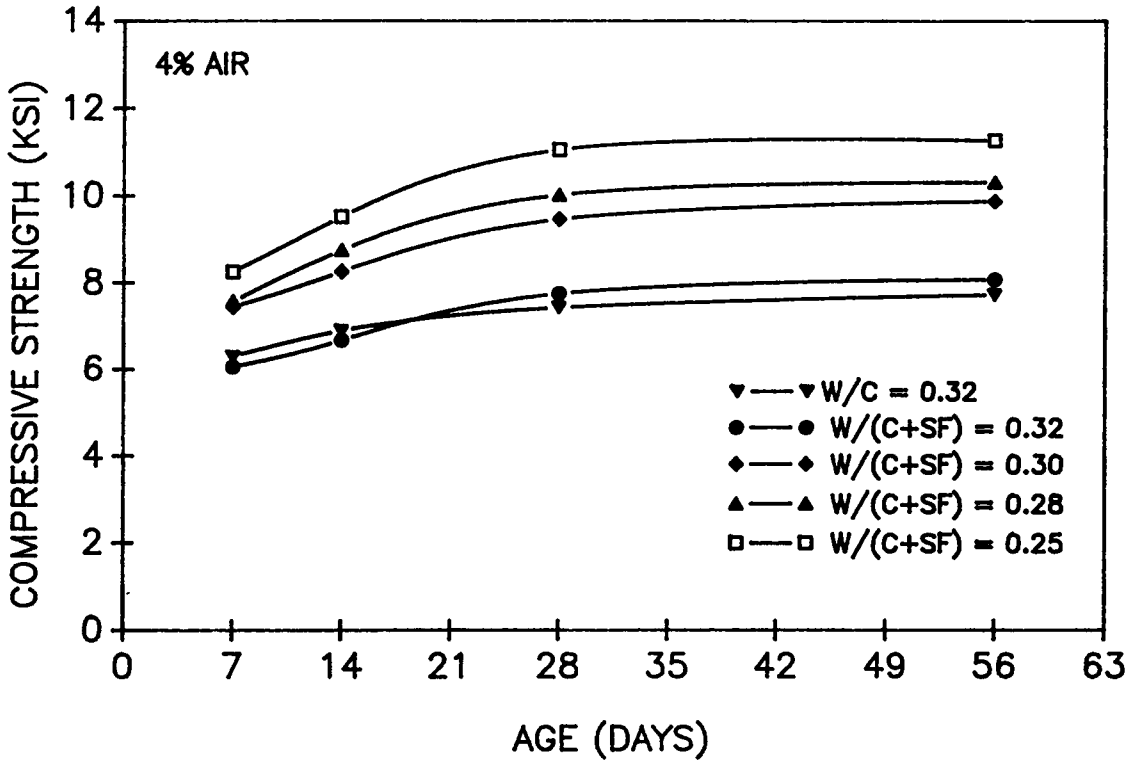

Figure 6.2. Compressive Strength Versus Age

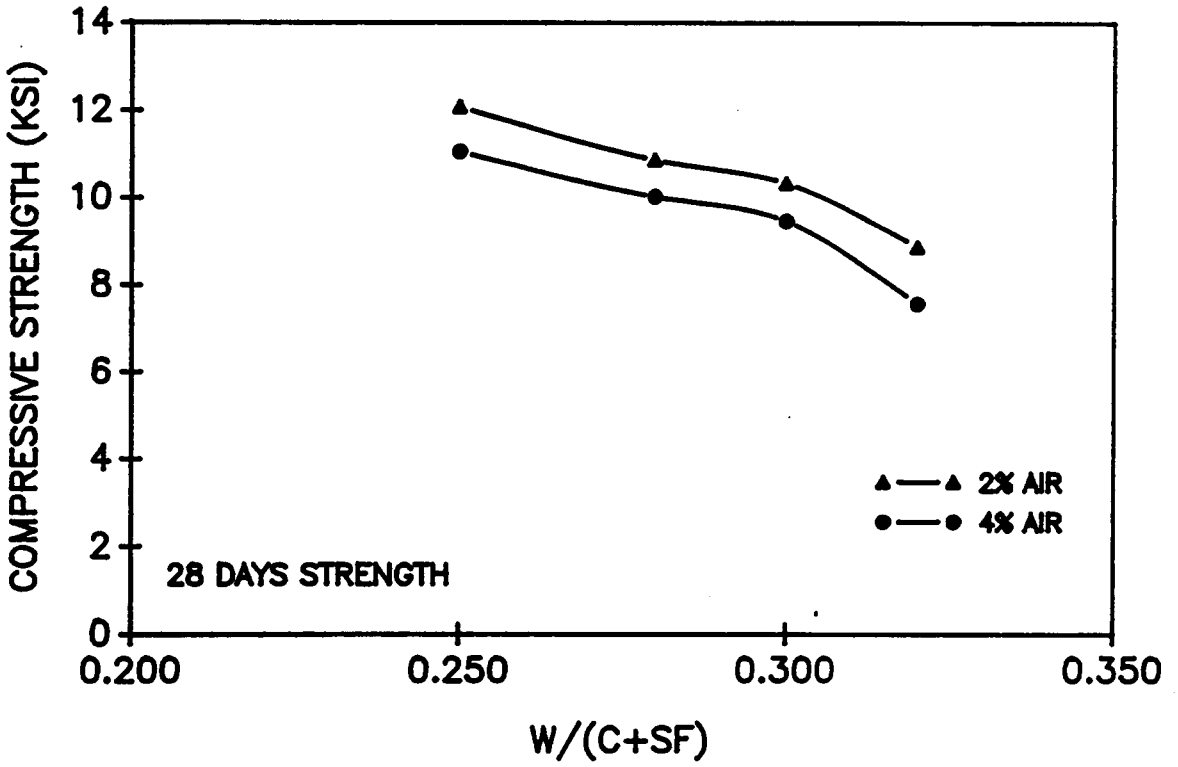

Figure 6.3. Effect of W/C Ratio on Compressive Strength.

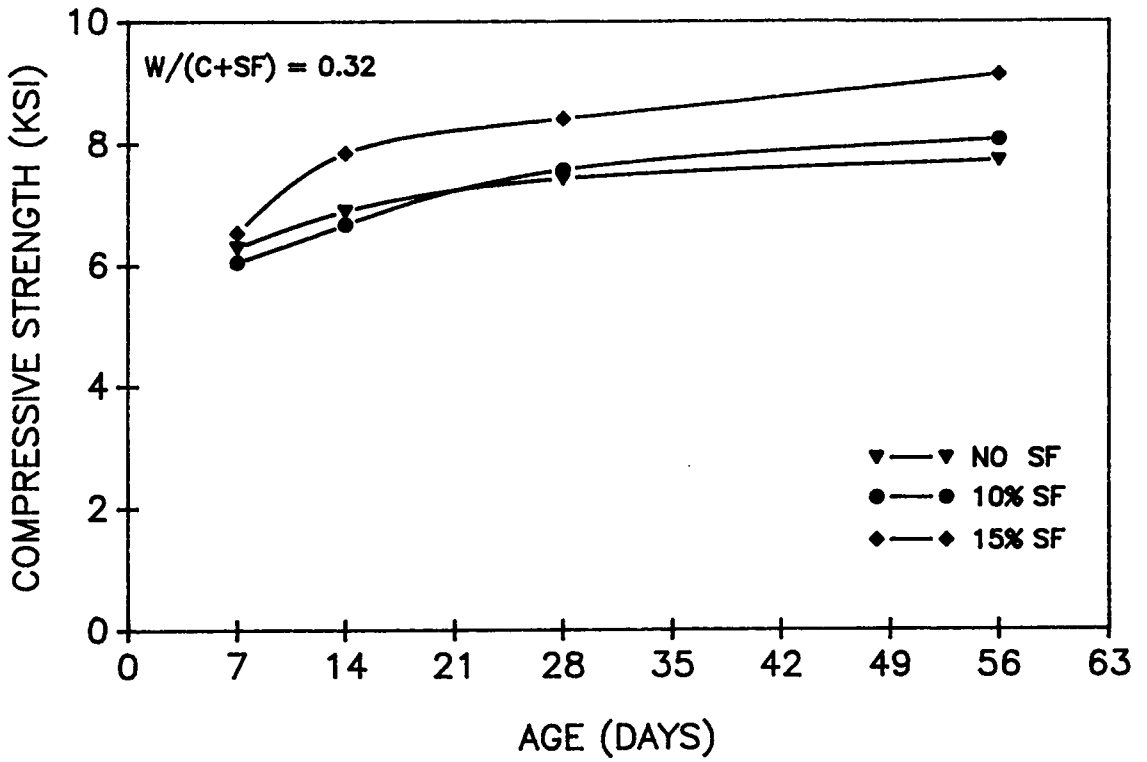

Figure 6.4. Effect of Silica Fume on Compressive Strength.

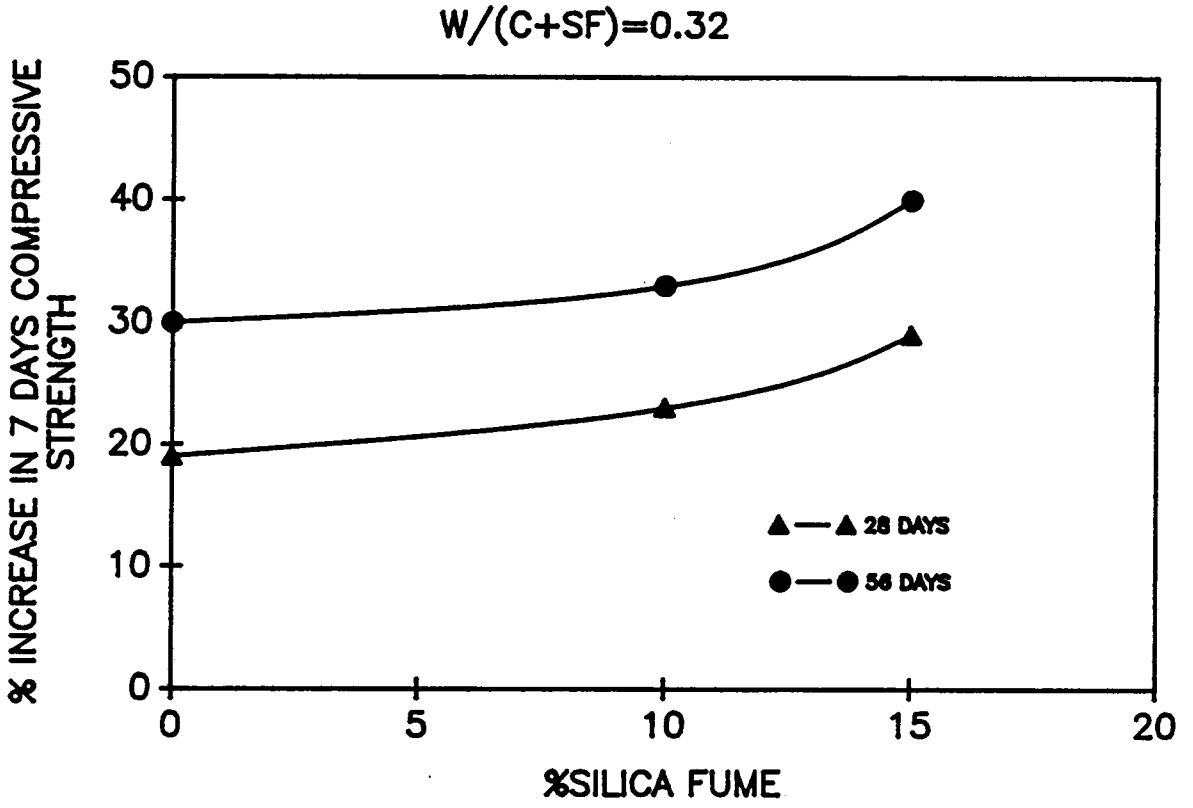

Figure 6.5. Rate of Increase in Seven Days Compressive Strength.

One noteworthy point here was that, in spite of such a low water to cementitious ratio and high cement content (9 bags per yd ^{3}), the average compressive strength even for the lowest water to cementitious ratio (0.25) did not go beyond 13,500 psi. There is literature (78) showing that concrete with similar W/C ratio had a compressive strength of about 16,000 psi. A close examination of the failed specimens showed that all the fracture lines, particularly at ages of 28 and 56 days pass through the aggregates. This indicated that the ultimate strength in these cases were controlled predominantly by the strength of aggregate. The larger aggregate particles (known as top size in coarse aggregate) are particularly prone to fail first, since the probability of natural flaws are higher with larger particles. The top size aggregate used in this study was one inch. This is primarily the reason for ACI Committee 363 recommendation to use a coarse aggregate with smallest possible top size. In ordinary concrete, compressive strength is normally controlled by the strength of paste.

6.2 EFFECT OF AIR ENTRAINMENT ON COMPRESSIVE STRENGTH

Figures 6.6 to 6.10, show the effect of air entraining on compressive strength of the concrete. The top curve on each graph represents the non air-entrained mixture and thus the air content shown, is the amount of entrapped air. All the air-entrained samples had a lower strength than non air-entrained ones, and typically one percent increase in air content caused a 5 percent decrease in compressive strength.

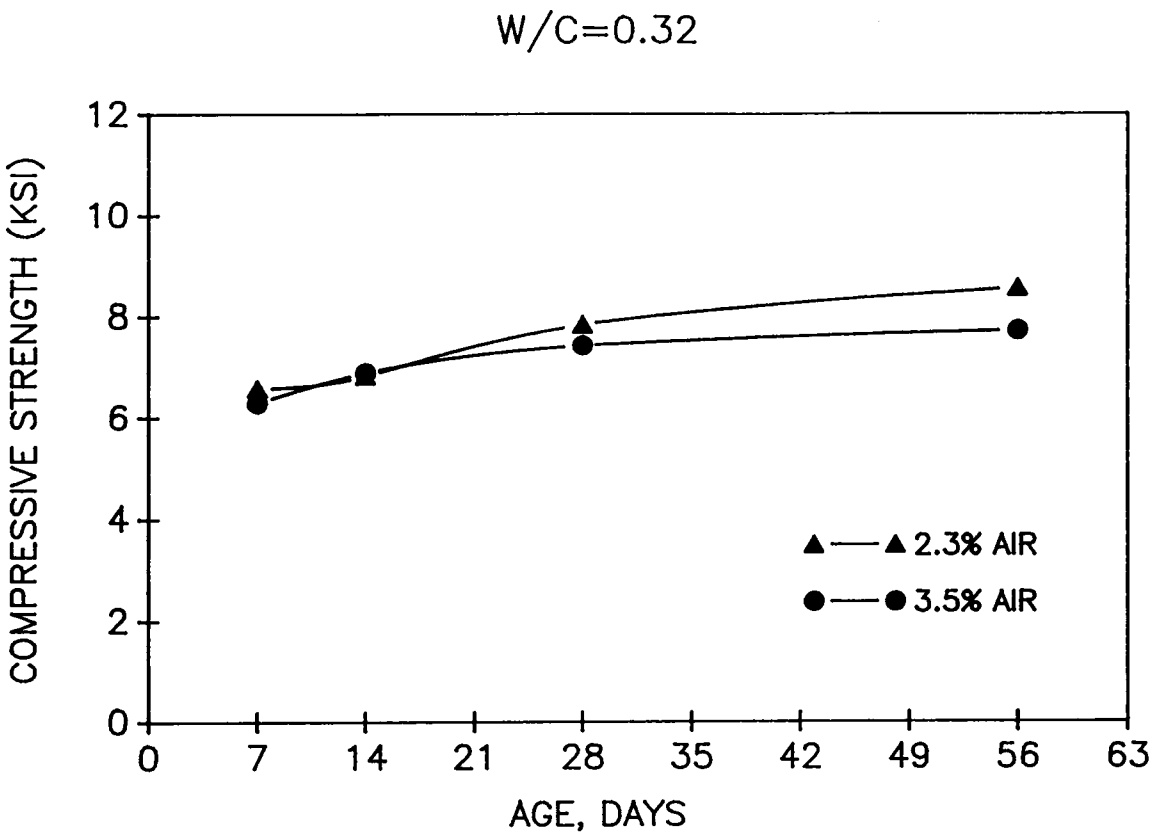

Figure 6.6. Effect of Air Entraining on Compressive Strength.

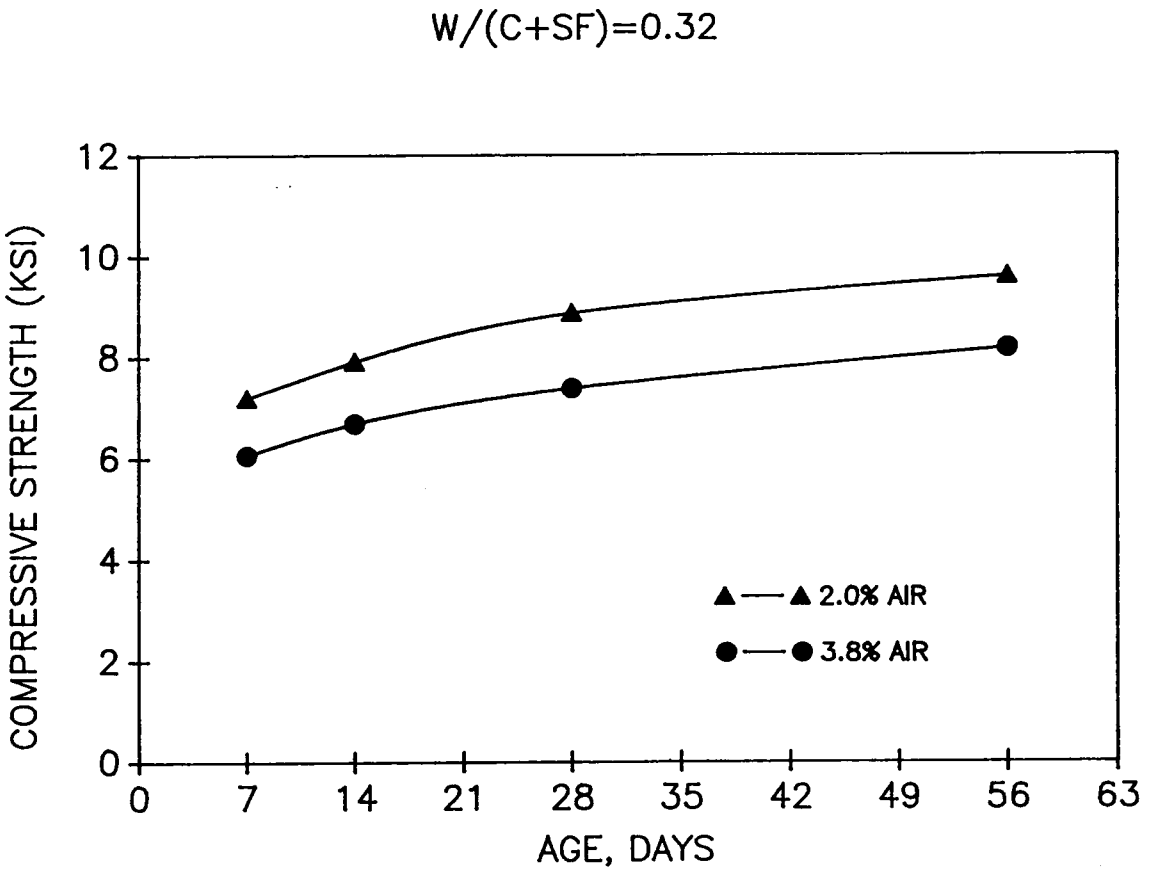

Figure 6.7. Effect of Air Entraining on Compressive Strength.

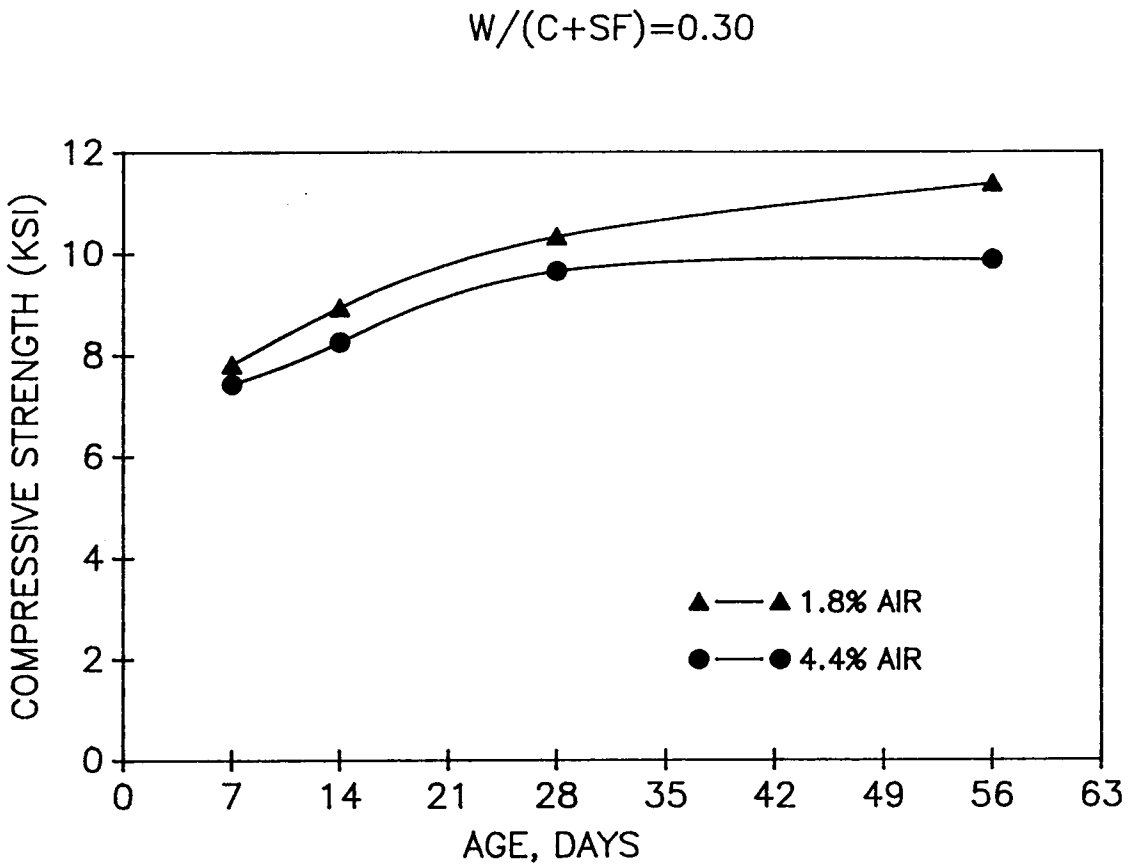

Figure 6.8. Effect of Air Entraining on Compressive Strength.

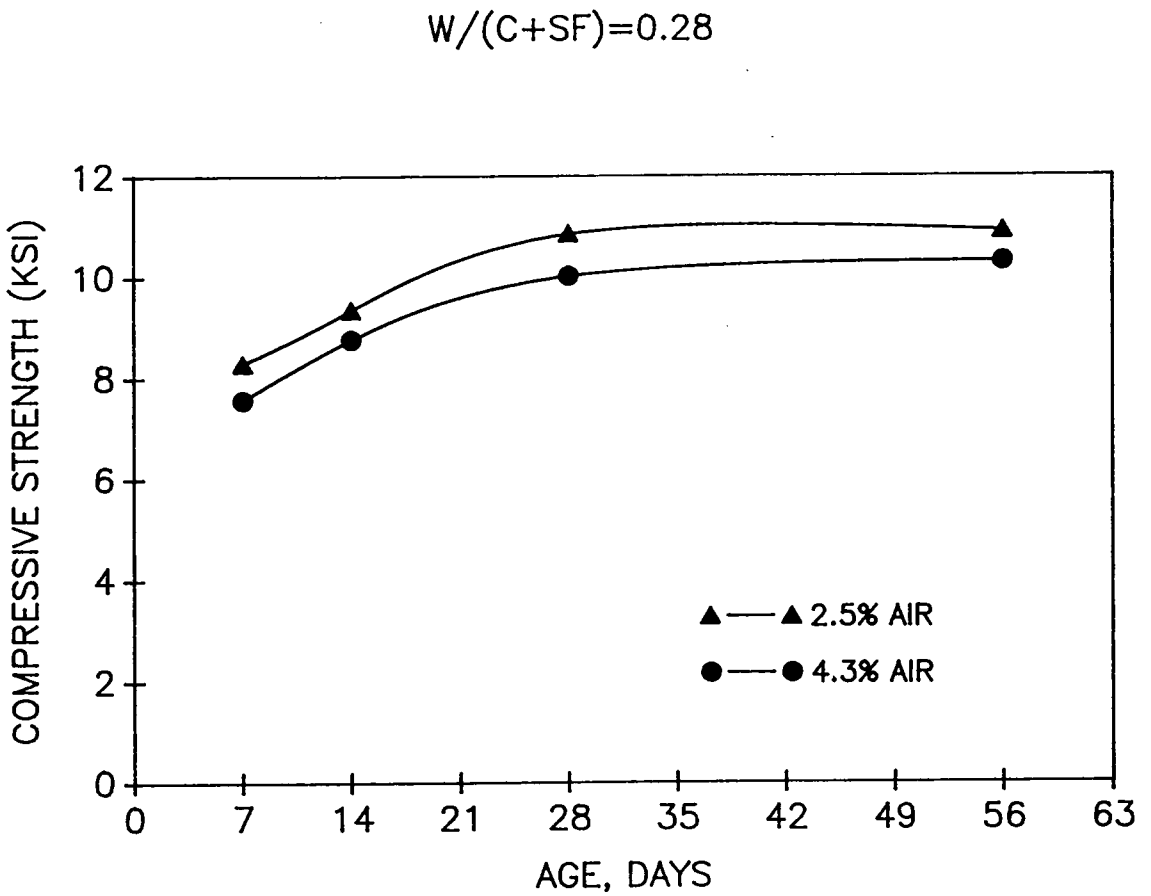

Figure 6.9. Effect of Air Entraining on Compressive Strength.

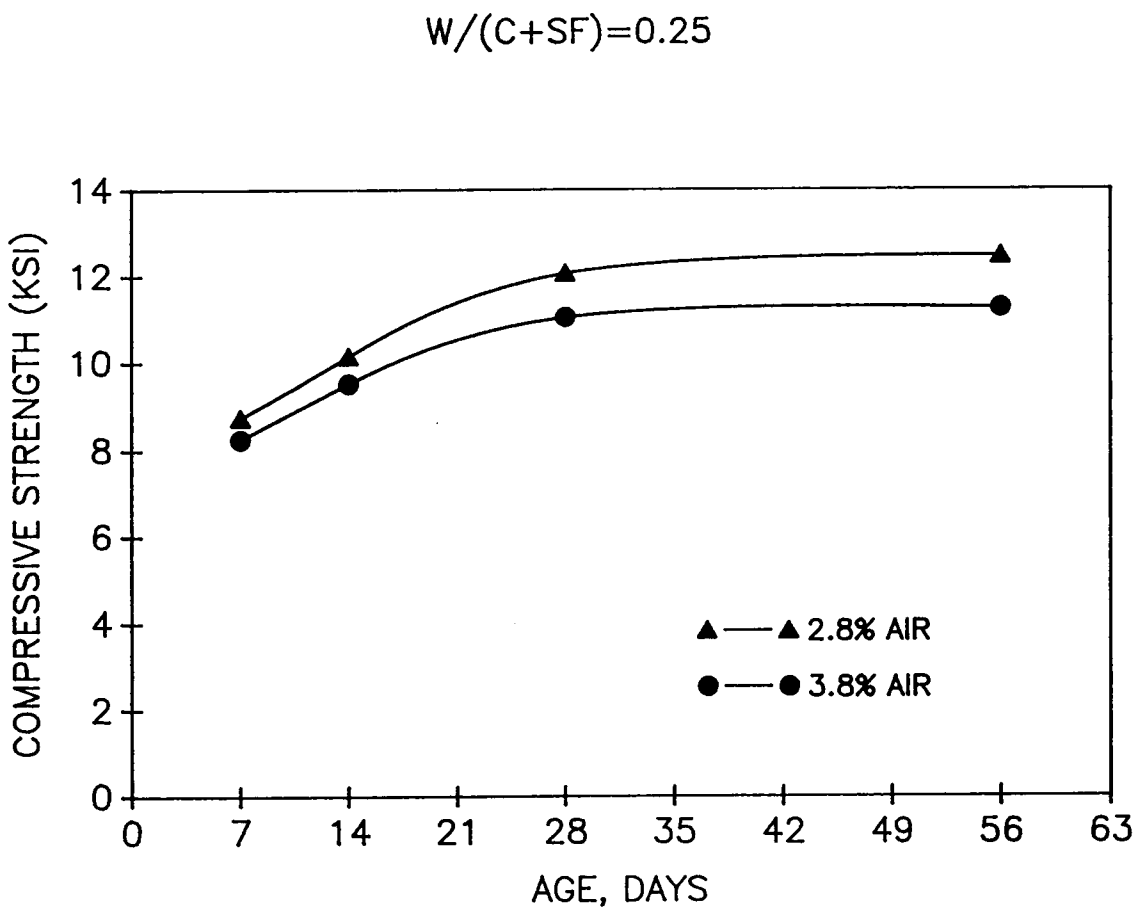

Figure 6.10. Effect of Air Entraining on Compressive Strength.

6.3 FREEZE-THAW DURABILITY

6.3.1 Phase 1 of Experiments

Twenty-two prisms (3x4x16 in) were tested according to ASTM C666 procedure A (freezing and thawing in water). All the specimens were made from concrete with water to cementitious ratio of 0.32. The specimens tested in this phase were cured for 28 days prior to testing. Six of the specimens were not air-entrained while the rest had different levels of air content. Table 6.1 presents the concrete mixtures tested in this phase along with their air content as measured by pressure meter (ASTM C231). The table also presents the results obtained from freeze-thaw testing of the specimens.

All the non air-entrained specimens tested, with the exception of one, failed to survive 300 cycles of freezing and thawing. Propagation of internal cracks was generally the mode of failure for the specimens. Several longitudinal cracks appeared on the surfaces of both of the 4x16 in sides of the prisms. The widest part of the cracks was located in the middle of the surface and several smaller cracks were branching out toward the ends and edges of the specimens. Failed specimens (A1-1,A1-2,A2-1,A3-1,A3-2) are presented in Figures 6.11 to 6.15. Figure 6.16 shows several specimens (one from each batch groups A,B,C,D) which survived 300 cycles of freeze-thaw testing.

Regardless of air content none of the specimens, not even the ones which had failed, lost any weight throughout the freeze-thaw testing period and there were no sign of scaling or surface disintegration.

The non air-entrained concrete with W/C ratio in normal range (above 0.4) generally fails during the first few cycles of exposure to freezing and thawing. But in this case the non air-entrained specimens (A1-A3) demonstrated more resistance to the destructive freeze-thaw forces.

Table 6.1. Characteristics of Concrete Tested in Phase 1.

MIX NO.	W/(C+SF)	SF[1] %	AEA[2] OZ	PM[3] %A	CURED DAYS	LT[4] %A	CYCLE NO. 1	CYCLE NO. 2	RDM[5] 1	RDM[5] 2
A-1	0.32	10	0	1.9	28	1.3	168	159	31	56
A-2	0.32	10	0	2.1	28	1.4	241	300	63	97
A-3	0.32	10	0	1.8	28	1.2	91	254	43	30
A-4	0.32	10	2	4.7	28	3.7	300	300	100	99
A-5	0.32	10	1	3.4	28	3.5	300	300	100	100
A-6	0.32	10	1	2.9	28	2.7	300	300	99	97
A-7	0.32	10	4	4.1	28	3.7	300	300	99	99
A-8	0.32	10	4	3.9	28	5.0	300	300	100	100
A-9	0.32	15	1	6.3	28	6.7	300	300	100	100
A-10	0.32	15	0.75	5.8	28	6.3	300	300	97	97
A-11	0.32	15	0.75	6.6	28	5.2	300	300	101	99

1.Silica Fume, 2.Air Entraining Agent (oz per 100 lb. of cement),
3.Pressure Meter, 4. Linear Traverse, 5. Relative Dynamic Modulus

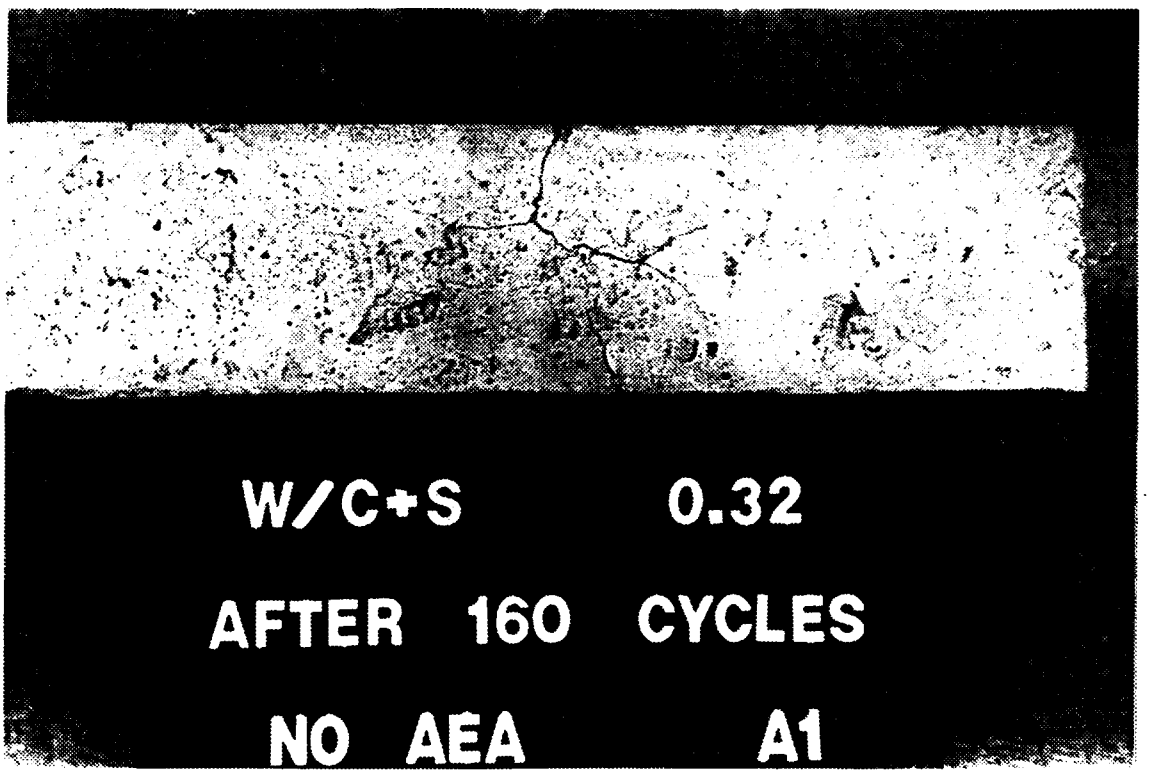

Figure 6.11. A failed Specimen Tested in Phase one

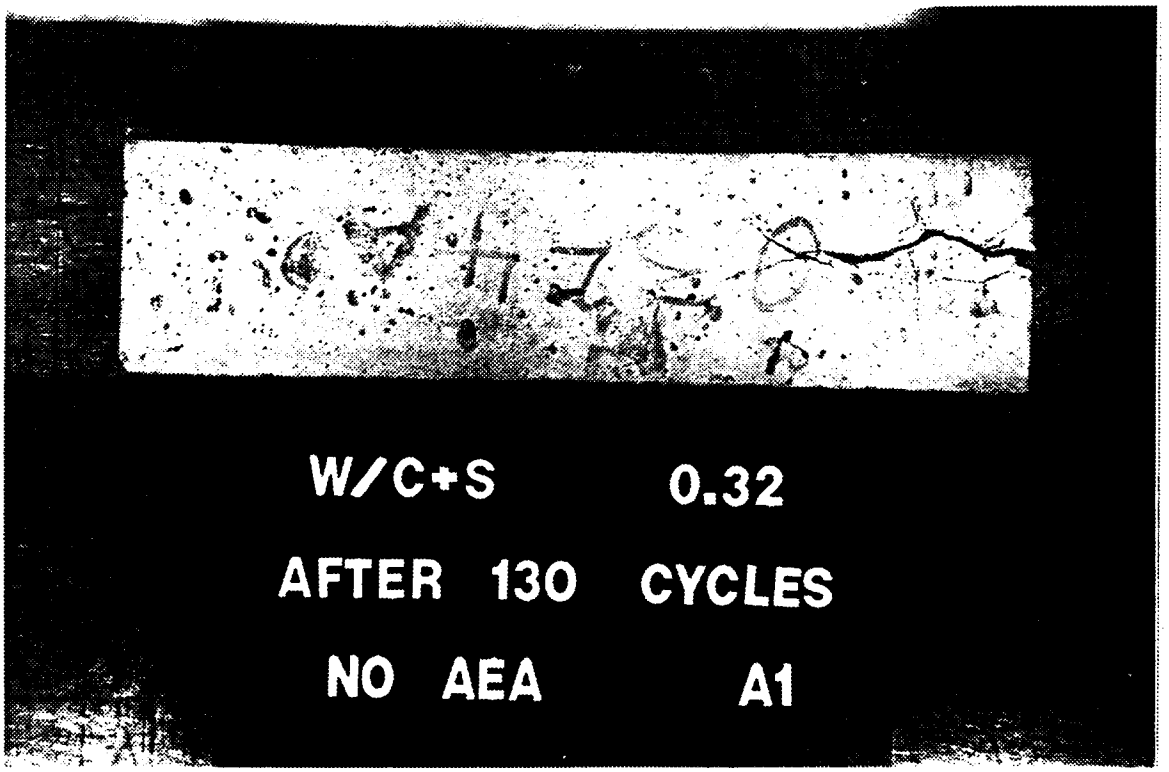

Figure 6.12. A failed Specimen Tested in Phase one

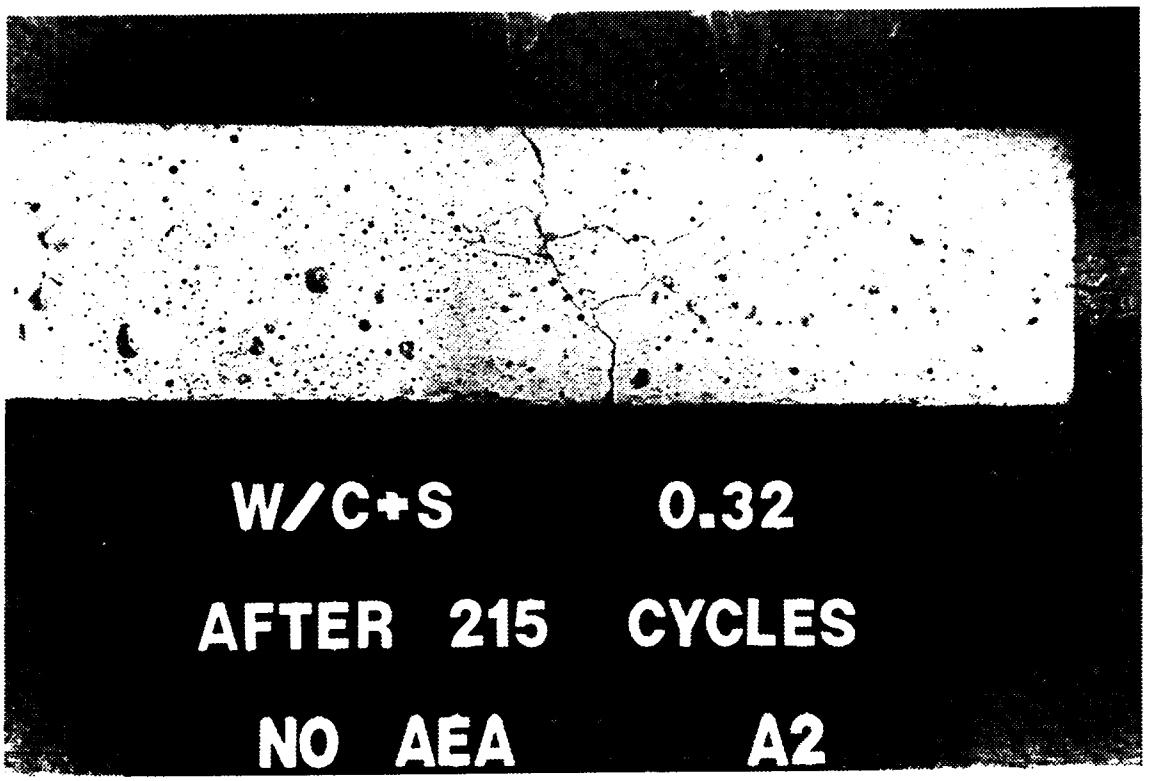

Figure 6.13. A failed Specimen Tested in Phase I

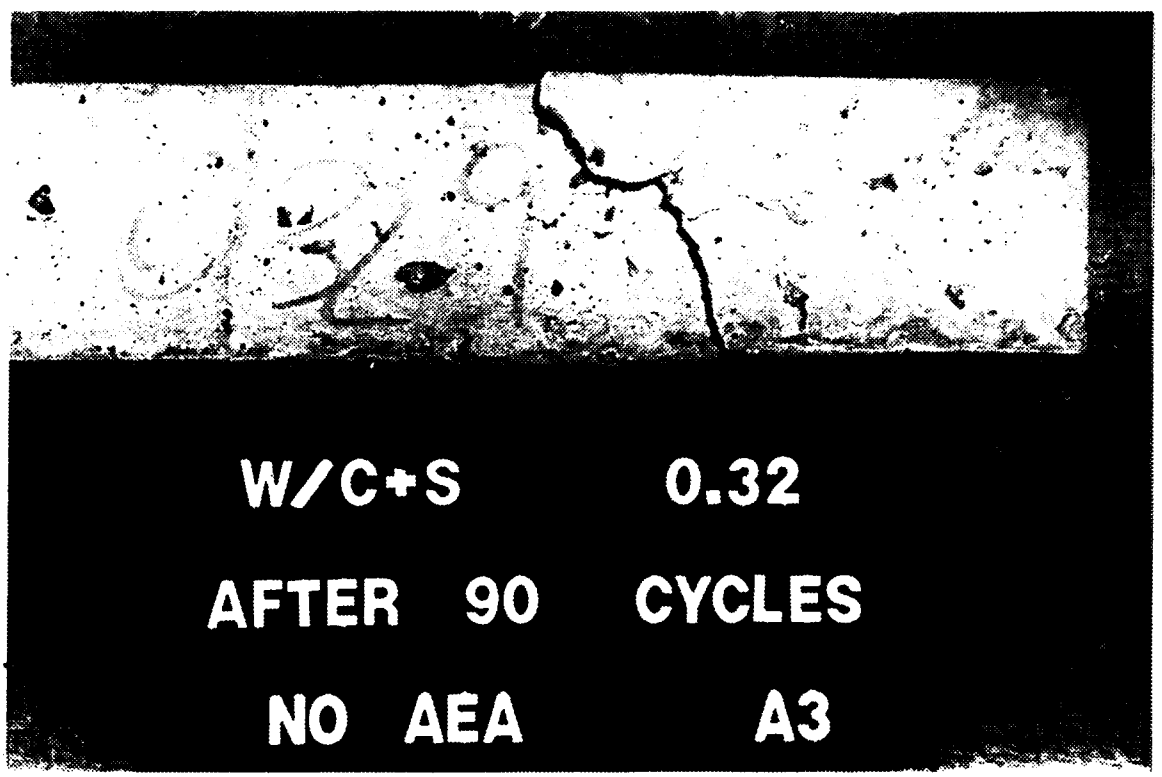

Figure 6.14. A failed Specimen Tested in Phase one

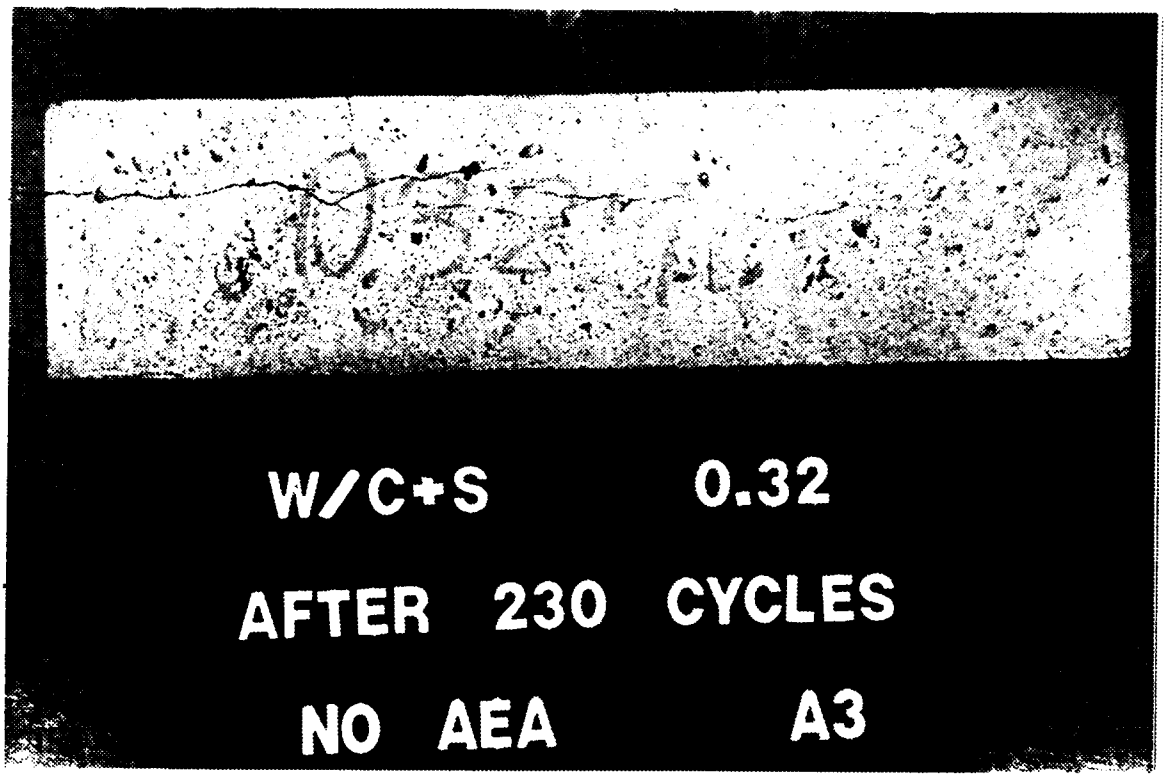

Figure 6.15. A failed Specimen Tested in Phase one

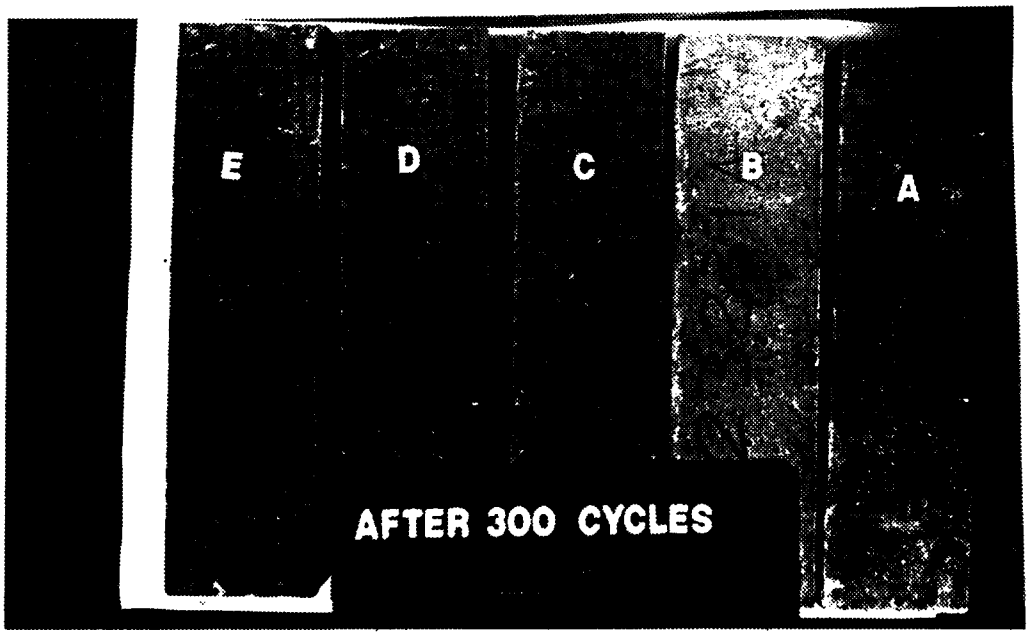

Figure 6.16. Typical Specimens Survived 300 Cycles of Testing

They survived an average of 190 cycles of freezing and thawing and when they failed, it was in a relatively short period. For example, two prisms from mix A1 tested for resonant frequency after 135 cycles of exposure had a relative dynamic modulus of 99 percent. When they were tested again after 160 cycles of exposure (20 cycles later), they had fallen to 31 percent. Most normal concrete generally fails in a more gradual process. Figure 6.17 shows a relative dynamic modulus versus freeze-thaw cycles for the non air-entrained specimens tested in this phase.

All the air-entrained specimens regardless of their air content demonstrated an excellent resistance to freezing and thawing and their durability factor after 300 cycles of exposure were 98 to 100 percent.

6.3.2 Phase 2 of Experiments

In the second phase of the project a total of sixteen prisms from eight batches of concrete after 28 days of curing were tested for freeze-thaw durability. Water to cementitious ratio for these batches were 0.32, 0.30, 0.28, and 0.25. Table 6.2, summarizes the data pertaining to the concrete specimens tested in this phase.

All the specimens regardless of their air content survived the 300 cycles of freezing and thawing. With the exception of three beams from the mixtures D1 and E1, the specimens with and without air entrainment retained a relative dynamic modulus (RDM) of above 90 percent. Both beams from mix D1 and E1 had somewhat lower RDM after 300 cycles of testing. But none had any sign of deterioration. Figure 6.18 shows the relative dynamic modulus versus the number of freezing and thawing cycles for the specimens which exhibited any sign of decrease in dynamic modulus.

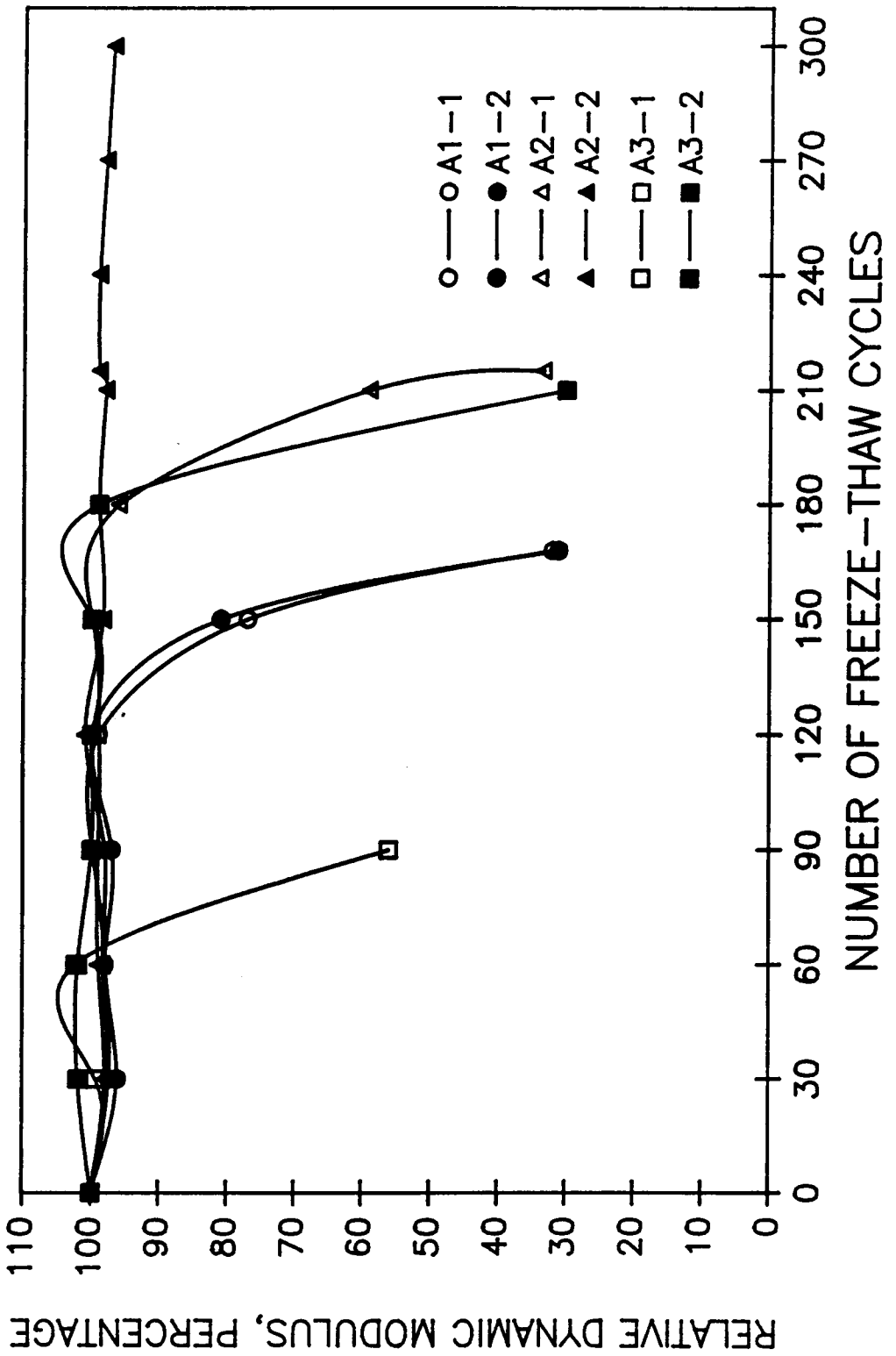

Figure 6.17. Relative Dynamic Modulus for Specimens Failed in Phase 1.

Table 6.2. Characteristics of Concrete Tested in Phase 2.

MIX NO.	W/(C+SF)	SF[1] %	AEA[2] OZ	PM[3] %A	LT[4] %A	CURED DAYS	CYCLE NO.	RDM[5] 1	RDM[5] 2
B-1	0.32	0	0	2.0	1.4	28	300	91	100
B-3	0.32	0	0.3	3.2	2.2	28	300	105	98
C-1	0.30	15	0	2.0	2.1	28	300	93	98
C-3	0.30	15	0.4	4.8	5.0	28	300	97	99
D-1	0.28	15	0	2.0	1.8	28	300	70	82
D-3	0.28	15	0.5	4.5	3.6	28	300	98	96
E-1	0.25	15	0	2.8	1.5	28	300	87	66
E-3	0.25	15	0.3	3.0	3.1	28	300	99	92

1.Silica Fume, 2.Air Entraining Agent (oz per 100 lb. of cement)
3.Preasure Meter, 4. Linear Traverse, 5. Relative Dynamic Modulus

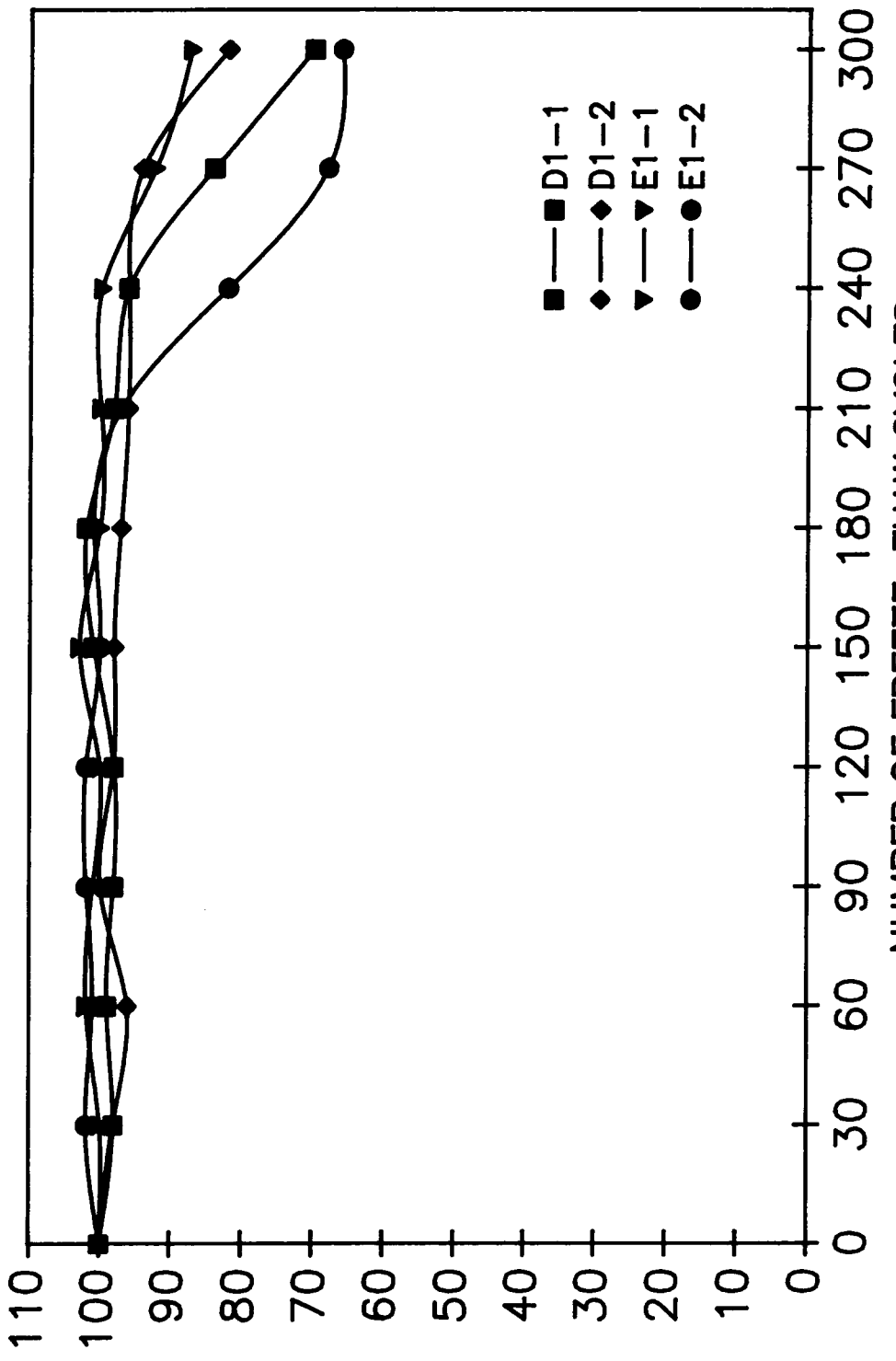

Figure 6.18. Relative Dynamic Modulus for Some Specimens Tested in Phase 2.

6.3.3 Phase 3 of Experiments

The specimens tested in this phase of the research were similar to the ones tested in the second phase. The only difference was that the prisms in this phase were all cured for 14 days prior to the testing. As it can be seen in Table 6.3 and Figure 6.19 all the specimens with, the exception of one survived 300 cycles of freezing and thawing. One beam from mixture D-2 (D2-2) failed after 281 cycles of exposure. The failure mode was similar to the ones failed in first phase of the project (Figure 6.20). Although the mixture D-2 was not air-entrained, the other companion beam tested from the same batch retained its 100 percent RDM throughout the 300 cycles of freeze-thaw testing. Changes in relative dynamic modulus for specimens D2-1, D2-2, E2-1, and E2-2 as the result of freeze-thaw testing are shown in Figure 6.19.

Like the samples tested in the last two phases, none of the samples tested here scaled or had any sign of surface deterioration.

6.4 AIR VOID PARAMETERS

A microscopical examination was performed on the polished sections of the hardened specimens from each batch of concrete. A CPM microprocessor based linear traverse apparatus was used for the task, and the measurements were in accordance with the ASTM C457-82 (linear traverse method). A brief description of the apparatus is presented in Appendix D. Each specimen was traversed for 95 inches and all the individual intercepted chords were measured at a magnification of X120, and stored on a computer disk. Subsequently the measured chords were used for calculating the air void parameters which are presented in Table 6.4.

The non air-entrained specimens had a spacing factor ranging from 0.018 to 0.035 in., and air-entrained specimens had a spacing factor of 0.006 to 0.01 inches. The specific surface calculated

Table 6.3. Characteristics of Concrete Tested in Phase 3.

MIX NO.	W/(C+SF)	SF[1] %	AEA[2] OZ	PM[3] %A	LT[4] %A	CURED DAYS	CYCLE NO. 1	CYCLE NO. 2	RDM[5] 1	RDM[5] 2
B-2	0.32	0	0	2.7	1.6	14	300	300	92	99
B-4	0.32	0	0.4	3.8	3.2	14	300	300	100	100
C-2	0.30	15	0	1.7	2.2	14	300	300	97	98
C-4	0.30	15	0.4	4.0	4.7	14	300	300	97	97
D-2	0.28	15	0	3.0	1.9	14	300	281	100	41
D-4	0.28	15	0.5	4.0	3.9	14	300	300	102	99
E-2	0.25	15	0	2.8	2.2	14	300	300	98	79
E-4	0.25	15	0.7	4.7	3.7	14	300	300	100	103

1.Silica Fume, 2.Air Entraining Agent (oz per 100 lb. of cement)
3.Pressure Meter, 4. Linear Traverse, 5. Relative Dynamic Modulus

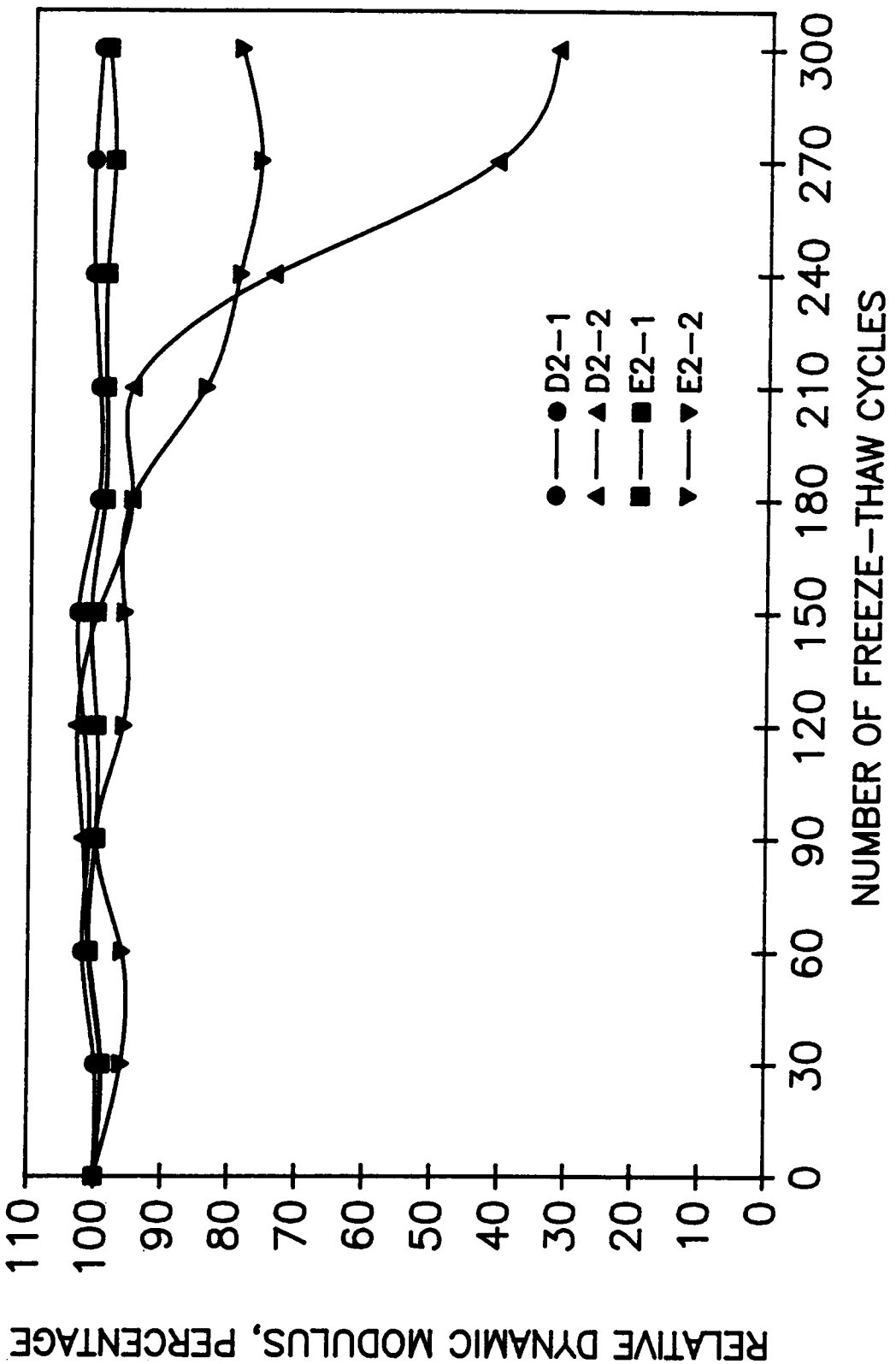

Figure 6.19. Freeze-Thaw Performance of Some Specimens Tested in Phase 3

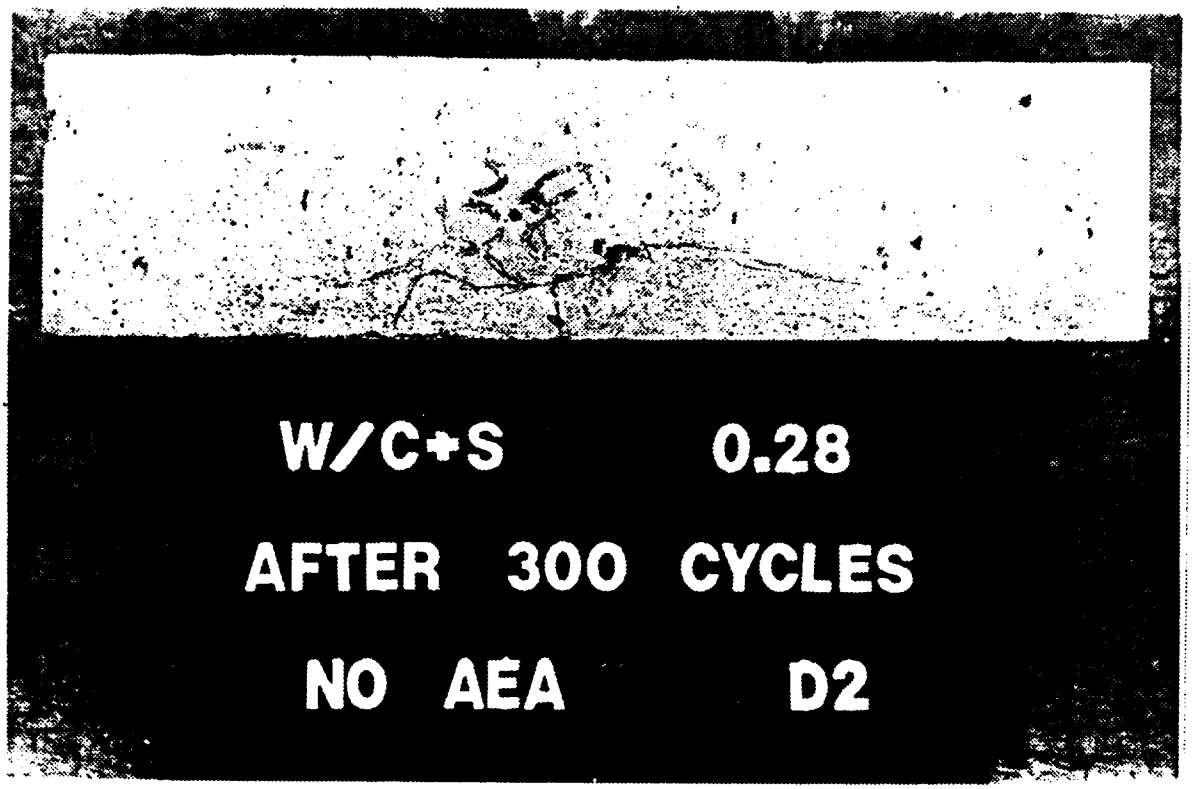

Figure 6.20. A Specimen Failed in Phase 3.

Table 6.4. Air Void Parameters Considering All the Chords

MIX NO.	W/(C+SF)	SF[1] %	PM[2] %A	LT[3] %A	$\bar{L}$[4] IN.	α[5] 1/IN	CURED DAYS	CYCLE NO.	RDM[6]
A-1	0.32	10	1.9	1.3	0.023	441	28	168	31
A-2	0.32	10	2.1	1.4	0.018	537	28	241	63
A-3	0.32	10	1.8	1.2	0.029	372	28	172	43
A-4	0.32	10	4.7	3.7	0.005	1265	28	300	100
A-5	0.32	10	3.4	3.5	0.007	982	28	300	100
A-6	0.32	10	2.9	2.7	0.010	780	28	300	98
A-7	0.32	10	4.1	3.7	0.006	1121	28	300	99
A-8	0.32	10	3.9	5.0	0.006	1009	28	300	100
A-9	0.32	15	6.3	6.7	0.005	981	28	300	100
A-10	0.32	15	5.8	6.3	0.007	688	28	300	97
A-11	0.32	15	6.6	5.2	0.006	795	28	300	100
B-1	0.32	0	2.0	1.4	0.035	283	28	300	95
B-2	0.32	0	2.7	1.6	0.033	290	14	300	95
B-3	0.32	0	3.2	2.2	0.018	455	28	300	100
B-4	0.32	0	3.8	3.2	0.012	555	14	300	100
C-1	0.30	15	2.0	2.1	0.018	453	28	300	95
C-2	0.30	15	1.7	2.2	0.020	409	14	300	97
C-3	0.30	15	4.8	5.0	0.007	758	28	300	98
C-4	0.30	15	4.0	4.7	0.008	715	14	300	97
D-1	0.28	15	2.0	1.8	0.035	261	28	300	75
D-2	0.28	15	3.0	1.9	0.022	396	14	300	68
D-3	0.28	15	4.5	3.6	0.008	811	28	300	97
D-4	0.28	15	4.0	3.9	0.009	697	14	300	100
E-1	0.25	15	2.8	1.5	0.026	367	28	300	77
E-2	0.25	15	2.8	2.2	0.019	423	14	300	89
E-3	0.25	15	3.0	3.1	0.011	622	28	300	95
E-4	0.25	15	4.7	3.7	0.010	626	14	300	100

1. Silica Fume, 2. Pressure Meter, 3. Linear Traverse
4. Spacing Factor, 5. Specific Surface, 6. Relative Dynamic Modulus.

for the non air-entrained mixtures were ranging from 261 to 537 in^2/in^3 and for the air entrained mixtures they varied from 455 to 1265 in^2/in^3. No correlation was found between the actual freeze-thaw performance and the air void parameters.

An observation made here was that mixtures A4,A7, and A8 had an air content ranging from 3.9 to 4.7 percent (as measured by pressure meter), but they all had a specific surface of greater than 1000 in^2/in^3, while the other mixtures with similar or sometimes higher air content had a specific surface much lower than 1000 in^2/in^3. This is because the mixtures A4,A7, and A8 were the only air entrained mixtures without high range water reducer (HRWR) (exclusive of the HRWR in the silica fume), and it is known that the HRWR in general cause the air bubbles to become coarser. Such a high specific surface and low spacing factor for a concrete with 4 percent air is probably due to the type of air entraining agent (MICRO AIR) used for this study.

Figure 6.21 shows the correlation between the air content as measured by pressure meter and linear traverse method. Performing a linear regression between the two indicates that the air content measured by pressure meter is higher. The regression line parameters are 0.98 for the intercept and 0.805 for the slope and R square is equal to 81 percent.

In search of a tangible connection between the air void system and the actual freeze-thaw performance, the measured chords were compiled in a personal computer and with the aid of a spread sheet program various factors (air void parameters) based on different assumptions were calculated. The entrapped air voids due to their coarseness and low numbers can not protect the concrete from frost damage. The chords greater than 1 mm are assumed (81) to represent the entrapped air voids and in order to find their impact, they were not considered in the calculation of the air void parameters. Table 6.5 shows the air void parameters calculated based on the chords smaller than 1 mm. Table 6.5 also shows the air void parameters calculated based on the chords smaller than 0.5 mm. The idea is that since the majority of the chords measured are within the size range of 0.1 to 0.5 mm., this may eliminate the bias introduced into the calculations by a few larger

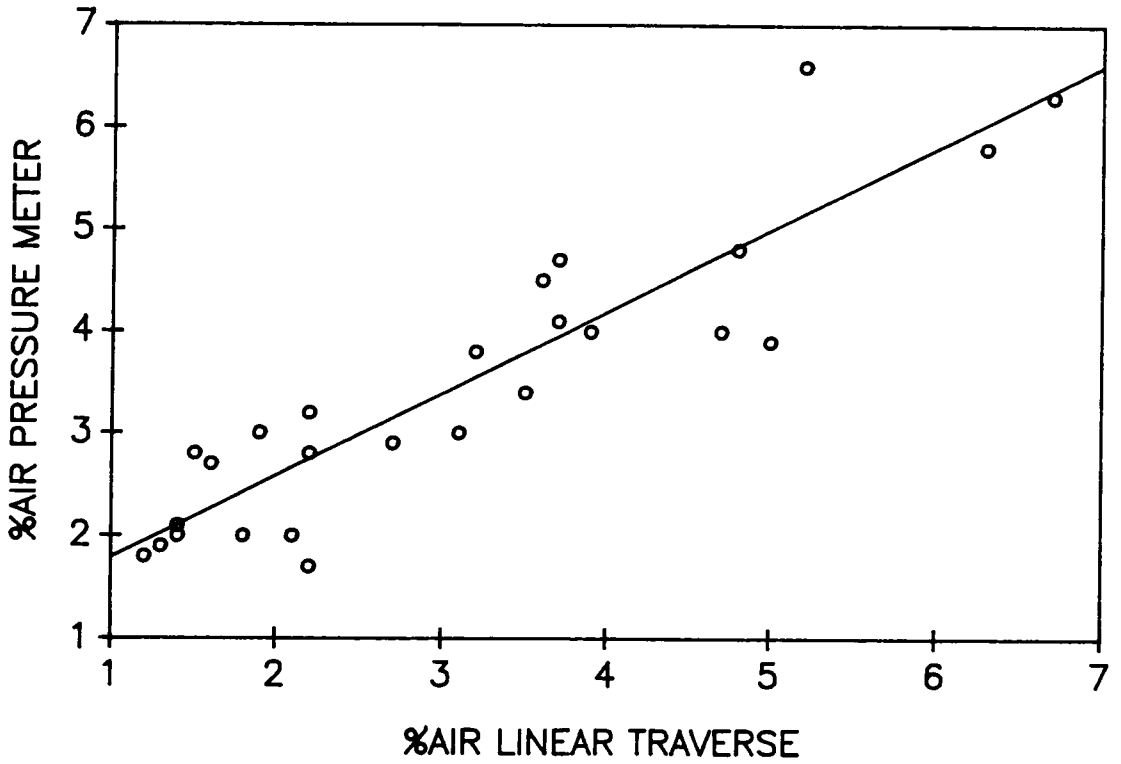

Figure 6.21. Air Content as Measured by Pressure Meter and Linear Traverse.

air voids in the system (82). No relation was found between these parameters and the freeze-thaw behavior of the concrete.

A noteworthy point is the progressive reduction of spacing factor as the result of eliminating the air voids larger than 1 mm from calculations. But in both cases the spacing factors for non air-entrained specimens are still higher than 0.008 inches as specified by ACI and can not explain the excellent freeze-thaw resistance observed here.

6.4.1 Philleo's Factor

The Philleo's factors were calculated based on the Willies equation for the number of voids per unit volume of paste (74), and the results are given in Table 6.5. No relationship between the Philleo's factor and the freeze-thaw testing results was found.

6.5 Results of Drying

Table 6.6 presents the results obtained from drying a cut section from each batch of concrete. In general the specimens lost approximately from 6.2 to 8.2 percent of moisture during 24 days of exposure to 240 °F heat. Statistical analysis (linear regression) showed a very poor correlation (R square of 18 percent) between the amount of water lost and water-cement ratio. It should be noted that the specimens at the time of testing were cured in moist room for different length of time ranging from 57 to 259 days. Lack of correlation might be due to this non uniformity.

Table 6.5. Air Void Parameters Considering the Chords less than 1 and 0.5 mm.

			Less Than 1 mm.			Less Than 0.5 mm.				
NO.	W/(C+SF)	PM[1] %A	L_T[2] %A	$\bar{l}$[3] IN.	α[4] 1/IN	L_T[2] %A	$\bar{l}$[3] IN.	α[4] 1/IN	s[5] CM.	RDM[6] %
A-1	0.32	1.9	0.9	0.019	620	0.8	0.018	710	0.015	31
A-2	0.32	2.1	1.1	0.016	663	1.0	0.015	752	0.015	63
A-3	0.32	1.8	0.8	0.024	515	0.6	0.022	646	0.013	43
A-4	0.32	4.7	3.2	0.005	1465	2.8	0.005	1639	0.008	100
A-5	0.32	3.4	2.7	0.006	1256	2.5	0.006	1327	0.009	100
A-6	0.32	2.9	2.0	0.008	1033	1.7	0.008	1204	0.009	98
A-7	0.32	4.1	2.9	0.005	1400	2.6	0.005	1542	0.008	99
A-8	0.32	3.9	3.7	0.005	1335	3.4	0.005	1463	0.009	100
A-9	0.32	6.3	5.9	0.004	1100	5.2	0.004	1228	0.008	100
A-10	0.32	5.8	5.5	0.006	767	4.6	0.006	892	0.008	97
A-11	0.32	6.6	4.3	0.006	928	3.8	0.006	1052	0.008	100
B-1	0.32	2.0	0.8	0.027	462	0.6	0.025	554	0.025	95
B-2	0.32	2.7	1.1	0.028	382	0.6	0.025	549	0.015	95
B-3	0.32	3.2	1.9	0.017	504	1.4	0.016	620	0.014	100
B-4	0.32	3.8	2.5	0.011	687	2.0	0.010	824	0.011	100
C-1	0.30	2.0	1.7	0.017	534	1.2	0.015	693	0.011	95
C-2	0.30	1.7	1.6	0.017	544	1.3	0.016	643	0.011	97
C-3	0.30	4.8	4.0	0.007	924	3.5	0.006	1048	0.013	98
C-4	0.30	4.0	3.7	0.007	896	2.9	0.007	1081	0.010	97
D-1	0.28	2.0	1.1	0.029	392	0.6	0.023	627	0.012	75
D-2	0.28	3.0	1.5	0.020	490	1.1	0.019	591	0.013	68
D-3	0.28	4.5	3.4	0.008	870	3.0	0.008	957	0.009	97
D-4	0.28	4.0	3.2	0.009	830	2.7	0.008	968	0.010	100
E-1	0.25	2.8	1.1	0.023	479	0.9	0.022	534	0.012	77
E-2	0.25	2.8	1.6	0.017	557	1.2	0.016	666	0.015	89
E-3	0.25	3.0	2.7	0.011	691	2.2	0.010	835	0.011	95
E-4	0.25	4.7	2.6	0.009	884	2.1	0.008	1034	0.010	100

1. Pressure Meter, 2. Linear Traverse, 3. Spacing Factor,
4. Specific Surface, 5. Philleo's Factor, 6. Relative Dynamic Modulus.

Table 6.6. Results of Drying.

SPECIMEN NO.	SATURATED W (gr)	DRY W (gr)	LOSS (gr)	LOSS %
A1	482.2	449.5	32.7	7.3
A2	502.0	468.2	33.8	7.2
A3	485.1	452.9	32.2	7.1
A4	479.4	444.2	35.2	7.9
A5	469.7	434.1	35.6	8.2
A6	468.3	434.2	34.1	7.8
A7	486.4	452.4	34.0	7.5
A8	478.0	442.9	35.1	7.9
A9	461.6	431.7	29.9	6.9
A10	465.0	434.6	30.4	7.0
A11	462.8	433.7	29.1	6.7
B1	484.9	455.3	29.6	6.5
B2	488.4	456.0	32.4	7.1
B3	480.3	451.5	28.8	6.4
B4	490.3	458.3	32.0	7.0
C1	493.7	461.0	32.7	7.1
C2	465.2	433.5	31.7	7.3
C3	480.1	448.9	31.2	6.9
C4	483.9	453.3	30.6	6.7
D1	499.7	464.6	35.1	7.5
D2	478.7	445.8	32.9	7.4
D3	470.0	437.7	32.3	7.4
D4	469.5	437.4	32.1	7.3
E1	471.9	443.3	28.6	6.4
E2	486.1	456.9	29.2	6.4
E3	482.2	454.2	28.0	6.2
E4	475.2	444.8	30.4	6.8

6.6 Summary Discussion

None of the parameters calculated above seem to have any correlation with the way specimens behaved in actual freeze-thaw testing. This is further evidence that the remarkable durability encountered in these experiments can only be attributed to the low permeability and lack of freezable water, and these two are the consequence of very low water to cement ratio concrete used for this research.

6.7 FAILURE MECHANISMS

6.7.1 Surface Scaling

As mentioned above, none of the specimens tested throughout this study exhibited any sign of surface distress (scaling). There is evidence (48) showing that the progress of scaling in non air-entrained concrete is much lower for silica fume concrete as compared to ordinary concrete. But the ASTM specification for testing concrete's resistance to freezing and thawing (ASTM C666), is not generally a rigorous test method. Various apparatus and procedures are employed in different laboratories which make the reproduction of test results between laboratories a difficult, if not an impossible task. Therefore the comparison of test results without an accurate knowledge of the procedure employed can be misleading. On the subject of concrete's scaling as a result of freezing and thawing, the type of apparatus used is even more critical, since the scaling is very much a function of the freezing condition imposed on the specimen.

In Logan type machines (the one used for this study) the specimens are laid horizontally and freezing proceeds from bottom of the specimens toward the top. The pressure produced by freezing water around the specimens are relieved from the top, through a rather short distance (4 in.). In

some of the other freeze-thaw machines the samples are placed vertically in the boots and freezing proceeds from top toward the bottom. This will cause the pressure of freezing water around each specimen to be exerted on the surface, producing more severe scaling. Previous experience in the Virginia Tech laboratory showed that (76), non air-entrained specimens from ordinary concrete exhibit both modes of freezing and thawing damage, surface scaling and internal cracking. However scaling occurs much later in Logan machines as compared to some other types of freeze-thaw machines. For example scaling in an air-entrained specimen of ordinary concrete starts after 100 cycles of exposure in Logan freeze-thaw equipment, were in others it occurs as early as the first 50 cycles.

Since scaling occurs only when concrete is frozen under water, it is probably related to the saturation of the capillary pores in the paste close to the surface of concrete. The lack of scaling observed in this study even though the specimens were submerged in water for the entire curing and freeze-thaw testing periods can only be explained by the following hypothesis.

The size of capillary in a hardened paste have a direct impact on the temperature where freezing can initiate. The relation is defined by the following equation known as Thompson's equation (62).

$$T_r = T_s \exp - \left(\frac{2\sigma M}{r_c Q d}\right)$$

where

T_r = Fusion temperature of an ice crystal with the radius r_c.

$T_s = 273°K$.

σ = Interfacial energy between ice and water = 10.2 dynes/cm.

M = Molecular weight of ice = 18.02 gr/mol.

Q = Molar heat of fusion = 14,400 cal/mol.

d = Density of ice = 0.917 gr/cm^3

In a capillary channel of cement paste regardless of temperature, a film of unfrozen water remain absorbed on the solid surface. The thickness of this film varies slightly with temperature but it is approximately 4 molecular layers of water. An ice crystal in a capillary with a diameter equal to D can only exist when its diameter is smaller than (D + 2ut), where:

u = The number of molecular mono-layers of water = 4

t = The thickness of a mono-layer of water = 3.1 Å.

In an study done by Bager et al (79), the heat of fusion released by the capillary water at the time of freezing was measured for several saturated specimens of neat cement paste. The mixtures varied in water-cement ratio from 0.60 to 0.35. The results are shown in Figure 6.22 which is reproduced from reference (79). Each peak in the top graphs corresponds to the initiation of freezing of water in a specific capillary size. The curve $W_{ice}(RT)$ in the bottom plot shows the total amount of water frozen when temperature was decreased to -55 °C (-67 ° F).

Using Thompsons's equation the diameter of the largest capillary where freezing started was calculated. For the specimen with the lowest water-cement ratio (0.35), the largest capillary where water started to freeze is equal to 42 Å, and this corresponds to -20° C (-4° F). The next peak on the graph (Figure 6.22) is at $-40°F$ considerably below the temperature experienced ($-15°F$) in our machine (see Appendix B) and the recommendation of ASTM C666 ($0°F$) Figure 6.23 shows the capillary size restriction on freezing corresponding to the freezing temperature in the range of concern in this research. Considering the above, the saturated capillaries in the paste matrix of low water-cement ratio (perhaps less than 0.32) concrete are so small that the exposure to the freezing condition with the temperature in the range of 32 to $-15°F$ was not capable of freezing the water to induce any surface damage.

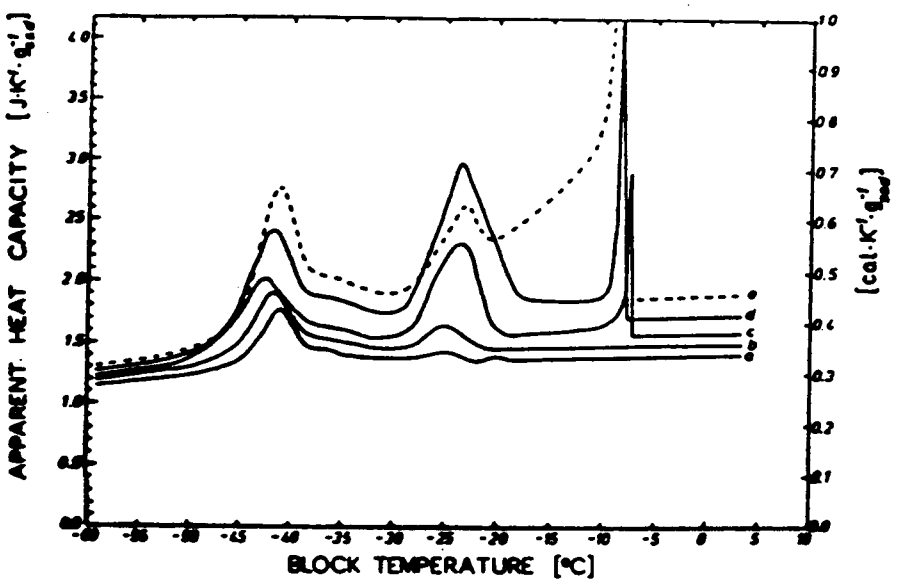

Apparent heat capacity curves.
A: Cooling and B: Heating. a, b, c, d, e represent water/cement ratios of 0.35, 0.40, 0.45, 0.50, and 0.60, respectively.

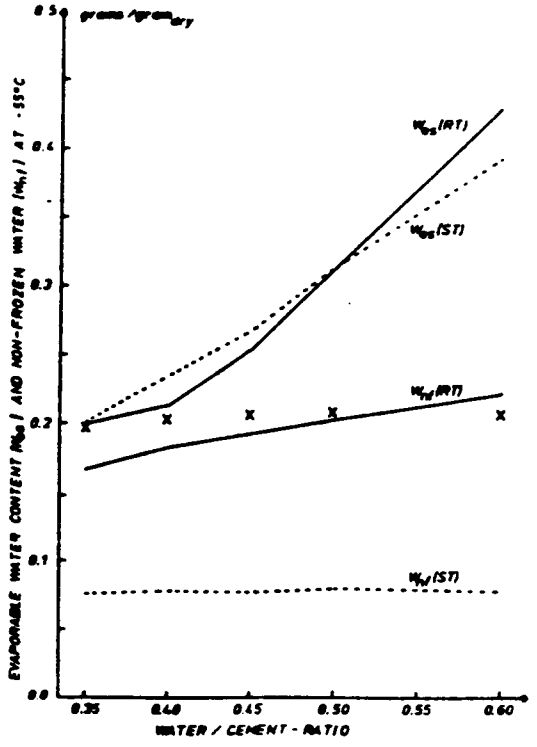

Amounts of total evaporable water (w_{es}) for virgin saturated specimens and non-frozen water at -55° C (w_{nf}) as a function of water/cement ratios, both for room temperature (RT) and steam (ST) cured pastes. "X" marks the calculated amount of non-frozen water in RT pastes according to de Fontenay (3).

Figure 6.22. Heat Capacity and Total Freezing Water

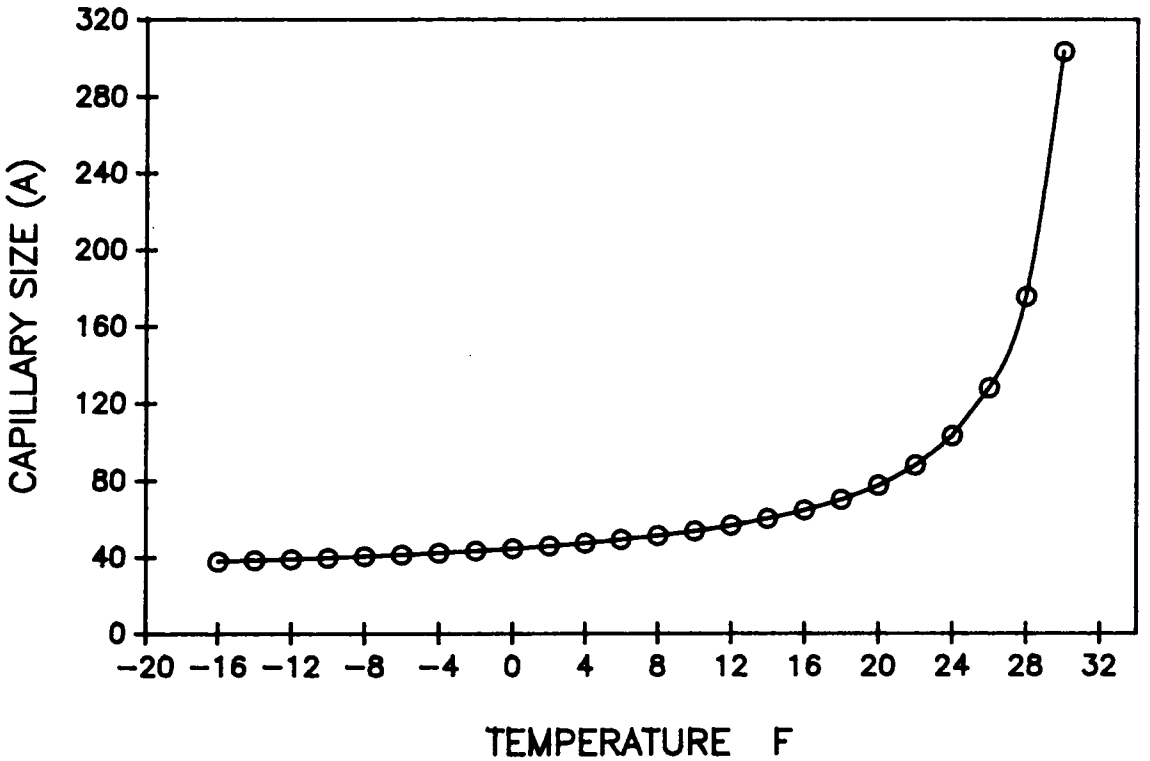

Figure 6.23. Plot of Thompson's Equation.

6.7.2 Internal Cracking

In an ordinary concrete, residual capillary water remaining from incomplete hydration reactions at early ages or later saturation (due to high permeability) is responsible for the frost damage. In such a concrete failure occurs rather early since capillaries are numerous and the destructive internal pressure is produced throughout the paste matrix at the onset of the freezing front.

When water-cement ratio is reduced, and specially for high strength concrete and when pozzolans are used, high cement content causes a rapid depletion of water in early age and this will eliminate the potential for the creation of a great percentage of capillary channels. The natural consequence is the reduction of concrete's permeability and porosity. The porosity is specially reduced by pozzolanic reaction of silica fume which is shown to drastically refine the paste's pore structure (28,39,41). According to Litvan (69), in a concrete where permeability and porosity are both low, if freezing initiates at a site such as a saturated flaw and there are no adequate air void systems, the rapid process of freezing can produce such a high rate of water expulsion that an orderly migration of the excess water is not possible and as a result enough pressure will be created to initiate the internal fracturing process.

This can explain why the non air-entrained concrete with water-cementitious ratio of 0.32 incorporating 10 percent silica fume failed, but similar concrete without silica fume, regardless of the length of curing period survived the 300 cycles of freezing and thawing. The specimens with silica fume had a lower permeability and porosity compared to the ones without silica fume. Once some site inside the silica fume concrete specimens became saturated (during an average of 190 cycles of exposure to freezing and thawing under water), the lack of adequate porosity could not accommodate the rapid migration of the excess water and it caused the speedy failure. The higher porosity and permeability in the concrete without silica fume allowed the orderly migration needed for the small amount of expelled water without producing the damaging pressure. When the water to cementitious ratio were decreased further than 0.32, the system became so impermeable that ei-

ther water could not permeate through for saturating the cavities, or a much longer period of time (beyond the period under water during curing and freeze-thaw testing) was needed for the water to saturate the flaws and cavities inside the concrete in order to cause failure.

According to Philleo (80) the concrete that is gaining strength has a capacity for freezable water, since a concrete can gain strength only if there is available space for depositing hydration products. He also points out that even the highest strength concrete cannot contain the pressure produced by the freezing of freezable water which exerts a force in excess of 30,000 psi. Results obtained from this study contradict such a view, since all the non air-entrained concrete specimens tested here, regardless of their water to cementitious ratio, significantly gained in strength beyond the freeze-thaw testing ages of 14 and 28 days (Figure 6.1 and 6.2). According to the above theory all theses samples should have failed. This gives rise to the hypothesis that although both water and space were available for the hydration activities to continue, the spaces were small enough that water could not freeze. The ones that failed (D1) were most likely due to the pressure created in a few saturated freezing sites such as flaws created by shrinkage cracks.

Chapter VII

CONCLUSIONS AND RECOMMENDATIONS

7.1 CONCLUSIONS

Based on the preceding experiments, following conclusions can be drawn.

1. General Conclusions.

1. The effectiveness of air entraining agents in producing air in plastic concrete (with low water cement ratio) is much more sensitive to the concrete's workability than the dosage of agent added.

2. The entrainment of air into high strength concrete causes a loss of 5 percent in compressive strength for each 1 percent of air-entrained.

3. The addition of silica fume into concrete significantly increases its compressive strength.

4. Reduction of water-cement ratio significantly improves its compressive strength and freeze-thaw durability of concrete.

2. Freeze-Thaw performance.

1. The 0.32 for water-cementitious ratio (and 10% SF) is the limit point at (and above) which concrete have to be air-entrained in order to be frost resistant.

2. Concrete with water-cementitious ratio of less than 0.32 does not need air-entrainment

3. Lack of failure in non air-entrained specimens can only be attributed to the lack of freezable water.

4. Capillary pore system in concrete with water-cement ratio less than 0.32 is smaller than 40 Å and for water to freeze in such a small voids, the temperature have to reach far below -15 ° F.

5. Propagation of cracks as the result of ice expansion in the internal flaws of hardened paste is most likely mechanism of failure (Litvan's hypotheses).

3. Effect of Curing Time.

1. Increasing the curing period from 14 days (ASTM C666 recommendation) to 28 days did not have any significant effect on the resistance of concrete with W/C ratio of 0.32 and less to freezing and thawing.

2. The hypothesis here is that due to high cement content in high strength concrete and specially when silica fume is used, internal self desiccation and highly reduced permeability depletes the system from a substantial amount of freezable water in a short period of time (perhaps less than 14 days).

3. Failure basically is due to saturation of flaws such as shrinkage cracks in the paste matrix, and this process for the concrete with water-cement ratio of 0.32 took at least 100 cycles. While non air-entrained ordinary concrete fails in the first few cycles of exposure to freezing and thawing.

4. Air Void Parameters.

1. Concrete with water-cementitious ratio of 0.32 even with a low air content of 2.9 percent (A-6) performed exceptionally well in a freezing and thawing environment.

2. Spacing factor for all the non air-entrained specimens was (0.018 to 0.035 in.) exceeding the requirement by ACI (0.008 in.), and for air-entrained specimens they varied from 0.005 to 0.018 in.

3. Specific surface for non air-entrained specimens are from 261 to 537 $\frac{in^2}{in^3}$ and for air-entrained specimens the range is 455 to 1265 $\frac{in^2}{in^3}$.

4. Philleo's factor for non air-entrained specimens are ranging from 0.011 to 0.025 in. and for air-entrained specimens they are 0.008 to 0.014 in..

5. When measured chords greater than 1 mm. was not considered in the calculation of air void parameters, the specific surface increased but it caused a decrease in spacing factor. No correlation was found between these calculated parameters and the freeze-thaw performance.

6. Same conclusion (lack of correlation) was obtained when chords greater than 0.5 mm. was excluded from the calculations.

7. Freeze-thaw performance of concrete with water-cement ratio of less than 0.32 is independent of the air void parameters.

7.2 RECOMMENDATIONS FOR FURTHER RESEARCH

1. Specimens from similar concrete should be tested in accordance with ASTM C671. This can be particularly beneficial since in this method the expansion rather than dynamic modulus is measured and the temperature corresponding to the initiation of dilation can be used to find the capillary pore size where freezable water exist.

2. The change in permeability as the result of curing should be monitored for concrete with water to cement ratio less than 0.32 with and without silica fume.

3. The non air-entrained concrete with water cementitious ratio of 0.32 and 10 percent silica fume failed to survive the 300 cycles of exposure to freezing and thawing. It is recommended to increase the silica fume content to 15 percent or even higher, since this might decrease the permeability to a level where saturation is not possible. Another suggestion is to allow a period of air drying before exposure to freezing and thawing.

4. The cement content of the concrete tested in this research were fairly high (9 to 10 bags/ Yd^3), which makes the concrete relatively expensive. It is recommended to decrease this to 7 or 8 bags per cubic yard (W/(C+SF) of 0.32 to 0.25) and repeat similar experiments.

REFERENCES:

1. Skalny J., " Concrete Durability-An Issue of National Importance", Concrete Durability, Katharine and Bryent Mather International Conference, ACI SP-100, Vol 1, PP.265-280,1987.

2. Powers T.C., and Copeland H.," Permeability of Portland Cement Paste ", Journal of ACI, Vol 26, No.3, PP. 285 - 298, Nov.1954.

3. Powers T.C. and Brownyard T.l., " Studies of the Physical Properties of Hardened Portland Cement Paste ", In nine parts, Journal of ACI, from October 1946 to April 1947.

4. Philleo Robert E., " Freezing and Thawing Resistance of High Strength Concrete ", NCHRP Synthesis of Highway Practice 129, TRB, Dec. 1986.

5. ACI Committee 201, " Guide to Durable Concrete ", ACI Manual of Concrete Practice, Part 1., PP. 201.2R-1 - 201.2R-37, 1987.

6. American Concrete Institute, " Standard Practice For Concrete Highway Bridge Deck Construction ", ACI 345-74 Proposed Revision, Concrete International, Design and Construction, Design and Construction, Vol. 3, No. 9, Sep. 1981

7. American Concrete Institute, " High Strength Concrete ", ACI Special Publication 87, 1985.

8. American Society of Testing Materials, " Annual Book of ASTM Standards ", Section 4, Construction, Volume 04.02, Concrete and Aggregate, 1987.

9. American Concrete Institute," State-of-the-Art Report on High Strength Concrete ", ACI committee 363. ACI Manual of Concrete Practice, PP. 363R-1 - 363R-48, 1987.

10. Peterman M.B. and Carrasquillo R.L. " Production of High Strength Concrete ", Noyes Publication of High Strength Concrete", Noyes Publications N.J., 1986.

11. " Structural Trends in New York City Buildings, " Civil Engineering ASCE vol.53, no.1., PP. 30 - 37, January 1983.

12. Rixom M.R. and Mailvaganam N.P., " chemical Admixtures for concrete " , Second Edition, E.& F.N. spon LTD, London, 1986.

13. Ramachandran V.S., " Concrete Admixtures Handbook, Properties, Science and Technology ", Noyes Publications, N.J. 1984.

14. ACI Committee 226, " Silica Fume in Concrete " , ACI Material Journal, PP. 158-165, March-April 1987.

15. Ozgildirim C., " Laboratory Investigation of Concrete Containing Silica Fume for use in overlays ", ACI Materials Journal, PP. 3-7, Jan-Feb 1987.

16. Elkem Chemicals, Inc., " Using EMSAC™ F-100T Concrete Admixture in Ready-mixed Concrete " , EMSAC™ User Notes, Elkem Chemicals Inc., Feb. 1987.

17. Grutze M.W., Atkinson, Roy D.M. , " Mechanism of Hydration of Condensed Silica Fume in Calcium Hydroxide Solutions ", Fly Ash, Silica Fume, Slag, & other Mineral By-Products in Concrete, ACI Special Publication No. 79, vol.2, PP. 643-664, 1983.

18. Cheng-Yi H. and Feldman R. F., " Influence of Silica Fume on the Micro Structural Development in Cement Mortars " Cement and Concrete Research, vol 15, PP. 285 - 294, 1985.

19. Sarkar S.L. and Aitcin P.C., " Dissolution Rate of Silica Fume in very High Strength Concrete ", Cement and Concrete Research, vol. 17, PP. 591-601, 1987.

20. Sellevold E.J. and Radjy F.F., " Condensed Silica Fume (Microsilica) Concrete: Water Demand and Strength Development ", Fly Ash,Silica Fume, Slag & Other Mineral By-Products in Concrete, Vol. II, ACI publication SP-79, PP. 677 - 694, 1983.

21. Sellevold E.J., " Condensed Silica Fume in Concrete: A World Review ", Elkem Chemical, Feb. 1986.

22. Jahren P., " Use of Silica Fume in Concrete ", Fly Ash,Silica Fume, Slag & Other Mineral By-Products in Concrete, Vol. II, ACI Publication SP 79, PP. 677 - 694, 1983.

23. Carette G. and Malhotra, " Early Age Strength Development of Concrete Incorporating Fly Ash and Condensed Silica Fume ", Fly Ash,Silica Fume, Slag & Other Mineral By-Products in Concrete, Vol. II, ACI Publication SP 79, PP. 765 - 784, 1983.

24. Ramakrishnan V. and Srinivasan V., " Performance Characteristics of Fiber Reinforced Condensed Silica Fume Concrete ", Fly Ash,Silica Fume, Slag & Other Mineral By-Products in Concrete, Vol. II, ACI Publication SP 79, PP. 797 - 812, 1983.

25. Skrastins J.I. and Zoldners N.G., " Ready Mixed Concrete Incorporating Condensed Silica Fume " Fly Ash,Silica Fume, Slag & Other Mineral By-Products in Concrete, Vol. II, ACI Publication SP 79, PP. 813 - 829, 1983.

26. Regourd M., Mortureux B., and Hornian H., " Use of Condensed Silica Fume as Filler in Blended Cements ", Fly Ash, Silica Fume, Slag & Other Mineral By-Products in Concrete, Vol. II, ACI Publication SP-79, PP. 847 - 865, 1983.

27. Pierre-Claude A. and Vezina D.," Resistance to Freezing and Thawing of Silica Fume Concrete ", Cement, Concrete, and Aggregate, ASTM, PP. 38 - 42, 1984.

28. Sandvik M., and Gjorv, " Effect of Condensed Silica Fume on the Strength Development of Concrete ", Fly Ash, Silica Fume, Slag, and Natural Pozzolans in Concrete, Proceedings of Second International Conference, Madrid, Spain, vol. 2, ACI SP-91, PP. 893 - 901, 1986.

29. Malhotra V.M., " Mechanical Properties, and Freezing -and-Thawing Resistance of Non-Air-Entrained and Air-Entrained Condensed Silica Fume Concrete Using ASTM Test C666 Procedures A & B ", Fly Ash, Silica Fume, Slag, and Natural Pozzolans in Concrete, Proceedings of Second International Conference, Madrid, Spain, Vol. 2, ACI SP-91, PP. 1069 - 1094, 1986.

30. Yamato T., Emotoy. Soeda M., " Strength and Freezing -and-Thawing Resistance of Concrete Incorporating Condensed Silica Fume ", Fly Ash, Silica Fume, Slag, and Natural Pozzolans in Concrete, Proceedings of Second international Conference, Madrid, Spain, Vol. 2, ACI SP-91,PP. 1095 - 1117, 1986.

31. Kahno K. and Komatsu H., " Use of Ground Bottom Ash and Silica Fume in Mortar and Concrete ", Fly Ash, Silica Fume, Slag, and Natural Pozzolans in Concrete, Proceedings of Second International Conference, Madrid, Spain, Vol. 2, ACI SP-91, PP. 1279-1292, 1986.

32. Christensen D.W, Sorenson E.V.,and Radjy F.F., " Rockbond^{TM} : A New Microsilica Concrete Bridge Deck Overlay Material ", Proceedings of the First International Bridge Conference, Pennsylvania, PP. 151 - 160, June 1984.

33. Fistilli, M.F. & Rau G., and Cechner R., " The Variability of Condensed Silica Fume from a Canadian Source and its Influence on the Properties of Portland Cement Concrete ", Cement, Concrete, and Aggregate, ASTM, PP. 33-37, 1984.

34. Pigeon M., Pirre-Claude A., and Laplante P., " Comparative Study of the Air-Void Stability in a Normal and a Condensed Silica Fume Field Concrete ", ACI Materials Journal, PP. 194-199, May-June 1987.

35. Yogendran V., Langan B.W., Haque M.N., and Ward M.A., " Silica Fume in High Strength Concrete ", ACI Material Journa, PP. 124-129, March-April 1987.

36. Carles-Gibergues A., Grandet J., Ollivier J.P., "Contact Zone between Cement Paste and Aggregate", Bond in Concrete, Applied Science Publishers, PP. 24-33, 1982.

37. Mehta K.," Pozzolanic and Cementitious By-products as Mineral Admixtures for Concrete- A critical Review ", Fly Ash, Silica Fume, Slag & Other Mineral By-Products in Concrete, ACI Publication SP-79, Vol. I, PP. 1 - 46, 1983.

38. Feldman R.F., " Influence of Condensed Silica Fume and Sand/Cement Mortars ", Fly Ash, Silica Fume, Slag, and Natural Pozzolans in Concrete, Proceedings of the Second International Conference, vol. 2, PP. 973-989, Madrid, Spain, 1986.

39. Mindess S. and Gray R. J., " Effect of Silica Fume Addition on the Permeability of Hydrated Portland Cement Paste and the Cement-Aggregate Interface ", Proceedings of Symposium on Technology of Concrete When Pozzolans, Slag, and Chemical Admixtures are used. ACI and RILEM, Monterry, Mexico, 1985.

40. Gjorv E.O., " Durability of Concrete Containing Condensed Silica Fume " ,Fly Ash, Silica Fume, Slag & Other Mineral By-Products in Concrete, ACI Publication SP-79, Vol. II, PP. 695 - 708, 1983.

41. Nagataki S. and Ujike I. " Air Permeability of Concrete Mixed with Fly Ash and Condensed Silica Fume ", FA, SF, S, Proceeding ACI, 1986.

42. Traetteberg A., " Frost Action in Mortar of Blended Cement with Silica Dust ", Durability of Building Materials and Components, ASTM ST P-691, PP. 536-548, 1980.

43. Virtanen J. " Freeze-Thaw Resistance of Concrete Containing Blast-Furnace Slag, Fly Ash or Condensed Silica Fume ", Fly Ash, Silica Fume, Slag & Other Mineral By-Products in Concrete, ACI Publication SP-79, Vol. II, PP. 923 - 942, 1983.

44. Radjy F.R., Loeland K.E., " Microsilica Concrete: A Technological Break through Commercialized " , Proceedings of Material Research Symposium", vol. 42, PP. 305-312, 1985.

45. Carette G.G., Malhotra V.M., " Mechanical Properties, Durability, and Drying Shrinkage of Portland Cement Concrete Incorporating Silica Fume", Cement, Concrete, and Aggregate, ASTM, PP. 3-13, Summer 1983.

46. Sorensen E.V.," Freezing and Thawing Resistance of Condensed Silica Fume (Microsilica) Concrete Exposed to Deicing Chemical ", Fly Ash, Silica Fume, Slag & Other Mineral By-Products in Concrete, ACI Publication SP-79, Vol. II, PP. 709 - 718, 1983.

47. Malhotra V.M., Painter K.A., and Bilodeau A. " Mechanical Properties and Freeze and Thawing Resistance of High-Strength Concrete Incorporating Silica Fume ", Cement, Concrete and Aggregates, ASTM, PP. 65-79, 1987.

48. Pigeon M., Pleau R., Aitcin P.C., " Freeze-Thaw Durability of Concrete with and without Silica Fume in ASTM C666-Procedure A Test Method: Internal Cracking Versus Scaling ", Cement, Concrete, and Aggregates, vol 8., No.2, PP.76-85, 1986.

49. Pigeon M., Gange R., Foy C., " Critical Air-Void Spacing Factors for Low Water-Cement Ratio Concrete with and without Condensed Silica Fume ", Cement and Concrete Research, vol. 17, No. 6, PP. 896-906, 1987.

50. Whiting D., " Durability of High-Strength Concrete ", Concrete Durability , Katharine and Bryant Mather International Conference, ACI SP-100, vol 1, PP. 169-186, 1987.

51. Foy C., Pigeon M., Banthia N., " Freeze-Thaw Durability and Deicer Salt Scaling Resistance of A 0.25 Water-Cement Ratio Concrete ", Cement and Concrete Research, vol.18, PP. 604-614, 1988.

52. Khalil S.M. Ward M.A., Morgan D.R., " Freeze-Thaw Durability of Non Air-Entrained High Strength Concrete Containing Super Plasticizers ", Durability of Building Materials and Components, ASTM STP-691, PP. 509-519, 1980.

53. Cordon W., "Freezing and Thawing of Concrete-Mechanism and Control," ACI Monograph No. 3, 1966.

54. Chung-Hsing Lin, " The Effect of Freezing Rates on the Durability of Concrete, " PhD Dissertation, Virginia Polytechnic Institute and State University, June 1974.

55. Cady P. D.," A Brief Guide for Preliminary Visual Identification of the Most Common Forms of Distress in Portland Cement and Asphaltic Concrete ", June 1979, Handout given in CE. 5980, Virginia Tech, spring 1986.

56. Powers T. C., " Basic Consideration Pertaining to Freezing and Thawing Test ", ASTM Proc. Vol. 55, 1955.

57. Powers T. C.,Mann H. M., " Flow of Water in Hardened Portland Cement Paste ",Highway Research Board Special Report No.40, PP 308-323,1959

58. Powers T. C., " Physical Properties of Cement Paste ", Fourth International Symposium on Chemistry of Cement, Washington DC. PP 577-613,1960

59. Powers T. C.,Helmuth R. A.," Theory of Volume Change in Hardened Portland Cement Paste During Freezing ", Highway Research Board Proc. 32,PP 285-297,1953

60. Powers T. C., " The Air Requirement of Frost resistant Concrete ",Highway Research Board, Vol. 29,PP 184-202, 1949

61. Helmuth R. A., " Frost Action in Concrete ",Discussion on the Paper by Nernst P.,Proceedings of Fourth International Symposium on Chemistry of Cement, Vol 2, Washington DC.,1960

62. Helmuth R. A., "Capillary Size Restriction on Ice Formation in Hardened Portland Cement Paste ",Fourth International Symp. on Chemistry of Cement,Vol. 2,PP 855-869, Washington DC.,1960

63. Fontenay C. S., " Ice Formation in Hardened Cement Paste -1.Mature Water Saturated Paste ", ASTM, STP 691, PP 438-455, 1980

64. Litvan G. G.," Phase Transition of Adsorbates: IV.Mechanism of Frost Action in Hardened Cement Paste " ,Journal of American Ceramic Soc.,Vol. 55, No.1, PP. 38 - 42,January 1972

65. Beaudoin J. J., " The Mechanism of Frost Damage in Hardened Cement Paste " ,Cement and Concrete Research,Vol. 4, PP 139-147, 1974

66. Helmuth R. A., " Dimensional Changes in Hardened Portland Cement Paste ",Highway Research Board Proc. Vol. 40,PP 315-336,1961

67. Litvan G. G.," Frost Action in Cement Paste ",Materials and Structures,Vol. 6, No. 34, PP. 293 - 298,1973

68. Litvan G. G., " Freeze-Thaw Durability of Porous Building Materials " ,Durability of Building Material and Component, ASTM STP 691,PP 455-463,1980

69. Litvan G. G., " Frost Action in Cement in The Presence of De-Icers ",Cement and Concrete Research,Vol. 6, No. 3,PP 351-356,1976

70. Brown L.S. and Pierson C.U., " Linear traverse Technique for Measurement of Air in Hardened Concrete ", Journal of the ACI, PP 117-123, October 1950

71. Philleo R.E., " A Method For Analyzing Void Distribution in Air-Entrained Concrete ", Cement, Concrete, and Aggregate, Vol. 5, No. 2, PP. 128 - 130, Winter 1983.

72. American Concrete Institute, Committee 116, " Cement and concrete Terminology " , ACI Manual of Concrete Practice, Part 1, PP. 116-1 to 116-58, 1988

73. Lord G.W. and Willis T.F.," calculation of Air Bubbles Size Distribution from Rosiwal Traverse of Areated concrete ", ASTM Bulletin, PP 56-61, Oct. 1951.

74. Larson T.D.,Cady P.D., and Malloy J.J., " The protected Paste Volume Concept Using New Air-Void Measurement and Distribution Techniques ", Journal of Materials, PP. 202-226, .?

75. Chung-Hsing L., " The Effects of Freezing Rate on the Durability of Concrete ", Doctor of philosophy Dissertation, Virginia Polytechnic Institute and State University, June 1974.

76. Dr. Richard D. Walker, " Personal Conversation ", Virginia Tech, August, 1988.

77. Whiting W., " Air Content and Air Void Characteristics in Low Slump Dense Concrete ", ACI Journal, PP. 716-723, Sep-Oct 1985.

78. Radjy F.F., Bogen T., Sellevold E.J., Loeland K.E., " A Review of Experiences With Condensed Silica Fume Concrete and Products ", Proceedings of the Second International Conference, Fly Ash, Silica Fume, Slag, and Natural Pozzolans in Concrete, SP-91, Vol. 2, PP. 1135-1152, 1986.

79. Bager D.H., Sellevold E.J.," Ice Formation in Hardened Cement Paste, Part I.- Room Temperature Cured Pastes With Variable Moisture Content ", Cement and Concrete Research, Vol. 16, PP. 709 - 720, 1986.

80. Philleo R., " Frost Susceptibility of High-Strength Concrete ", Concrete Durability: Katharine and Bryant Mather International Conference, ACI SP-100, Vol. 1, PP. 819-842, 1987.

81. Whiting D. and Schmitt J., " Durability of In-Place Concrete Containing High-Range Water-Reducing Admixtures ", NCHRP Program Report No. 296, TRB, Sep. 1987.

82. Roberts L.R. and Scheiner P., " Air Void System and Frost Resistance of Concrete Containing Superplasticizers ", Developments in the Use of Superplasticizers, ACI Special Report No. 68, ACI, 1981

83. Malhotra V.M., " Testing Hardened Concrete: Nondestructive Methods " , ACI Monograph No. 9, 1976.

Appendix A

MIXTURE DATA

Table A.1. Coarse and Fine Aggregate Characteristics

	BULK SG.	UNIT WEIGHT lb./ft^3	ABSORPTION %	FINENESS MODULUS
C AGGREGATE	2.83	102	0.48	--
F AGGREGATE	2.53	94	1.67	2.80
SILICA FUME	2.20	39	--	--

Table A.2. Coarse and Fine Aggregate Gradations

SIEVE SIZE	C AGGREGATE %PASSING	F AGGREGATE %PASSING
1 in.	100	--
3/4	87	--
1/2	25	--
3/8	8	100
NO.4	1	100
NO.8	--	94
NO.16	--	76
NO.30	--	42
NO.50	--	7
NO.100	--	1
NO.200	--	0.2

Table A.3. Concrete mixture Data

MIXTURE NO.	W/(C+SF)	CEMENT lbs	SF lbs	CA lbs	FA lbs	WATER lbs	AEA oz*	HRWR oz*
A1-A3	0.32	952	95	1510	1109	335	0.0	0.0
A4-A8	0.32	952	95	1510	936	335	2.0	0.0
A9-A11	0.32	715	107	1547	1261	263	0.7	12.5
B1,B2	0.32	1047	0	1529	1121	335	0.0	12.3
B3,B4	0.32	1047	0	1529	1036	335	0.4	16.2
C1,C2	0.30	870	130	1579	1157	300	0.0	14.6
C3,C4	0.30	870	130	1579	1074	300	0.4	9.7
D1,D2	0.28	994	149	1475	1081	320	0.0	14.0
D3,D4	0.28	994	149	1475	996	320	0.5	11.0
E1,E2	0.25	974	146	1551	1134	280	0.0	24.0
E3,E4	0.25	974	146	1551	1048	280	0.5	24.0

* Ounces per 100 lbs. of cement.

Table A.4. Concrete's Plastic Characteristics

MIX NO.	W/(C+SF)	SLUMP IN.	TEMP. F	AIR %	UNIT WEIGHT Lb./Ft^3	R/YILED %
A-1	0.32	1.5	-	1.9	150	99
A-2	0.32	2.0	-	2.1	149	100
A-3	0.32	1.0	80	1.8	150	99
A-4	0.32	2.5	-	4.7	146	98
A-5	0.32	2.5	-	3.4	147	97
A-6	0.32	1.5	80	2.9	149	96
A-7	0.32	1.5	75	4.1	146	97
A-8	0.32	2.5	77	3.9	146	97
A-9	0.32	3.0	82	6.3	145	100
A-10	0.32	2.5	75	5.8	141	103
A-11	0.32	2.0	77	6.6	144	101
B-1	0.32	3.5	80	2.0	151	99
B-2	0.32	3.5	77	2.7	149	101
B-3	0.32	3.0	79	3.2	149	99
B-4	0.32	3.5	78	3.8	148	99
C-1	0.30	2.5	76	2.0	151	95
C-2	0.30	2.5	77	1.7	150	97
C-3	0.30	3.0	79	4.8	147	98
C-4	0.30	3.5	79	4.0	148	97
D-1	0.28	1.5	78	2.0	150	99
D-2	0.28	2.0	79	3.0	148	101
D-3	0.28	2.5	80	4.5	146	101
D-4	0.28	1.0	81	4.0	147	100
E-1	0.25	2.5	80	2.8	149	102
E-2	0.25	1.5	80	2.8	150	102
E-3	0.25	2.0	79	3.0	149	100
E-4	0.25	2.5	84	4.7	147	101

Appendix B

MONITORING THE FREEZE-THAW APPARATUS

In order to asses the true performance of the freeze-thaw apparatus, a concrete prism was made with four thermocouples placed at its core at different depths. Type T (Copper-Constantan) thermocouples were casted inside the prism at the depth of 3.5, 3, 2, and 0.75 In.. The data was collected during a completed freeze-thaw cycle, using an Apple-based data acquisition system (ISAAC). Temperature data from each thermocouple was collected at 5 minutes intervals. The temperature monitoring was conducted with the specimens in each one of the seventeen locations available in the freeze-thaw apparatus.

Figures B-1 to B-6 shows the typical temperature variations within the specimen at different locations. As it can be seen in the Figures B-1 to B-6 the freezing and thawing rate in all the seventeen locations is approximately the same. At the peak of thawing period there was a difference of 10 to 20 & deg. F from top to the bottom of the specimen. At the bottom of freezing period there was a temperature difference of 10 to 30 ° F between top and bottom of the specimen. The temperature at the depth of 2 In. when the apparatus was operating at the bottom of the freezing period, varied from -5 to -10 ° F in different locations within the freeze-thaw machine. The tem-

perature specified by ASTM C666 is at the middle of the specimen. Figure B-7 shows a picture of the specimen with the thermocouples in the freeze-thaw apparatus.

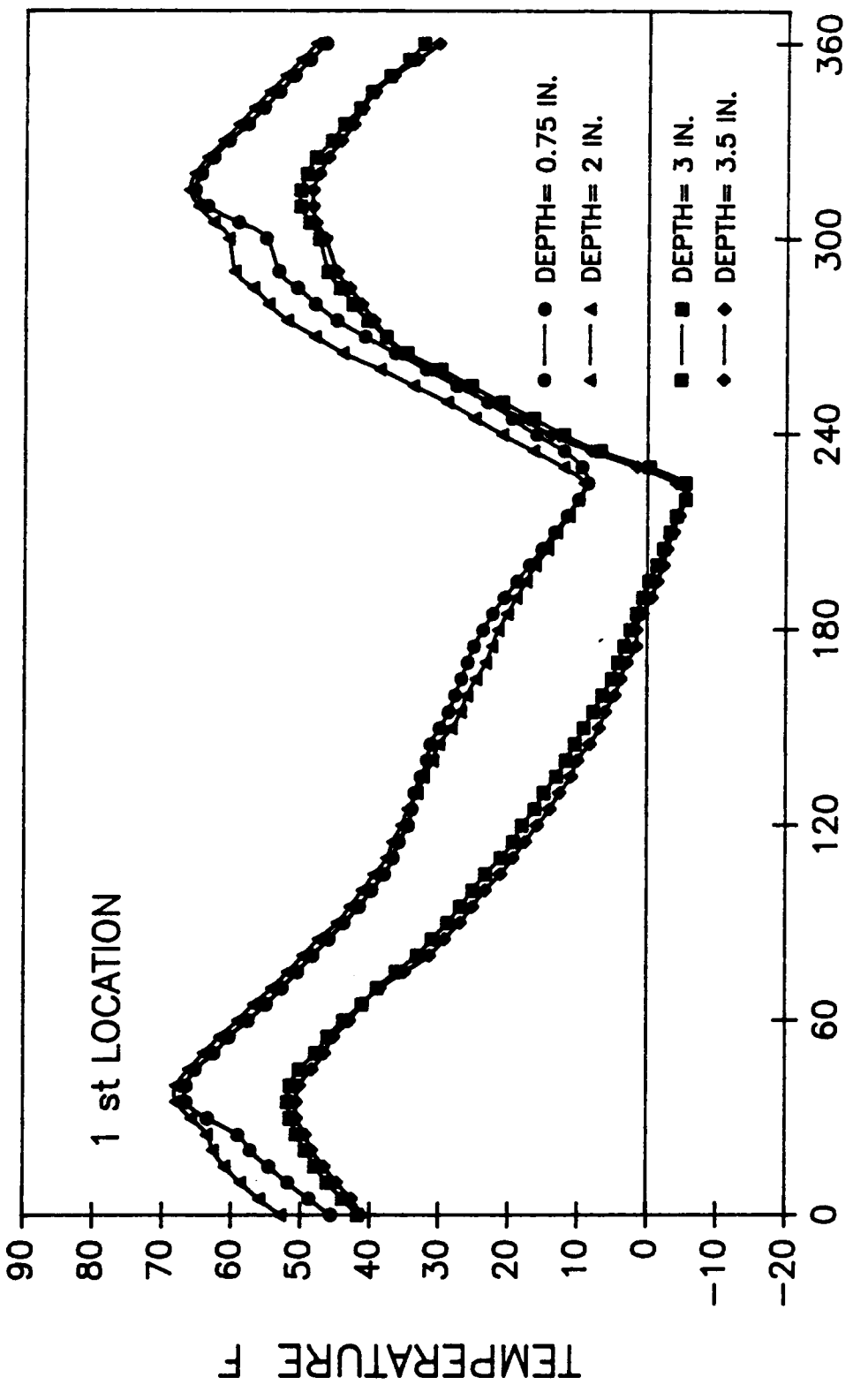

Figure B.1. Temperature Variation Within The Specimen Depth

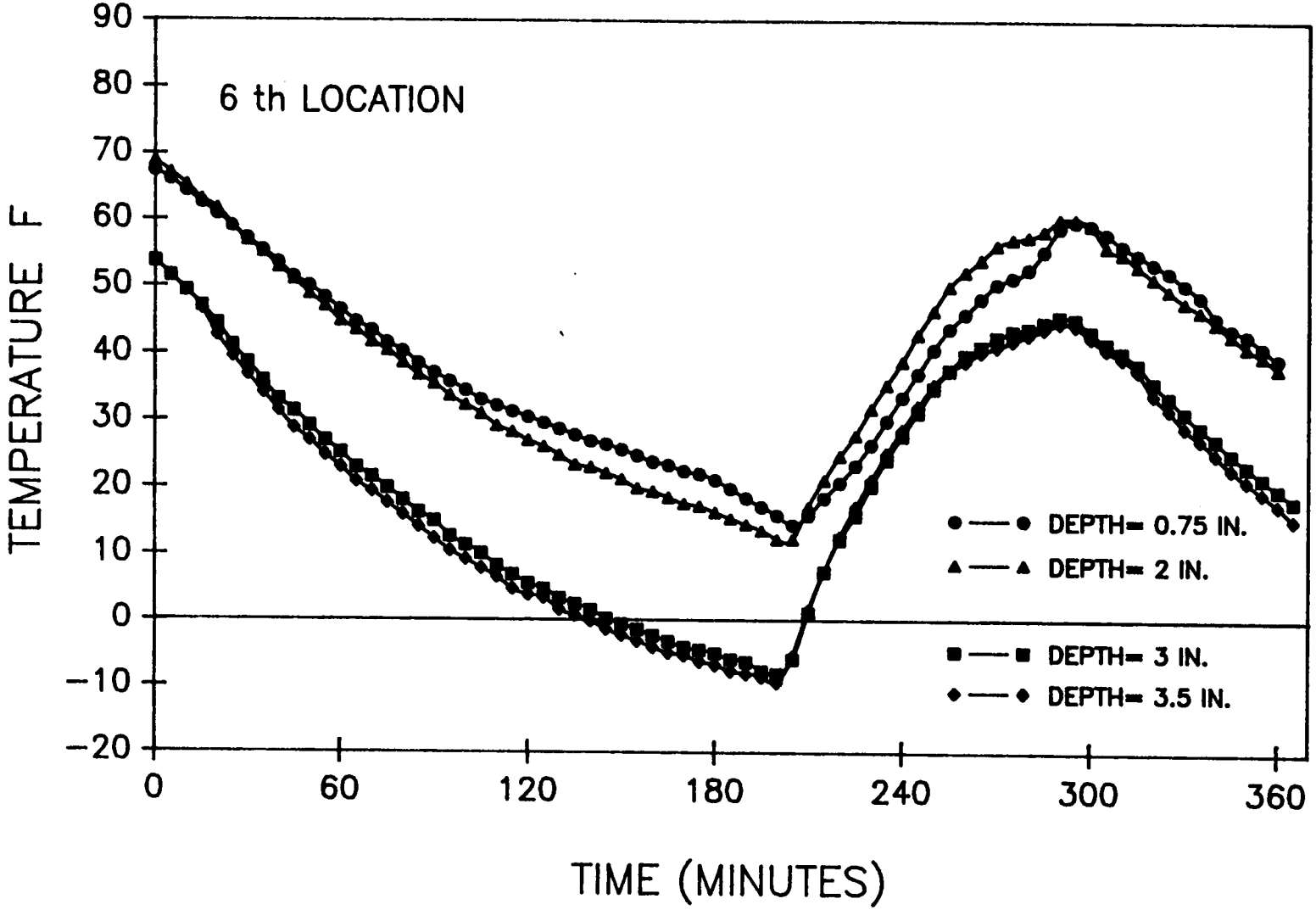

Figure B.2. Temperature Variation Within The Specimen Depth

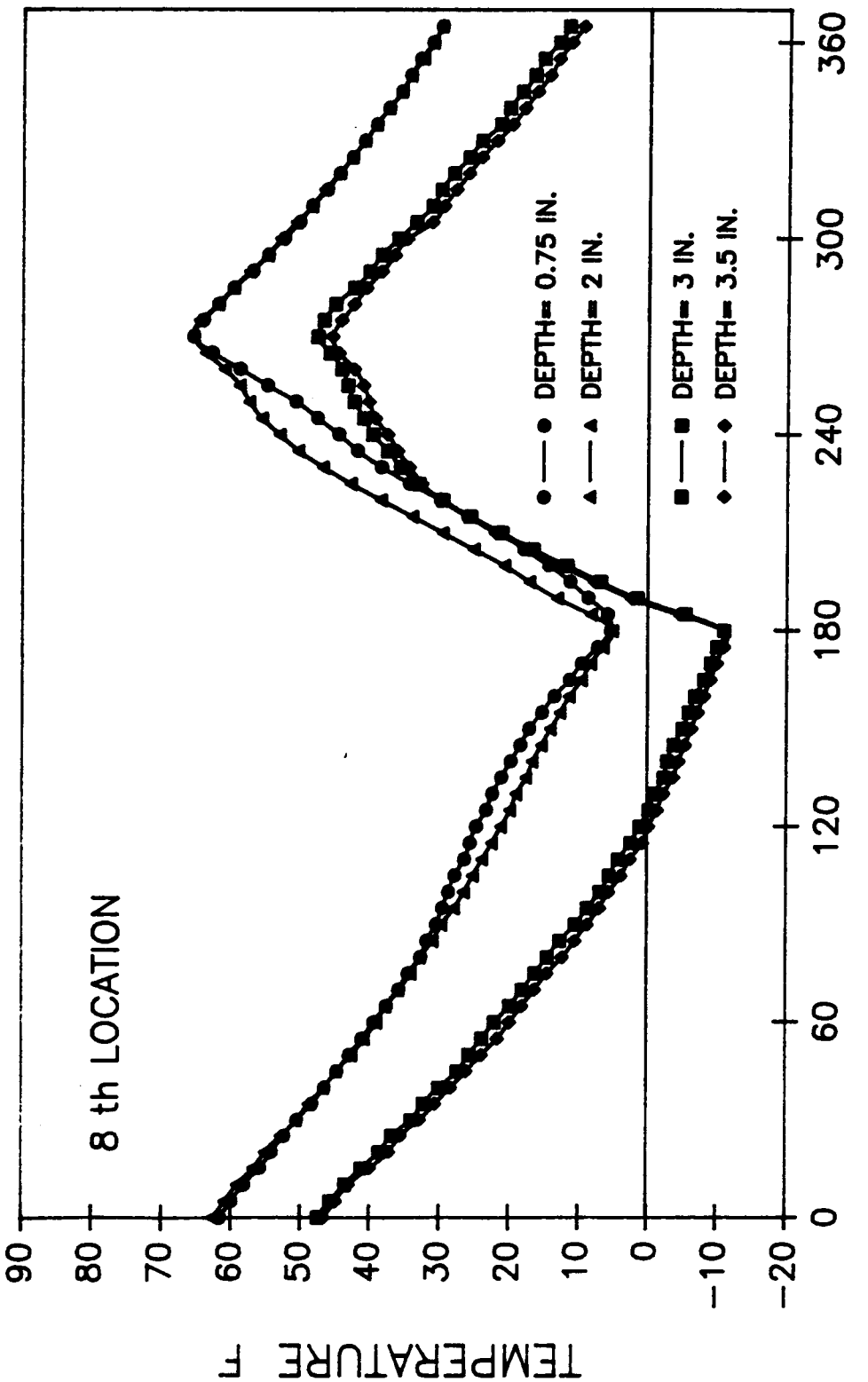

Figure B.3. Temperature Variation Within The Specimen Depth

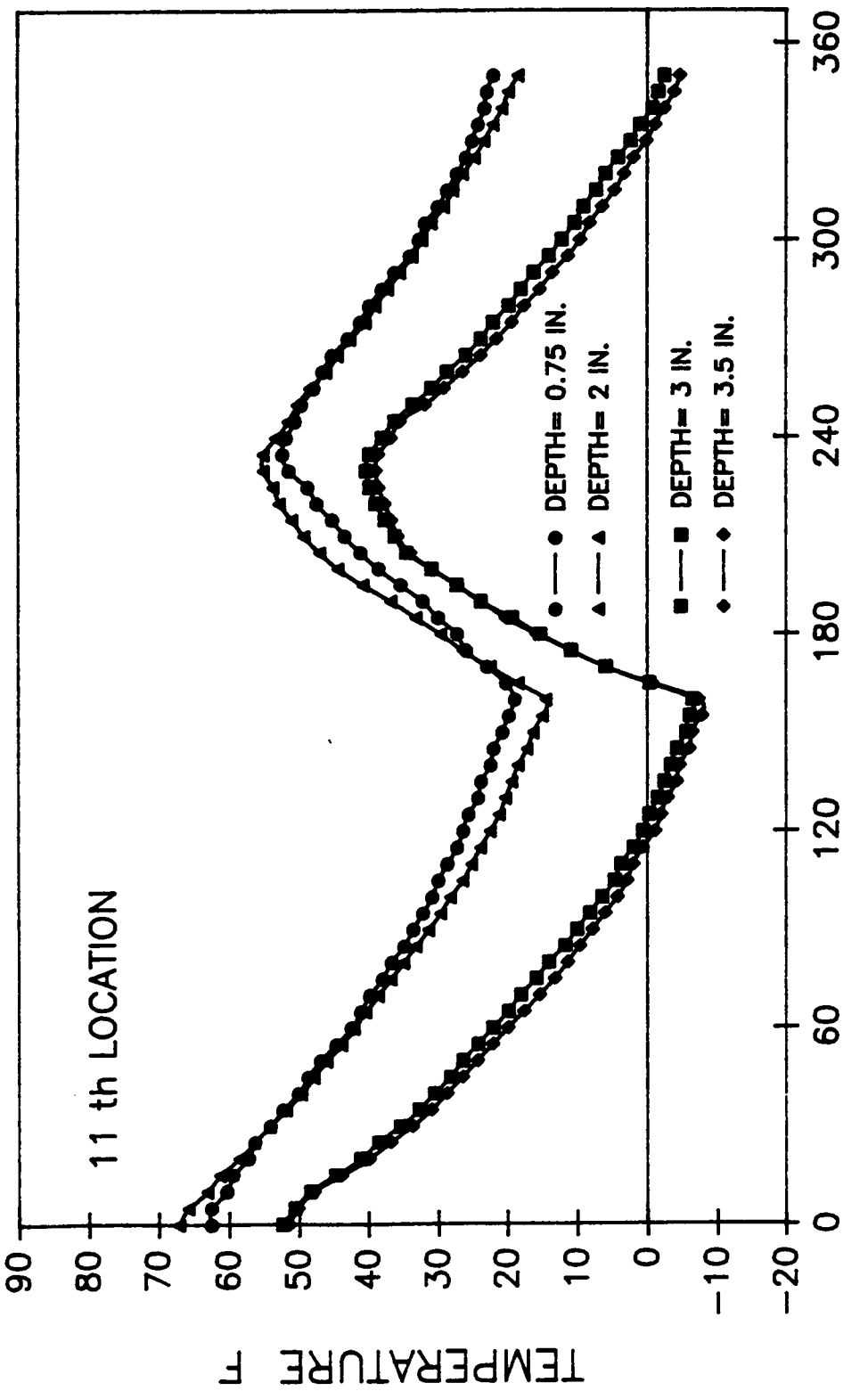

Figure B.4. Temperature Variation Within The Specimen Depth

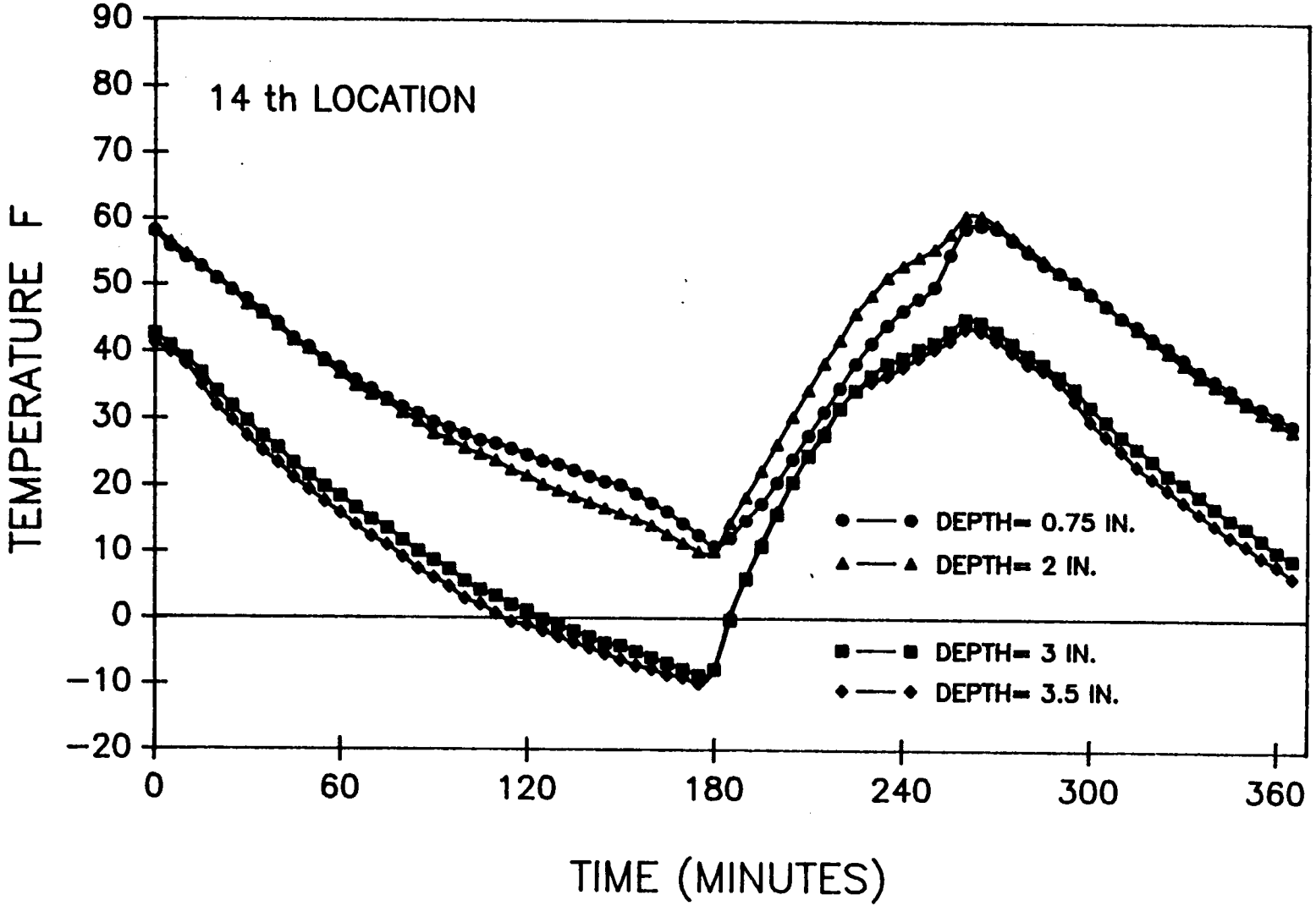

Figure B.5. Temperature Variation Within The Specimen Depth

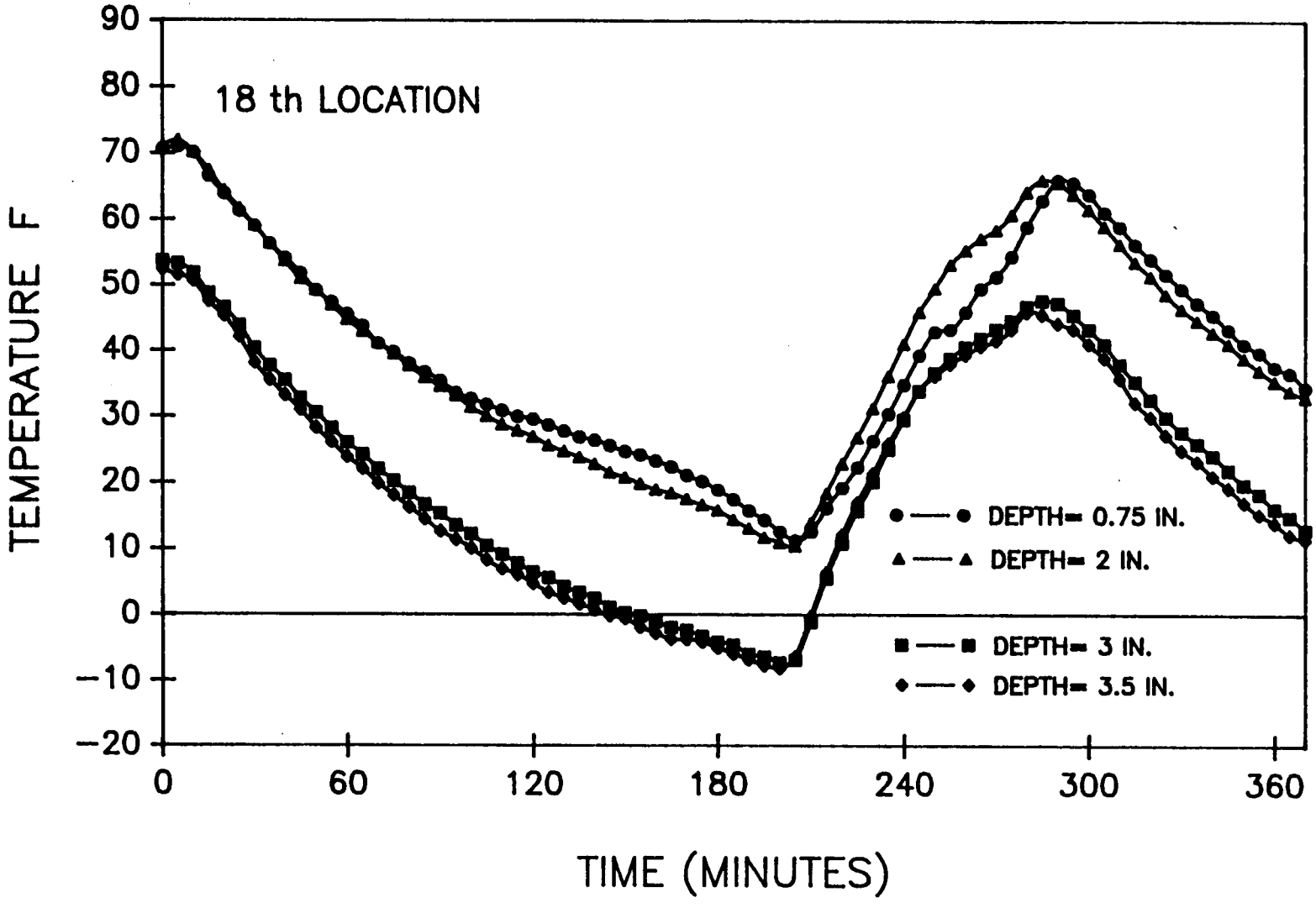

Figure B.6. Temperature Variation Within The Specimen Depth

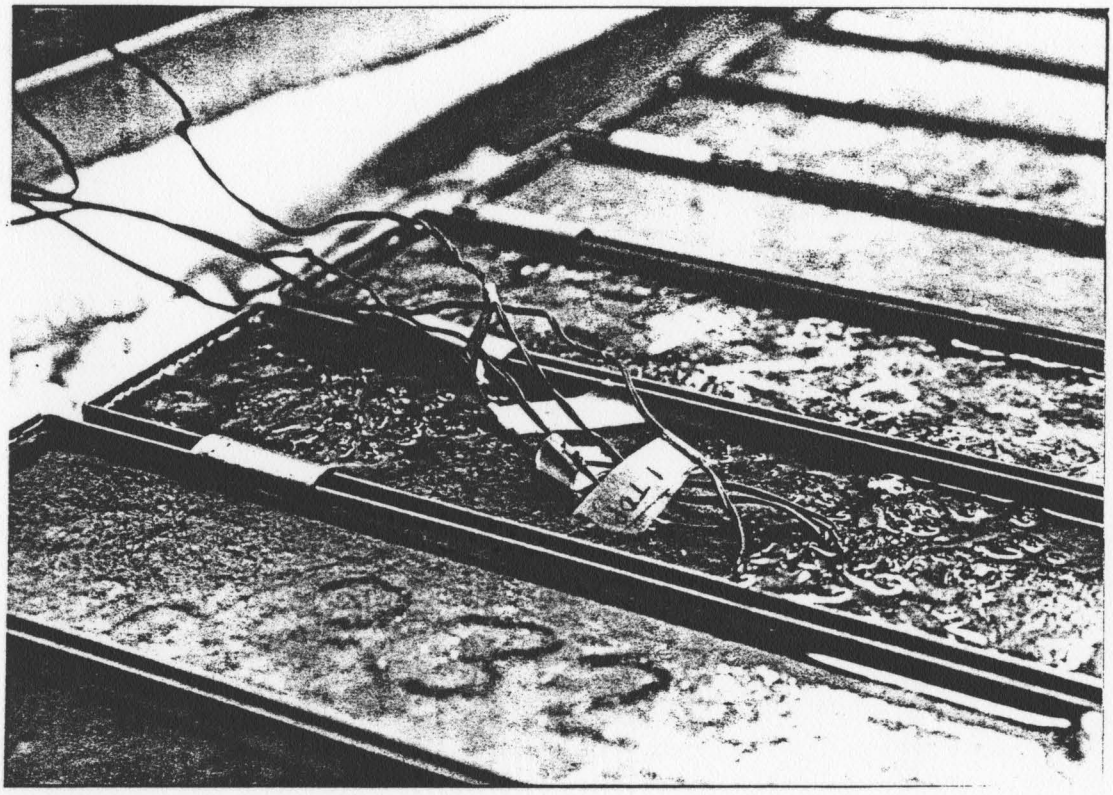

Figure B.7. The Beam With Thermocouples

Appendix C

DYNAMIC MODULUS

In concrete industry the strength is the major criterion for the quality and its direct determination requires one to load a specimen to failure. In order to detect the gradual effect of time-dependent deleterious forces such as freezing and thawing, the only alternative is to test the concrete through a nondestructive method. There are several nondestructive methods such as Schmidt rebound hammer, resonant frequency, ultrasonic pulse velocity, X and gamma rays transmission, and acoustic emission. The resonant frequency designated by ASTM C215 as standard test method for fundamental transverse, longitudinal and torsional frequencies of concrete specimens (8) is primarily used in the laboratories for the durability study on the concrete.

The concrete specimen which is usually a prism or cylinder is tested in the following fashion: The specimen is vibrated by a variable oscillator and it is tuned until there is a resonant frequency with the highest amplitude is the one of concern.

The testing apparatus primarily consists of an audio frequency counter. During testing the oscillator generates an audio-frequency voltage. The voltage is amplified to a level suitable for producing mechanical vibration. The specimen is caused to vibrate and its vibrations are sensed by a magnetic or a piezoelectric pick-up unit. The output is amplified and fed to the oscilloscope

and the counter. As the driver oscillator is tuned to the proper frequency, visible indication of the fundamental modes of vibration can be obtained. The frequency where the amplitude of the output vibration is at maximum, is measured by the counter and recorded (83). An schematic of the apparatus as given by the ASTM C215 is shown in the Figure C-1 and Figure C-2 shows a picture of the sonic testing machine used during this research.

Although the resonant frequency value can be used to calculate Young's dynamic modulus of elasticity, its prime use for durability study is to calculate the relative dynamic modulus of elasticity. The numerical value of the relative dynamic modulus of elasticity as specified by ASTM C666 is calculated as following:

$$P_c = \frac{n_1^2}{n^2} x100$$

where

P_c = Relative dynamic modulus of elasticity after c cycles of freezing and thawing

n = Fundamental transverse frequency at 0 cycle of freezing and thawing

n_1 = Fundamental transverse frequency after c cycles of freezing and thawing

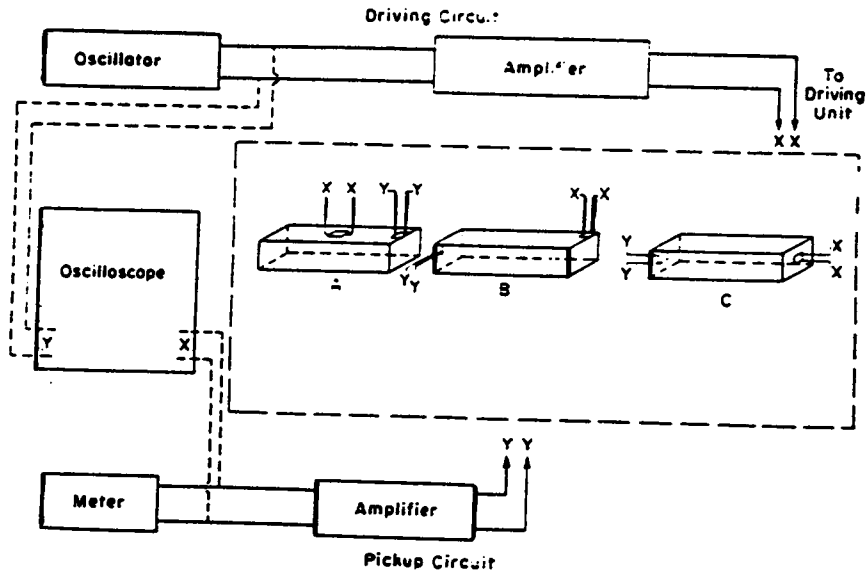

—Schematic diagram of a typical apparatus showing driver and pick-up positions for the three types of vibration. A. Transverse resonance. B. torsional resonance. C. longitudinal resonance. (After ASTM C 215-60.)

Figure C.1. Schematic of Sonic Testing Apparatus

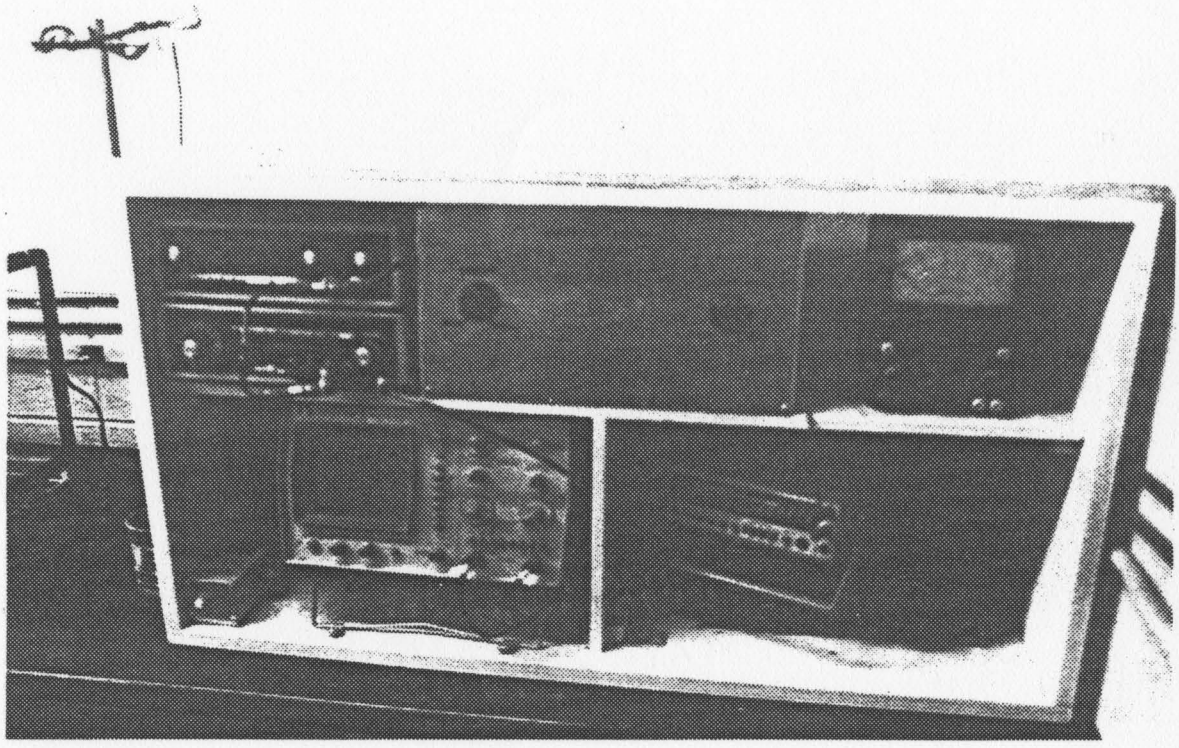

Figure C.2. The Sonic Testing Apparatus

Appendix D

LINEAR TRAVERSE APPARATUS

The linear traverse apparatus used during this study was manufactured by Frank E. Fryer Company, Inc. Carpentersville, ILL. and it is marketed under brand name of MCS-83. The MCS-83 offers a direct visual viewing by a steriomicroscope capable of magnification up to 120X and a motorized stage transport which automatically operates a X-Y coordinate for scanning. Traversed chords are measured using a small keyboard mounted on the base of the apparatus. For further information on the operation of this apparatus refer to the operation manual supplied by the manufacturer. The stage movement, speed, data collection, and basic calculation of the air void parameters are all performed by a microcomputer. The microcomputer utilizes a Z80A, 40 MHz microprocessor and CPM operating system. Figure D-1 shows the MCS-83 used for this research. Individual chords are saved (in Micron) on a 8 inches floppy disc. The data is transferred to a MS DOS base system using a reformatter and conversion system. This system includes an external 8 inches floppy drive, an internal control card, and a software. The transferred data is saved in standard ASCII format and can be imported by any data base or spread sheet program. For the purpose of this study the collected data was transferred to a Zenith personal computer. The data was imported by a spread sheet program (Supercalc 4) and subsequent manipulations was done

using this program. Following is the list of Supercalc4 overlay used for the calculations of the air void parameters. The capital letters refers to the column names in the spread sheet program.

A = measured chords imported to the program (Micron)

B = $\frac{A}{1x10^6}$ chords in mm

E = total number of voids

G = SUM (A1:Ax) total length of voids

where Ax refers to the row number of the last measured chord

I = G/E average void length (mm)

K = E/2413 average number of voids per mm of traverse

M = I x K x 100 percent air content

O = 4/I specific surface (1/mm)

Q = percent paste content

S = M/Q air to paste ratio

U = 1/S paste to air ratio

W = (3/O)(1.4(((Q/M) + 1)**0.333)-1) spacing factor (mm)

Y = W/25.4 spacing factor (in)

AA = O*25.4 specific surface (in)

For the calculation of air void parameters based on the chords less than 1 mm the data in column A (chord length) were sorted in an ascending order and chords greater than 1 mm were removed. Air void parameters were calculated in the same fashion as above. For the calculation of air void parameters based on chords less than 0.5 mm again same steps as above were followed, but this time the chords greater than 0.5 mm were dropped.

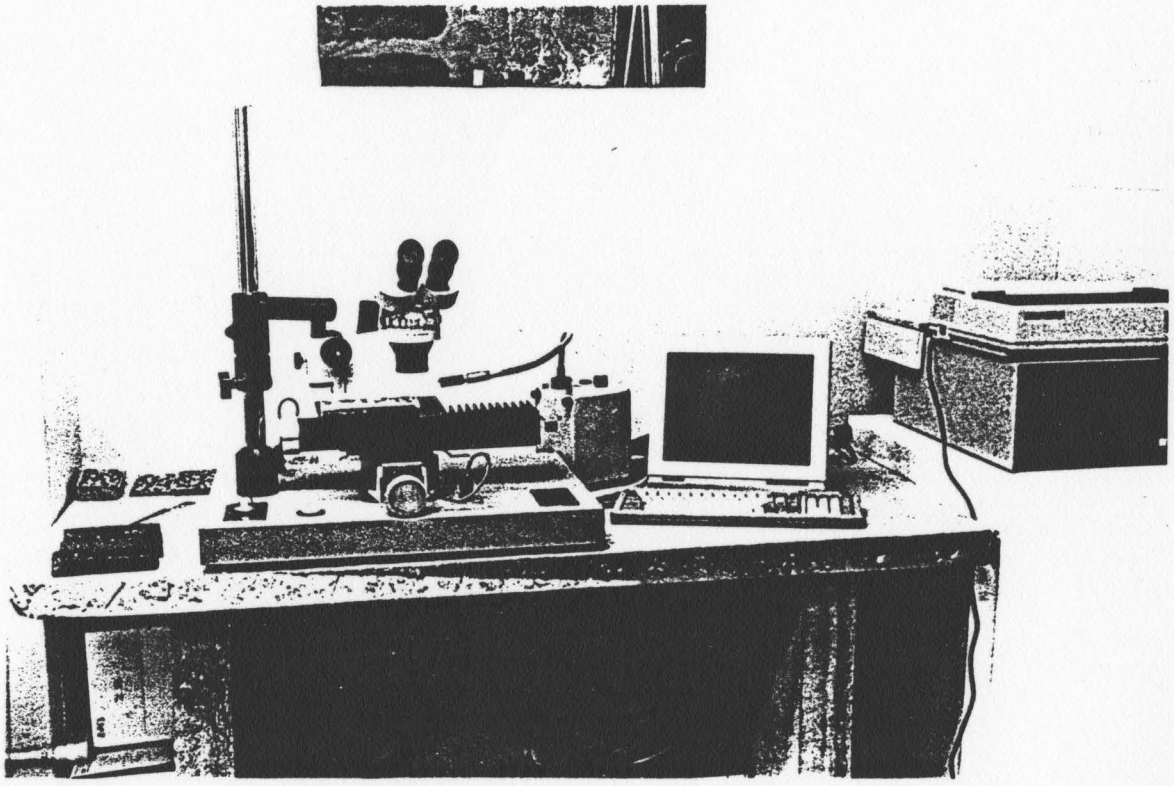

Figure D.1. The MCS-83 Linear Traverse Apparatus

The vita has been removed from the scanned document